MAGNETIC RESONANCE IMAGING OF ATHEROSCLEROTIC PLAQUE

STEPHEN G. WORTHLEY

M.B.,B.S., F.R.A.C.P.

Department of Medicine
University of Adelaide
Adelaide, SA, 5005
AUSTRALIA

AND

Zena and Michael A. Wiener Cardiovascular Institute
Mount Sinai School of Medicine
New York, NY, 10029-6574
UNITED STATES OF AMERICA

Submitted in the total fulfillment of the requirements
for the degree of Doctor of Philosophy
Department of Medicine
University of Adelaide
AUSTRALIA
August 2000

For my beautiful wife, Kirsten.

Thank you for your strength and love

during these memorable times.

DECLARATION

I performed the research presented in this thesis within the Department of Medicine, University of Adelaide, Adelaide, Australia and the Zena and Michael A. Wiener Cardiovascular Institute, Mount Sinai School of Medicine, New York, United States of America. There is no data presented within this thesis which has been accepted for the award of any other degree or diploma in any other institution and contains no material previously published or written by any other person, except where due reference is made in the text.

Dr. Stephen G. Worthley
Department of Medicine
University of Adelaide
Adelaide
South Australia 5000
AUSTRALIA

I give consent to this copy of my thesis, when deposited in the University Libraries, being available for photocopying and loan.

SIGNATURE: **DATE:** 10/8/2001

TABLE OF CONTENTS

ACKNOWLEDGEMENTS

I would firstly like to acknowledge the contribution my co-supervisors have made to my education and the production of this thesis. Associate Professor Juan Jose Badimon has been an outstanding and unrelenting leader and scientist, whose unwavering support has permitted the success of many research projects. I have learnt invaluable lessons from our association that have shaped and moulded my approach to both the research and clinical spheres of my career. Professor Philip Barter has provided wisdom and vision about my research and future, and in concert with his flexibility and persistence, have allowed this research venture I have embarked on to reach its potential. A special mention must be made to Professor Valentin Fuster, whose abilities as a clinician, a scientist and a leader have had a major impact upon me professionally.

To my many co-workers, without whose assistance many of the tasks that were required for this thesis would have been insurmountable, I give heart-felt thanks. In particular, I must make special note of two people. Dr. Gérard Helft's intellect and abilities as a clinician-scientist allowed the realisation of many productive projects together during this time. More importantly, I know that his friendship and camaraderie will remain forever. Dr. Azfar Zaman's perspective and teamwork allowed the forging of a superb work ethic, and I learnt much from his wisdom and years of experience.

I must thank the National Heart Foundation of Australia, South Australian Branch and especially the hard work of Mr. Bob McEvoy and all of the staff for believing in the initial undertaking that I proposed and providing the financial support to allow its completion.

To my parents, Janice and Lindsay Worthley, I am forever grateful for the love and support that has accompanied me throughout my life. So much of any successes I gain have their foundations firmly based on their love. My brothers Matthew and Daniel Worthley and their respective wives, Alex and Liza, have provided not only endless love and support throughout this time, but critical commentary on the quality of this research.

But, I owe the most to my wife Kirsten and my children, William and Phoebe, who have endured the hardships and celebrated the successes of this thesis.

THESIS RELATED PUBLICATIONS

ORIGINAL RESARCH

1. **Worthley SG**, Helft G, Fuster V, Fayad ZA, Fallon JT, Osende JI, Roque M, Zaman AG, Rodriguez OJ, Shinnar M, Verhallen P, Badimon JJ. High resolution ex vivo magnetic resonance imaging of in situ coronary and aortic atherosclerotic plaque in a porcine model. Atherosclerosis 2000;150:321-9.

2. **Worthley SG**, Helft G, Fuster V, Fayad ZA, Zaman AG, Osende JI, Fallon JT, Badimon JJ. Cardiac gated breath-hold blood black MRI of the coronary arteries: an in vivo and ex vivo comparison. Int J Card Imaging (in press).

3. **Worthley SG**, Helft G, Fuster V, Fayad ZA, Rodriguez OJ, Fallon JT, Zaman AG, Badimon JJ. Noninvasive in vivo magnetic resonance imaging of experimental coronary artery lesions in a porcine model. Circulation 2000;101:2956-61.

4. Helft G, **Worthley SG**, Fuster V, Osende JI, Zaman AG, Rodriguez OJ, Fayad ZA, Fallon JT, Badimon JJ. Atherosclerotic aortic component quantification by noninvasive magnetic resonance imaging. An in vivo study in rabbits. J Am Coll Cardiol 2001;37;1149-54.

5. **Worthley SG**, Helft G, Fuster V, Zaman AG, Fayad ZA, Fallon JT, Badimon JJ. Serial in vivo magnetic resonance imaging documents arterial remodeling in experimental atherosclerosis. Circulation 2000;101:586-9.

SPECIFIC CONTRIBUTION BY CANDIDATE TO EACH MANUSCRIPT

Development and management of the animal models, performance of the magnetic resonance imaging, euthanasia of animal models and specimen fixation, assistance in analysis of magnetic resonance images and histopathology, writing of all manuscripts (except reference 4, in which the manuscript writing was primarily by Helft).

REVIEWS

1. Zaman AG, Helft G, **Worthley SG**, Badimon JJ. The role of plaque rupture and thrombosis in coronary artery disease. Atherosclerosis 2000;149:251-66.

2. **Worthley SG**, Osende JI, Helft G, Zaman AG, Badimon JJ, Fuster V. Coronary artery disease: pathogenesis and acute coronary syndromes. Mt Sinai J Med 2001;68:167-81.

3. Helft G, **Worthley SG**, Zaman AG, Samama MM, Badimon JJ. Thrombolytic and adjunctive therapies in acute myocardial infarction. Haemostasis 2000;30:159-167.

4. **Worthley SG**, Helft G, Zaman AG, Fuster V, Badimon JJ. Atherosclerosis and the vulnerable plaque. Part 1 : Pathogenesis. Aust NZ J Med 2000;30:600-7.

5. **Worthley SG**, Helft G, Zaman AG, Fuster V, Badimon JJ. Atherosclerosis and the vulnerable plaque. Part 2 : Imaging. Aust NZ J Med 2000;30:704-11.

THESIS RELATED ABSTRACTS

1. **Worthley SG**, Helft G, Fayad ZA, Osende JI, Fallon JT, Aguinaldo G, Roque M, Shinnar M, Fuster V, Badimon JJ. High-resolution ex-vivo MR imaging of in-situ coronary wall components in a porcine model of atherosclerosis. Journal of Cardiovascular Magnetic Resonance 1999;1:285.

2. Helft G, **Worthley SG**, Fayad ZA, Osende JI, Fallon JT, Roque M, Shinnar M, Fuster V, Badimon JJ. High-resolution ex-vivo MR imaging of the aorta: a swine model of complex atherosclerotic plaque. Journal of Cardiovascular Magnetic Resonance 1999;1:289.

3. **Worthley SG**, Helft G, Fuster V, Fayad ZA, Rodriguez OJ, Fallon JT, Zaman AG, Badimon JJ. In vivo high-resolution MRI non-invasively defines coronary lesion size and composition in a porcine model. Circulation 1999;100:I-521.

4. **Worthley SG**, Helft G, Fuster V, Fayad ZA, Osende JI, Fallon JT, Roque M, Rodriguez OJ, Zaman AG, Badimon JJ. High-resolution magnetic resonance imaging of complex in situ coronary and aortic atherosclerosis ex vivo. Mt Sinai J Med 1999;66:368.

5. **Worthley SG**, Helft G, Fuster V, Fayad ZA, Rodriguez OJ, Fallon JT, Zaman AG, Badimon JJ. High-resolution in vivo magnetic resonance imaging of experimental coronary artery plaques. Mt Sinai J Med 1999;66:368.

6. Helft G, **Worthley SG**, Fuster V, Fayad ZA, Osende JI, Fallon JT, Zaman AG, Roque M, Rodriguez OJ, Badimon JJ. Non-invasive magnetic resonance imaging detects and quantifies atherosclerotic plaque components in rabbits. Mt Sinai J Med 1999;66:370.

7. **Worthley SG**, Helft G, Fayad ZA, Fuster V, Zaman AG, Fallon JT, Badimon JJ. MR Imaging Documents Coronary Artery Atherosclerotic Severity and Composition: Ex Vivo and In Vivo Studies in a Porcine Model. 27th Annual Meeting and Scientific Sessions of the North American Society for Cardiac Imaging (NASCI), Atlanta, November 1999.

8. Helft G, **Worthley SG**, Fayad ZA, Fuster V, Osende JI, Zaman AG, Fallon JT, Badimon JJ. In vivo Quantification of Atherosclerotic Plaque Components with MRI in a Rabbit Model of Atherosclerosis. 27th Annual Meeting and Scientific Sessions of the North American Society for Cardiac Imaging (NASCI), Atlanta, November 1999.

9. **Worthley SG**, Helft G, Fuster. V, Fayad ZA, Osende JI, Fallon JT, Zaman AG, Shinnar M, Badimon JJ. High Resolution MRI in a Novel Porcine Model of Complex Atherosclerosis: T1W, T2W and PDW Characteristics of Atherosclerotic Plaque Components. J Am Coll Cardiol 2000;35:A-479.

10. **Worthley SG**, Helft G, Fuster. V, Fayad ZA, Zaman AG, Fallon JT, Badimon JJ. Serial Noninvasive In Vivo MRI Monitors Progression and Regression of Individual Atherosclerotic Lesions in a Rabbit Model. J Am Coll Cardiol 2000;35:A-432.

11. Helft G, **Worthley SG**, Fuster V, Fayad ZA, Osende JI, Zaman AG, Fallon JT, Badimon JJ. In Vivo Quantification of Atherosclerotic Plaque Composition by Noninvasive High Resolution MRI in Rabbits: A Histopathological Correlation. J Am Coll Cardiol 2000;35:A-478.

12. Zaman AG, **Worthley SG**, Helft G, Fuster V, Fayad ZA, Fallon JT, Badimon JJ. In vivo quantification of atherosclerotic plaque components with MRI in a rabbit model of atherosclerosis. Heart Lung Circulation 2000:9(Suppl.);A146.

13. **Worthley SG**, Zaman AG, Helft G, Fuster V, Fayad ZA, Fallon JT, Badimon JJ. Noninvasive in vivo MRI documents arterial remodeling in a novel WHHL rabbit model. Heart Lung Circulation 2000:9(Suppl.);A127.

14. **Worthley SG**, Helft G, Zaman AG, Fuster V, Fayad ZA, Fallon JT, Badimon JJ. MR imaging of coronary artery atherosclerosis in a porcine model. Heart Lung Circulation 2000:9(Suppl.);A127.

THESIS RELATED AWARDS

1. Oral Presentation Winner: Cardiology
   17th Annual Samuel Bronfman Department of Medicine Research Day 1999
   Mount Sinai School of Medicine, New York.
   Abstract: High resolution magnetic resonance imaging of complex in situ coronary and aortic atherosclerosis ex vivo.
   Authors: **Worthley SG**, Helft G, Fuster V, Fayad ZA, Osende JI, Fallon JT, Roque M, Rodriguez OJ, Zaman AG, Badimon JJ.

2. First Place Poster Award
   27th Scientific Sessions of the North American Society for Cardiovascular Imaging 1999, Atlanta, Georgia
   Abstract: MR Imaging Documents Coronary Artery Atherosclerotic Severity and Composition: Ex Vivo and In Vivo Studies in a Porcine Model.
   Authors: **Worthley SG**, Helft G, Fayad ZA, Fuster V, Zaman AG, Fallon JT, Badimon JJ.

THESIS RELATED BOOK CHAPTERS

1. Fayad ZA, **Worthley SG**, Helft G, Foo T, Fuster V. Magnetic Resonance Imaging of the Vascular System Chapter 18B. Hurst's The Heart, 10th edition.

THESIS RELATED INVITED PRESENTATIONS

1. **Worthley SG**, MR Imaging Documents Coronary Artery Atherosclerotic Severity and Composition: Ex Vivo and In Vivo Studies in a Porcine Model. 4th Annual Scientific Meeting of the Cardiovascular Registrars Research Forum, Barossa Valley, May 2000.

2. **Worthley SG**. MR Imaging Documents Coronary Artery Atherosclerotic Severity and Composition: Ex Vivo and In Vivo Studies in a Porcine Model. 4th Annual Scientific Meeting of the Cardiovascular Registrars Research Forum, Barossa Valley, May 2000.

3. **Worthley SG**. Atherobiology, Imaging and Stroke. Melbourne Stroke Conference, July 2000.

4. **Worthley SG**. The Future in Imaging Atheroma. 4th International Monash Interventional Symposium – Millennium Stent Conference, Melbourne, August 2000.

5. **Worthley SG**. The Atherobiology of Stroke. Royal Australian and New Zealand College of Radiologists Scientific Meeting (Victorian Branch), Melbourne, August 2000.

LIST OF ABBREVIATIONS

AALAC	American Association for the Accreditation of Laboratory Animal Care
C-11	Carbon-11
CAC	Coronary Artery Calcium
CAM	Cellular Adhesion Molecule
CME	Combined Masson Elastin
CNR	Contrast-to-Noise
CT	Computerised Tomography
2IRFSE	Double Inversion Recovery Fast Spin Echo
EBCT	Electron Beam Computerised Tomography
ECG	Electrocardiograph
ESP	Echo Spacing
ETL	Echo Train Length
F-18	Fluorine-18
FDG	Fluoro-deoxyglucose
FGF	Fibroblast Growth Factor
FOV	Field Of View
FSE	Fast Spin Echo
Gd-DTPA	Gadolinium-DiethyleneTriamine PentaAcetate
GE	General Electric
HDL	High Density Lipoprotein
HU	Hounsfield Units
ICAM	Inter-Cellular Adhesion Molecule
IVUS	Intravascular Ultrasound
LAD	Left Anterior Descending
LCx	Left Circumflex
LDL	Low Density Lipoprotein
MCP-1	Monocyte Chemoattractant Protein-1
MHz	Megahertz
MMP	Matrix Metallo-Proteinase
MRI / MR	Magnetic Resonance Imaging / Magnetic Resonance
MWT	Mean Wall Thickness
N-13	Nitrogen-13
NMR	Nuclear Magnetic Resonance

NO	Nitric Oxide
NOS	Nitric Oxide Synthase
O-15	Oxygen-15
PAI-1	Plasminogen Activator Inhibitor-1
PBS	Phosphate Buffered Saline
PDGF	Platelet Derived Growth Factor
PDW	Proton Density Weighted
PET	Positron Emission Tomography
PGI_2	Prostacyclin
RCA	Right Coronary Artery
RF	Radiofrequency
SD	Standard Deviation
SEM	Standard Error of the Mean
T	Tesla
TE	Echo Time
TGF-β	Transforming Growth Factor-β
TI	Inversion Time
TIMP	Tissue Inhibitor of Metallo-Proteinase
TNF α and β	Tissue Necrosis Factor α and β
TOF	Time Of Flight
tPA	tissue-type Plasminogen Activator
TR	Recovery Time
T1W	T1 Weighted
T2W	T2 Weighted
VCAM-1	Vascular Cellular Adhesion Molecule-1
VEC	Velocity Encoded Contrast
VWA	Vessel Wall Area
vWF	von Willebrand Factor
WHHL	Watanabe Heritable HyperLipidaemic

SYNOPSIS

There is a need for an imaging modality (or modalities) that will provide information about the composition as well as the severity of atherosclerotic lesions, given the critical role that plaque composition plays in the acute thrombotic complications of atherosclerotic diseases. Magnetic resonance is a unique noninvasive imaging modality that affords a high intrinsic contrast between soft tissue structures using oscillating magnetic fields. Thus, before we can use magnetic resonance imaging (MRI) for the purpose of atherosclerotic plaque characterisation, validation of MRI with histopathology in models of complex atheroma would be required. This thesis builds on exciting early work with MRI and atherosclerosis by a systematic evaluation of its use in the ex vivo and in vivo setting, in the aorta and coronary arteries, in rabbit and porcine models and leaves us with the potential for human coronary atherosclerotic imaging.

Initially we assess the ability of MR imaging, in an ex vivo setting to be able to identify all of the components of complex atherosclerotic lesions in an experimental porcine model. This first step, provides the basis for the possibility that if the techniques used could be translated to the in vivo setting, then the potential for characterising atheroma in humans is possible.

The next step is towards translation of MR imaging techniques to in vivo coronary lesions, confirming the ability of the motion suppression techniques employed. Comparability of in vivo and ex vivo MR images from the same sites in the coronary arteries would provide compelling evidence that the imaging technique was robust for this purpose.

To confirm and extend the above described work, definitive confirmation that MR imaging was accurate in its representation of the atherosclerotic lesion would be required by providing comparative histopathological sections of the regions imaged. Using the porcine model, where the coronary anatomy is comparable to the human, the feasibility of now translating these techniques to patients with coronary artery disease would then be proven.

Rabbits models of atherosclerosis have utility in that they may have discrete fibrotic and lipidic plaque components. These two components of atherosclerosis appear critical in the determination of both risk of plaque rupture and subsequent thrombogenicity. Furthermore, the abdominal aorta of the rabbit is comparable in size to the human coronary artery. By utilising MR imaging techniques in a cholesterol fed rabbit model of atherosclerosis for the definition of both composition of the lesion, as well as the extent of atherosclerotic burden, we move closer towards the goal of being able to serially monitor changes in plaque composition.

Despite the pleiotropic postulates about the mechanisms involved for the risk reduction in mortality and recurrent coronary events in patients with coronary artery disease treated with lipid lowering therapy, in particular statins, the effect that these therapies have on the composition of atherosclerotic plaques is not definite. Despite pathological data, suggesting a reduction in lipidic and increase in fibrotic components of atherosclerotic lesions in response to dietary modification in animal models, the serial evaluation of the same lesions over time in response to a therapy will provide us with important data relevant to the concept of atherosclerotic plaque stabilisation.

Having discussed the theoretic ability of noninvasive MRI to serially image atherosclerosis, it remained to be shown that serial imaging at different time-points of the same atherosclerotic lesions could be performed. This crucial concept is central in the defining of compositional changes in atherosclerotic lesions. Having confirmed the ability of MRI to document the lipidic and fibrotic components of abdominal aortic atherosclerosis in the cholesterol fed rabbit model described in the previous chapter, the next step to serially image these lesions under circumstances of atherosclerotic progression and regression. This is crucial in confirming the ability of MRI to identify the same atherosclerotic lesions in the same individuals at different time-points and to document compositional changes in these lesions.

The ability of serial noninvasive MR imaging to document changes in aortic wall parameter in the Watanabe Heritable Hyperlipidaemic (WHHL) rabbit permits monitoring of the arterial remodelling process. We now know that significant atherosclerosis can exist without any compromise to the lumen. Furthermore, positive arterial remodelling appears to be associated with vulnerable atherosclerosis, thus enhancing the significance of its detection. This concept of arterial remodelling has been described for over 10 years. However, the mechanisms involved remain uncertain because of the difficulty in obtaining longitudinal studies over the lengthy time interval during which remodelling likely occurs, and because of limited data from relevant animal models. The feasibility of using MR imaging to document arterial remodelling in vivo permits future studies at multiple time points. Indeed it is clear that early arterial remodelling is not always positive. This further reinforces the need for an imaging modality that can serially and noninvasively provide information about the arterial remodelling process in humans. The ability of MR to provide serial and noninvasive information about the arterial wall in this model could provide us

with a useful imaging tool to assist the investigation of arterial remodelling in future studies.

Atherosclerotic imaging with MR has the potential to enhance our understanding of the patho-biology of this disease process and assist our understanding of the effect of therapies on atherosclerotic lesions. The ultimate goal of coronary artery atherosclerotic plaque characterisation and quantification is obtainable as demonstrated by the progression of findings on the uses of MRI in atherosclerotic imaging in this thesis.

Chapter 1

INTRODUCTION

TABLE OF CONTENTS

1. 1. BACKGROUND

The thrombotic complications of atherosclerotic diseases remain the leading causes of mortality in Western Society. In Australia, cardiovascular diseases are responsible for 1 in every 2.4 (41%) deaths and are the leading single cause of mortality. Furthermore, the presence of atherosclerotic disease (defined as thickening of the arterial wall through the accumulation of lipids, macrophages, T-lymphocytes, smooth muscle cells, extracellular matrix, calcium and necrotic debris) is more prevalent again and of itself rarely fatal. The crucial final common process for the conversion of a non-occlusive, often clinically silent, atherosclerotic lesion to a potentially fatal condition is plaque disruption. The mortality associated with atherosclerotic disease relates to the acute coronary syndromes, including acute myocardial infarction, unstable angina pectoris and sudden cardiac death. There is substantial clinical, experimental and post-mortem evidence demonstrating the central role that acute thrombosis upon a disrupted atherosclerotic plaque plays in the acute coronary syndromes. Therefore, therapeutic approaches to date have focused on reducing or resolving such thrombotic complications of atherosclerotic plaques (i.e. antiplatelet, anticoagulant and thrombolytic therapies) in order to reduce the socio-economic impact of these acute coronary syndromes.

1. 2. INTRODUCTION

It was in the 19th century that the first theories about the origin of atherosclerosis were proposed.

The thrombogenic, or incrustation theory, first proposed by Rokitansky in 1852 (von Rokitansky 1852), proposes that fibrin deposition and its subsequent organisation by fibroblasts is the critical intitial phase in atherogenesis. Lipid deposition occurred as a subsequent, secondary process, leading to intimal thickening. There has been recent corroborative data for this theory with the observation that platelet deposition on de-endothelialised areas may trigger the migration and proliferation of vascular smooth muscle cells (Ross 1986).

The lipidic theory, initially postulated by Virchow in 1856, suggests that lipid infiltration is the primary process leading to atherosclerosis and the consequence of an imbalance between the influx and efflux of cholesterol within the arterial wall.

Our current understanding integrates the above theories with more recent advances in our understanding of the cellular and molecular processes involved in atherogenesis into a more complex, unified theorem, often referred to as the "response to injury" hypothesis (figure 1. 1) (Fuster et al. 1992; Fuster et al. 1992).

Figure 1. 1

Multifactorial Theory on the Origin of Atherosclerosis

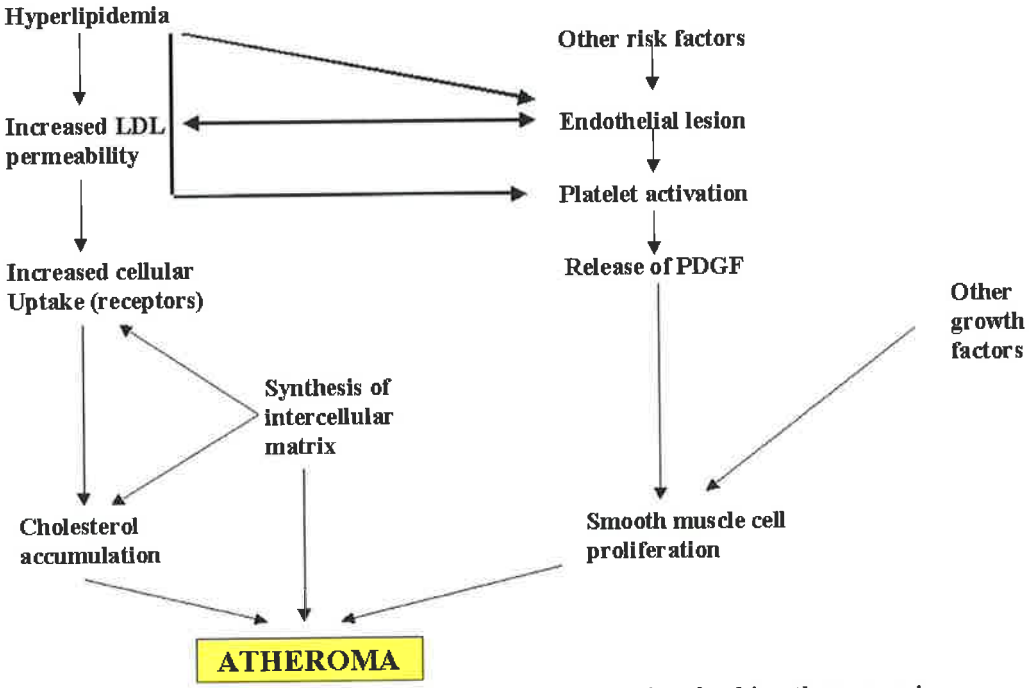

Summary of some of the important mechanisms and pathways involved in atherogenesis.

Endothelial dysfunction appears to be the critical initiating factor for the subsequent events that ultimately lead to atherosclerosis. This highlights the crucial role that a normally functioning endothelium plays in retarding the onset and progression of atherosclerosis. The strong relationship between known risk factors for atherosclerosis (including dyslipidaemia, smoking, hypertension, diabetes, obesity and inflammation) and endothelial dysfunction highlights this point. Despite the presence of these systemic risk factors, the clinical manifestations of atherosclerosis relate to focal disease. The explanation for this propensity for formation of focal atherosclerotic lesions at certain sites involves disturbances in the blood flow pattern; a concept related to shear stress.

1. 3. PATHOGENESIS

1. 3. 1. Rheological Factors

The arterial vessel wall, and thus the endothelial cells, are subject to mechanical forces including the hydrostatic force exerted by blood within the vessel, circumferential stress from motion of the vessel during the cardiac cycle and shear stress resulting from blood flow within the vessel. It is the last of these forces, shear stress, which appears to have the greatest impact upon events occurring at the blood-vessel wall interface because it stimulates the release of vasoactive substances, changes such cellular processes as gene expression, cell metabolism and cell morphology (Davies 1995). Shear stress refers to the force generated by the sliding motion of two adjacent planes. Blood flow can be described as an infinite number of laminae sliding across one another and thus each lamina experiences some frictional interference from the others. Blood flow in a non-obstructed, straight vascular segment is classically parabolic (so-called laminar flow). Moreover, this ordered laminar pattern of flow is pulsatile in association with the cardiac cycle. Thus, endothelial cells experience pulsatile shear stress with alterations in magnitude that result in a mean positive shear stress. At areas of abrupt curvature in the vessel (such as at the carotid bulb) the laminar blood flow is disrupted, resulting in recirculation vortices that lead to low mean shear stress and flow reversal. There is a strong correlation between endothelial dysfunction and areas of low mean shear stress and oscillatory flow with flow reversal (Ku et al. 1985). These sites demonstrate the appearance of cellular adhesion molecules on the endothelial cell surface, increased uptake of lipoproteins, inflammatory cell transmigration and the secretion of chemokines and cytokines leading to the proliferation of smooth muscle cells and macrophages within the vessel wall. Expression of vascular cellular adhesion

molecule 1 (VCAM 1), one of the earliest markers for fatty streaks and upregulated in areas of the endothelium associated with atherosclerosis, has an inverse relationship with shear stress (Ohtsuka et al. 1993; Ando et al. 1994; Ando et al. 1995; Sampath et al. 1995; Tsao et al. 1995; Walpola et al. 1995). This suggests that inflammatory cell binding would be enhanced under conditions of low mean shear stress. Furthermore, extensive monocyte adhesion has been noted under conditions of low mean shear stress, which has co-localised to areas of VCAM 1 expression (Walpola et al. 1995). Monocyte chemoattractant protein 1 (MCP 1), an important chemokine in monocyte recruitment to the vessel wall (Ross 1993), has been shown to be inhibited in conditions of pulsatile positive shear stress (Shyy et al. 1995). Thus, substantial evidence exists that high mean shear stress inhibits leukocyte binding and chemokine and cytokine expression, while low mean shear stress promotes inflammatory cell binding.

An important role of the endothelium is to provide an antithrombotic surface for the flowing blood. There is substantial data demonstrating that shear stress is an important stimulus for the secretion of prostacyclin (Grabowski et al. 1985; Ross et al. 1990) and nitric oxide (NO) (Rubanyi et al. 1986; Busse et al. 1989; Vanhoutte 1989), both of which are potent inhibitors of platelet aggregation. Furthermore, shear stress has been shown to regulate the production of thrombomodulin (Malek et al. 1994) which (through interaction with protein C and S) inactivates specific clotting factors, stimulates the expression of tissue plasminogen activator (Malek et al. 1994; Takada et al. 1994; Kawai et al. 1997) and reduces the secretion of plasminogen activator inhibitor type 1 (Kawai et al. 1997). The genes for the production of tissue factor, one of the most potent stimuli for thrombin generation via the extrinsic pathway of the coagulation cascade, are upregulated in conditions of low mean shear stress (Lin et al. 1997), leading to the existence of a prothrombotic endothelial

surface. Thus, it is clear that in conditions of low mean shear stress, there is not only the removal of anticoagulant mechanisms, but also the emergence of procoagulant ones.

Smooth muscle cell proliferation is an important feature of atherosclerotic lesions and is stimulated by endothelial factors, of which shear stress is one of the regulators (Kraiss et al. 1993). Low mean shear stress (which is pro-atherogenic) has been shown to be associated with increased production of endothelial platelet derived growth factor (PDGF) (Kraiss et al. 1993). High mean shear stress (which is anti-atherogenic or atheroprotective) has been associated with reduced production of endothelin 1 (Sharefkin et al. 1991) and angiotensin II (Rieder et al. 1997) (smooth muscle mitogens), and increased production of NO (Buga et al. 1991; Ohno et al. 1995) and transforming growth factor β (TGF-β) (inhibitors of smooth muscle cell growth). Thus, substantial evidence exists for shear stress mediated modulation of vascular smooth muscle cell proliferation.

This process is complicated a little by the concept of shear rate. This is different from shear stress and reflects the blood flow relative to the luminal size of the vessel. Thus, it directly influences the transit time that the above-described cellular and non-cellular substances have to gain entry into the vessel wall. As such, conditions of high shear rate decrease the time that these pro-atherogenic substances are in contact with a given endothelial cell and help to impede the development of atherosclerosis by affecting the rate of transport of cellular (i.e. monocytes, T-cells, platelets) and non-cellular (i.e. lipoproteins, cytokines, growth factors, fibrinogen etc.) pro-atherogenic substances into and away from the vessel wall. This concept is less defined than the previously described relationship between shear stress and endothelial dysfunction. However studies have shown that the concentration of LDL

at the surface of the vessel wall was inversely related to the shear rate, and that increased local LDL concentration resulted in an increased rate of lipid infiltration into the vessel wall (Deng et al. 1995). Thus areas exposed to low mean shear rates and flow reversal appear to be relatively permeable to LDL and other macromolecules, accounting for the predilection of lipid accumulation at these sites.

NO appears to be one of the critical factors accounting for the anti-atherogenic properties of high mean shear stress on the vessel wall. This substance inhibits platelet aggregation and leukocyte binding to the endothelium, vascular smooth muscle proliferation and alters lipoprotein metabolism (Vanhoutte 1989). The production of NO is dependent on an enzyme called nitric oxide synthase (NOS) (Janssens et al. 1992; Nishida et al. 1992; Sessa et al. 1992). Shear stress is one of the most potent physiological stimuli for the production of NO by endothelial cells. Recent research implicates the activation of the synthetic enzyme nitric oxide synthase (NOS) as the mechanism by which shear stress up-regulates NO production by the endothelial cells (Corson et al. 1996; Fleming et al. 1997).

Exactly how the endothelial cell response to shear stress is mediated remains unclear, although such signalling pathways as G-proteins, intracellular calcium, gene expression and kinase activity have all been implicated.

1. 3. 2. Endothelial Dysfunction

The endothelium also plays a central role in arterial haemostasis, through the regulation of plasma lipoprotein permeability and leukocyte adhesion, and the production of prothrombotic and antithrombotic factors, growth factors and vasoactive substances (figure 1. 2).

Figure 1. 2

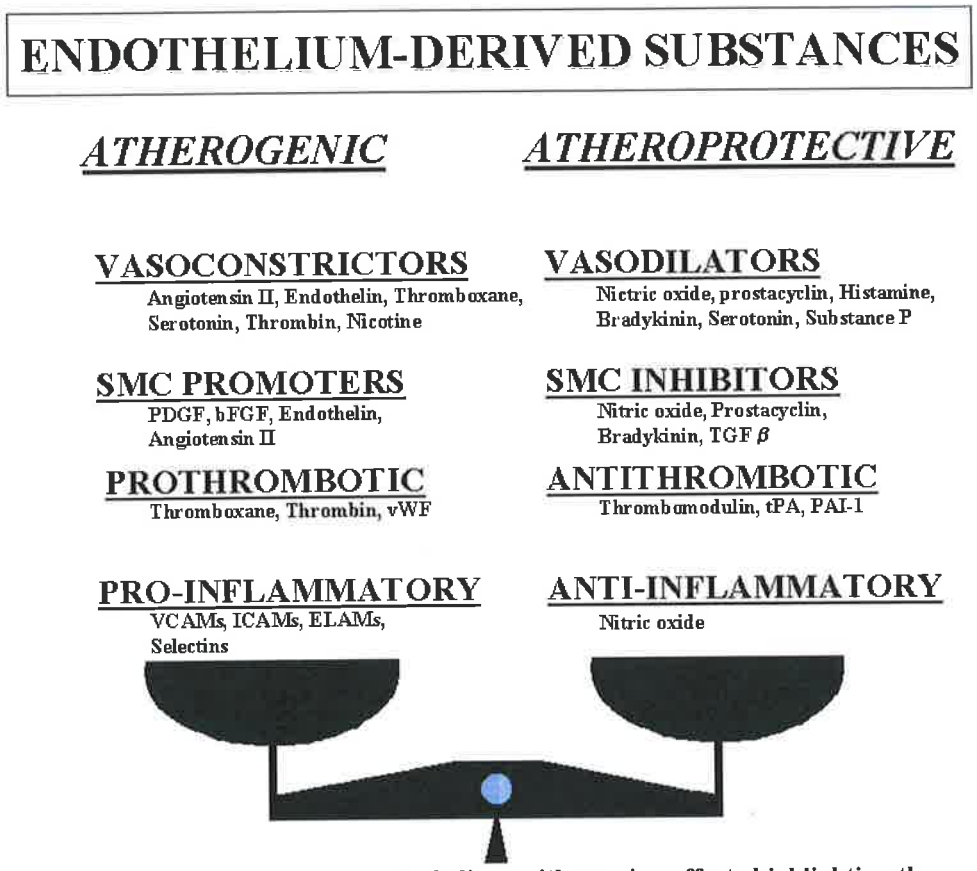

The numerous factors produced by the endothelium with varying effects highlighting the central homeostatic role of a normally functioning endothelium.

Initially it was proposed that endothelial denudation was the first step in atherosclerosis (Ross et al. 1973), although it is now clear that endothelial dysfunction rather than denudation is a far more important process. Many of these processes have been described above as shear stress acts through the endothelium in order to exert its effects. Dysfunctional or activated endothelial cells may express a series of cellular adhesion molecules (CAMs) called selectins that induce inflammatory cells such as the monocyte to marginate, roll and attach to the endothelial surface (Springer et al. 1996). Thereafter, a different series of CAMs called integrins (i.e. Vascular CAM or VCAM and intercellular CAM or ICAM) are expressed resulting in the adherence and subsequent migration into the subendothelial space (Springer et al. 1996). Plasma lipids accompany monocyte migration into the arterial wall, and subsequently these cells transform into tissue

macrophages acting as lipoprotein scavengers and modifiers. The continued internalisation of this lipidic material by macrophages leads to the formation of foam cells. Dysfunctional endothelium, rather than possessing the normal anticoagulant properties, appears procoagulant and expresses vasoactive molecules, cytokines and chemokines as described earlier. Furthermore, these dysfunctional endothelial cells, monocytes and platelet aggregates produce an assortment of chemotactic, inhibitory and stimulatory growth factors for other inflammatory cells (i.e. T-cells) and smooth muscle cells. These smooth muscle cells subsequently produce extracellular matrix and with further receptor mediated lipid accumulation and connective tissue synthesis lead to continued plaque growth. These processes describe the phenomenon of slow and predictable atherosclerotic progression (figure 1. 3) (Fuster et al. 1992; Fuster et al. 1992). Impairment of these functions of the endothelium is intrinsically linked to the development of atherosclerosis.

Figure 1. 3

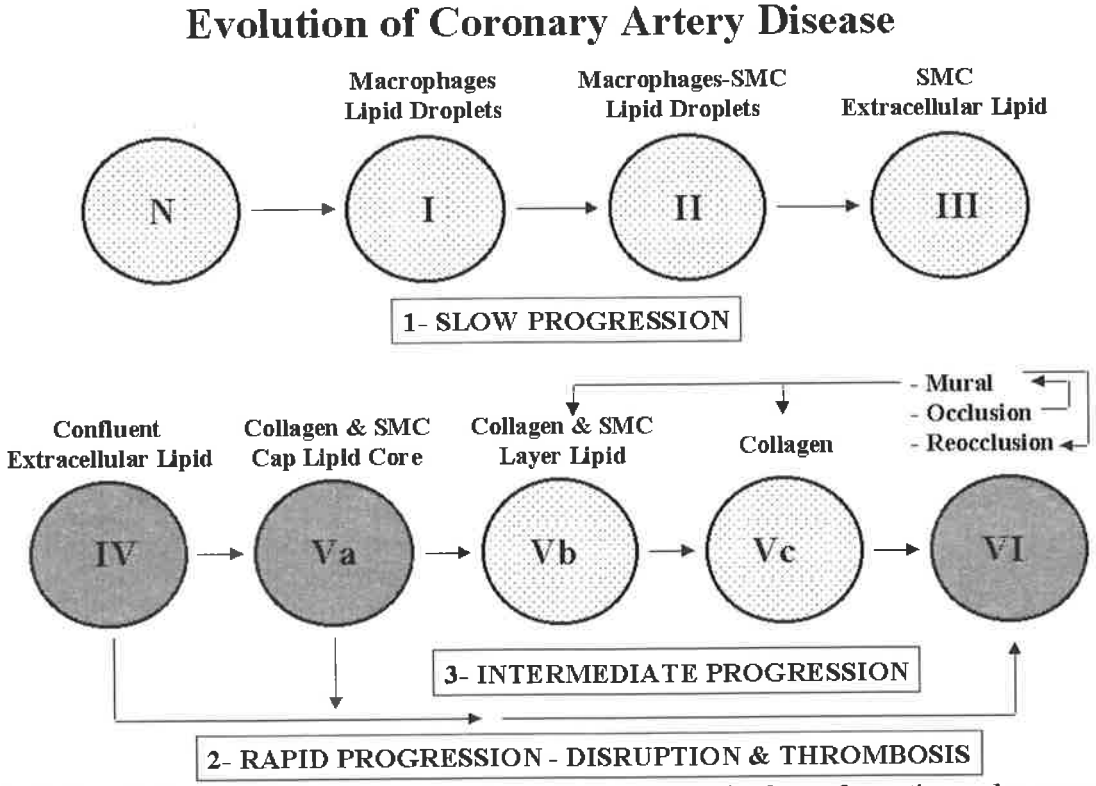

Schematic flow chart representing the various stages of atherosclerotic plaque formation and progression.

One of the most important causes of endothelial dysfunction, low mean shear stress has been described in detail above. However, many of the known risk factors for atherosclerotic disease are known to be associated with endothelial injury or dysfunction, including hyperlipidaemia (in particular LDL), diabetes (in particular hyperglycaemia), hypertension, smoking, elevated serum homocysteine, and infective agents such as herpes viruses and chlamydial organisms (Ross 1999).

1. 3. 3. Inflammation

The recruitment of monocytes into the vessel wall is an early step in the formation of an atherosclerotic lesion. The fatty streak, the precursor for atherosclerotic lesions, contains macrophages and T lymphocytes exclusively (Stary et al. 1994), although the deposition of lipidic material precedes this inflammatory cellular influx in patients with hypercholesterolaemia (Simionescu et al. 1986; Napoli et al. 1997). Inflammatory processes are intimately associated with endothelial dysfunction and important components of many if not all stages of atherosclerotic development. Whether it is the presence of systemic inflammatory processes that initially incites endothelial dysfunction, or a dysfunctional endothelial leads to the up-regulation of cellular adhesion molecule expression and inflammatory cell activation, the end result is a perpetuation and augmentation of the cellular and non-cellular responses of inflammation. This ultimately results in the migration of monocytes and T-cells into the vessel wall. Cellular adhesion molecules act as the receptors for these inflammatory cells, including selectins, intercellular adhesion molecules and vascular cell adhesion molecules (Springer et al. 1996). The subsequent migration of leukocytes across the endothelium depends on chemotactic factors such as monocyte

chemoattractant protein 1 and oxidised LDL (Rajavashisth et al. 1990) as well as adhesion molecules such as platelet-endothelial cell adhesion molecules (Muller et al. 1993). Factors such as monocyte colony stimulating factor appear to be important for the survival and multiplication of macrophages within the growing atherosclerotic lesions (Qiao et al. 1997; de Villiers et al. 1998). T-cells are similarly dependent on interleukin 2 (Ross 1999). Many other inflammatory factors are implicated in the pathogenesis of atherosclerotic lesions (including interferon γ, CD 40, heat shock protein 60, the disintegrins etc.), however their exact roles are yet to be accurately defined (Ross 1999).

Macrophages produce many growth factors (including PDGF, basic FGF, and epidermal growth factor) in addition to the inflammatory factors described above (Libby et al. 1996). However, it is the production of matrix degrading substances (in particular the matrix metalloproteinases and heparanses) which are crucial to the perpetuation and growth of the early lesion (Celentano et al. 1997). In order for smooth muscle cell migration to occur from the media to the intima (where atherosclerotic lesions reside), the extracellular matrix surrounding the smooth muscle cells and the basement membrane which separates the media from the intima must be degraded. Matrix metalloproteinases (MMPs) can perform this task (Celentano et al. 1997). Furthermore, cytokines released by macrophages have been shown to stimulate smooth muscle cells to produce these MMPs themselves (Galis et al. 1994). Included in this family of proteinases is an interstitial collagenase (MMP 1), gelatinase A (MMP 2), stromelysin 1 (MMP 3) and gelatinase B (MMP 9). Gelatinase A (MMP 2) degrades the collagen found in the basement membranes, and appears to be critical in allowing smooth muscle migration through the basement membrane (Pauly et al. 1994). The major control of MMP activity, once activated from the inactive zymogen, lies with the production of tissue inhibitors of MMPs

(TIMPs) (Celentano et al. 1997), of which three have been identified to date. These TIMPs are secreted by macrophages and most connective tissue cells and different TIMPs appear to have different effects on the various MMPs. Thus, it appears that the ratio of MMPs to TIMPs is crucial in determining whether the necessary conditions favor connective tissue and basement membrane breakdown or not. This area continues to be a source of on-going research. The role that MMPs play in promoting plaque disruption will be discussed later.

Lymphocytes, including CD4 and CD8 positive T-cells, have been identified in significant numbers within atherosclerotic lesions, and invariably play a role in the inflammatory processes in plaque genesis and progression (Jonasson et al. 1986; van der Wal et al. 1989). These T-cells are activated when they bind antigens processed and presented by both macrophages and smooth muscle cells. One such antigen may be oxidised LDL (Stemme et al. 1995). This results in the secretion of cytokines (including interferon γ, TNF α and β) that augment the inflammatory process. Other inflammatory cells have also been identified in atherosclerotic lesion (i.e. Mast cells) however their exact role remains unclear.

1. 3. 4. Smooth Muscle Cells

Smooth muscle cells, despite their apparent homogeneity within the media of the vessel wall, have a heterogeneous embryonic origin, depending on the vascular bed described. Thus it has been postulated that the smooth muscle cells in different arterial beds may respond differently to the stimuli that generate atherosclerotic lesions (Chamley-Campbell et al. 1981; Babaev et al. 1990; Koyama et al. 1996). Furthermore, even within the same site, smooth muscle cells appear to express one of two phenotypic states (Frid et al. 1997). One, a contractile (non-synthetic) state, the

normal form, the other a proliferative (synthetic) state, whereby the smooth muscle cell is able to produce matrix proteins and replicate. It is the latter of these forms that appears central in the progression of atherosclerotic lesions (Wight 1989).

The mechanism by which smooth muscle cells appear to migrate to the intima has been described earlier. It is worth to re-iterate that under the effect of cytokines, chemokines and growth factors released from the macrophages as well as oxidised LDL itself, the smooth muscle cells migrate into the intima where they proliferate and secrete matrix proteins, including collagen (important in determining a plaques' stability). Moreover, smooth muscle cells have the ability to secrete MMPs, and thus perpetuate the migration of further smooth muscle cells into the intima (Galis et al. 1994).

The effect of a unique growth factor, transforming growth factor β (TGF β), is worth mentioning briefly, as it appears to have bi-directional effects. It tends to inhibit smooth muscle cell proliferation while at the same time promoting the formation of extracellular matrix (Amento et al. 1991; Gibbons et al. 1992). Its role in atherosclerotic progression remains unclear.

1. 3. 5. Hypercholesterolaemia

Another substance that causes endothelial injury is Low-Density Lipoprotein (LDL) (Morel et al. 1983; Navab et al. 1996; Griendling et al. 1997). It is especially potent when modified by oxidation, glycation or associated with immune complexes (Khoo et al. 1988; Khoo et al. 1992; Griendling et al. 1997; Steinberg 1997). Oxidised LDL is avidly taken up by tissue macrophages within the vessel wall either via LDL receptors (which are subject to down-regulation as the intracellular lipid content

increases) or scavenger receptors (which are not subject to any feedback mechanisms) leading to the accumulation of cholesterol esters and eventually foam cell formation (Brown et al. 1983). This process is initially protective as the sequestration of oxidised LDL stops its deleterious effects on endothelial and smooth muscle cells (Falcone et al. 1991; Diaz et al. 1997; Han et al. 1997). However, uptake of oxidised LDL by the macrophages induces the release of more inflammatory cytokines and chemokines (i.e. monocyte colony stimulating factor (Quinn et al. 1987; Rajavashisth et al. 1990) and monocyte chemoattractant protein 1 (Leonard et al. 1990). This further promotes the migration of more inflammatory cells and enhancing the uptake of oxidised LDL by macrophages and smooth muscle cells. Thus a perpetuating cycle of inflammation, endothelial injury and lipoprotein modification and uptake may be established. Highly oxidised LDL is cytotoxic to the endothelium, macrophages and smooth muscle (Cathcart et al. 1991). The uptake of oxidised LDL by macrophages is unregulated through the scavenger receptor system, leading to the accumulation of large quantities of lipid and thus the formation of foam cells (Goldstein et al. 1979). These foam cells may under necrosis under direct cytotoxic effects from the modified LDL or a process of programmed cell death called apoptosis, induced by certain inflammatory cytokines such as interferon γ (Libby et al. 1996; Ross 1999). These two processes lead to the accumulation of extracellular lipid that may coalesce to form a lipidic, necrotic core, the clinical significance of which we will discuss later.

The density, not just the quantity, of the LDL particles has been shown to correlate with risk of atherosclerotic disease (Slyper 1994). It seems likely that small dense LDL particles are more susceptible to peroxidation (de Graaf et al. 1991; Tribble et al. 1992), and thus promote atherogenesis by the mechanisms described above.

As described above, LDL in its modified (especially oxidised) form is particularly atherogenic and inflammatory. Thus, many antioxidants have been proposed to potentially attenuate this factor of atherogenesis. Antioxidants have been shown to reduce the size of atherosclerotic lesions (Carew et al. 1987; Kita et al. 1987; Sasahara et al. 1994; Chang et al. 1995; Navab et al. 1996) and fatty streaks (Chang et al. 1995) in animal models. This last finding has suggested that antioxidants may have an anti-inflammatory effect, by modulating the expression of adhesion molecules for monocytes (Fruebis et al. 1997). Antioxidants have been shown to increase the resistance of human LDL to oxidation ex vivo, commensurate with the plasma vitamin E levels (Reaven et al. 1993). Although the incidence of myocardial infarction has been reduced by vitamin E supplementation in some preliminary clinical trials (Rimm et al. 1993; Stampfer et al. 1993; Stephens et al. 1996), other antioxidants (i.e. β-carotene) appear to have no such benefit (Reaven et al. 1993; Hennekens et al. 1996; Omenn et al. 1996).

High-density lipoprotein (HDL) fractions appear to counter the atherogenic effects of LDL, although it is unclear of which mechanism(s) is responsible. There do appear to be both lipid dependent and independent effects (Barter et al. 1996). Clearly, the role of HDL in reverse cholesterol transport (the removal of cholesterol from peripheral, extrahepatic sites including the vessel wall and returning it to the liver for metabolism or excretion) can explain some of its atheroprotective effect (Barter et al. 1996). However, HDL (of which there are discrete subfractions with variable effects) has also been shown to have both antioxidant (Decossin et al. 1995) and anti-inflammatory effects (Ulevitch et al. 1981), and thus the atheroprotective mechanisms of HDL may impact at more than one pathway.

1. 3. 6. Infective Agents

Recent interest in the role of infective agents in the pathogenesis of atherosclerosis has resurfaced. It is true that some evidence does support an association between some infective agents (notably chlamydia pneumoniae and herpes viruses, but recently also helicobacter pylori and hepatitis A) and the onset of atherosclerosis (Adam et al. 1987; Saikku et al. 1988; Grattan et al. 1989; Thom et al. 1992; Mendall et al. 1994; Sorlie et al. 1994; Rathbone et al. 1996; Danesh et al. 1997; Ossei-Gerning et al. 1997; Ossewaarde et al. 1998; Pasceri et al. 1998; Zhu et al. 1999). Certainly, in experimental models, chlamydia pneumoniae has been shown to increase atherosclerosis, both in a rabbit model and an apo-E knockout mouse model of atherosclerosis (Muhlestein et al. 1998; Rosenfeld et al. 1998) and cytomegalovirus (a herpes virus) has been shown to increase atherosclerosis in the apo-E knockout mouse (Hsich et al. 1999). This led to the postulate that perhaps direct antibiotic therapy may help retard atherosclerotic progression and complications. However, despite preliminary data suggesting that antibiotic therapy may reduce the incidence of complications associated with acute coronary syndromes (Gurfinkel et al. 1997), further larger scale trials have had negative results (Anderson et al. 1999; Gurfinkel et al. 1999). However, to date it must be emphasized that there is no direct and definitive evidence that these organisms can cause the lesions of atherosclerosis. However, we are unable to completely rule out the possibility that in some patients, in combination with other factors, infective organisms may play a role in atherogenesis.

1. 3. 7. Calcification

During the progression of atherosclerotic lesions the accumulation of calcium is often noted. There still exists debate about the clinical significance of this substance within an atherosclerotic lesion, especially in light of the publication of recent studies relating non-invasive estimations of coronary artery calcification with clinical outcomes (Arad et al. 1996; Secci et al. 1997). However, active cellular processes appear to regulate its accumulation. Smooth muscle cells may express osteopontin (Giachelli et al. 1995), and the expression of other factors may act on the vessel wall to promote the mineralisation of atheroma. Degradative processes appear to be important also, and macrophages within the atherosclerotic plaque may serve an osteoclastic function in calcified lesions. It appears that coronary calcification is a complex, regulated process, similar to bone formation, that is related to, yet distinct from, atherosclerosis (Doherty et al. 1999).

1. 3. 8. Thrombotic Factors

Both platelet and thrombin rich thrombi are intimately linked to the initiation and perpetuation of atherosclerotic lesions. The pro-coagulant nature of dysfunctional endothelium has been described above, and this can lead to the deposition of platelet and thrombin rich microthrombi. Platelet derived growth factors (such as PDGF) and thrombin itself leads to the migration and proliferation of smooth muscle cells and macrophages (Bombeli et al. 1998).

There is evidence from angiographic and pathological studies that not all growth of atherosclerotic lesions abides by the above-described linear, predictable laws. A rapid, faster process has been noted by serial angiographic studies where the

presence of a mild or moderately stenotic plaque (<50%) was the most frequent cause of acute ischaemic events (Ambrose et al. 1988; Little et al. 1988; Nobuyoshi et al. 1991; Giroud et al. 1992). It was further noted that even in the absence of clinical symptoms, some minor lesions had rapidly progressed in size over a short period in time. Post-mortem studies of patients dying from ischaemic events have elucidated the cause of both the above to be intimately related to plaque associated thrombosis (Davies et al. 1985; Falk 1992; Falk et al. 1995; Davies 1996; Mann et al. 1996; Felton et al. 1997). The atherosclerotic lesions that appeared susceptible or prone to such thrombotic phenomenon were noted to have common identifiable characteristics. These so-called "vulnerable" plaques are more prone to plaque disruption and subsequent thrombus formation. They are histologically characterised by the presence of an eccentric plaque, containing a soft lipid-rich core that is separated from the arterial lumen by a thin fibrous cap (Davies et al. 1985; Falk et al. 1995; Mann et al. 1996). The lipid core of such vulnerable plaques contains activated macrophages and T-cells, especially concentrated at the shoulder areas of an eccentric plaque; the very site where the fibrous cap is most likely to rupture and expose the very thrombogenic lipid core to the flowing blood (Falk et al. 1995; Ross 1999). Thus the inflammatory cells within the plaque are important factors in not only atherosclerosis progression, but also plaque disruption.

1. 3. 9. Miscellaneous

For completeness we need to briefly mention two concepts that have not arisen in the above discussions.

Firstly, the role of vasospasm in atherogenesis needs to be addressed. Certainly many of the pro-atherogenic and pro-thrombotic factors linked to the pathogenesis of

atherosclerosis (including thromboxane A2, endothelin 1 and angiotensin II) have vasoconstrictor properties. Moreover, many of the atheroprotective factors (including NO and PGI2) have vasodilator properties, and thus in their absence there is a further propensity to vasoconstriction. The intrinsic importance of vasoconstriction in atherogenesis remains unclear and many believe that it may simply represent an epiphenomenon of the processes of atherogenesis.

Secondly, the concept of vascular remodelling and its association with atherosclerosis needs to be considered. It is a well described phenomenon that as atherosclerotic lesions grow in size, there may be an initial outward remodelling (dilatation) of the vessel wall such there the end result is that there is no absolute change in the luminal area (Glagov et al. 1987). Thus, imaging modalities that rely on opacification of the arterial lumen for atherosclerotic detection (coronary angiography) will significantly underestimate the atherosclerotic burden of a given artery. However, the degree to which this remodelling occurs varies widely, even between different segments of the same atherosclerotic artery (Davies 1998). The concept of remodelling has implications for atherosclerotic detection and disease presentation, as high-grade stenoses (leading to symptoms of angina pectoris) are associated with a failure of this positive remodelling. However, remodelling does not appear to have a role in the pathogenesis of atherosclerosis, just in its manifestations.

1. 4. PLAQUE DISRUPTION AND THROMBOSIS

We have discussed some of the features that of an atherosclerotic plaque that predispose to complications of thrombosis leading to one of two broad events. One, non-occlusive luminal thrombosis leading to silent, rapid plaque growth, or two, occlusive (transiently or permanently) luminal thrombosis associated with unstable

angina pectoris, acute myocardial infarction or sudden cardiac death). Plaques containing a large atheromatous core are more prone to disruption, and indeed three-quarters of such plaques are responsible for the atherothrombotic complications leading to the acute coronary syndromes (Falk 1983; Richardson et al. 1989; Frink 1994; van der Wal et al. 1994). Most of the other cases are associated with plaque thrombosis atop a macrophage rich intimal erosion in a more fibrotic plaque, often in association with a severe arterial stenosis (Falk 1983; Richardson et al. 1989; van der Wal et al. 1994). However, it is worth to explore these concepts more thoroughly, including factors for both plaque disruption and subsequent thrombosis.

Plaque disruption is a central feature of atherothrombotic syndromes, and the risk that this will occur relates to intrinsic properties of the plaque (its vulnerability) and extrinsic factors (triggers).

1. 4. 1. Intrinsic Factors

Atherosclerotic plaque disruption tends to occur at those sites where the fibrous cap is thinnest and most heavily infiltrated with macrophage derived foam cells (i.e. its weakest point). This tends to be at the shoulder region of eccentric lesions (Richardson et al. 1989) (the juncture between the normal vessel wall and the atherosclerotic plaque). Factors that have been shown to be associated with risk of rupture of the fibrous cap are the following;

1. Size of the atheromatous core
2. Thickness, collagen content and smooth muscle cell content of the fibrous cap.
3. Inflammation within the fibrous cap.
4. Cap fatigue

It is true that the composition of most atherosclerotic lesions is mainly fibrotic however a significant atheromatous core does exists in the majority of so-called culprit lesions for acute coronary syndromes as we described earlier (Falk 1989). A number of studies have been performed confirming the association between size of the atheromatous core and risk for subsequent plaque rupture. One study found that in aortic plaque, an atheromatous core of > 40% of the plaque content was at a particularly high risk of disruption and subsequent thrombosis (Davies et al. 1993). This concept helps to explain the postulated mechanism by which lipid lowering is felt to reduce clinical events. Based on numerous animals studies, lipid-lowering therapy is believed to decrease the lipid content of the plaque (i.e. decrease the size of the lipid-rich core) resulting in a more fibrotic and stable plaque (Wagner et al. 1980; Small 1988; Loree et al. 1994).

Fibrous caps vary widely in their thickness and composition, however there is a tendency for them to be thinnest at the previously described shoulder regions of the plaques (Richardson et al. 1989). Collagen (in particular type 1 collagen) is a critical determinant of fibrous cap strength and in disrupted aortic plaques, smooth muscle cells (the source of collagen in the cap) and the collagen content itself is decreased (Davies et al. 1993; Majno et al. 1995). One mechanism postulated for the reduction of smooth muscle cells in the fibrous cap is apoptosis (Majno et al. 1995), although it is uncertain if this is the only mechanism responsible.

Evidence of active inflammation (with immunohistochemical stainings of pathological samples) within the fibrous cap at sites of disruption is strong, and studies have shown macrophage infiltration at the disrupted shoulder regions of fibrous caps (Constantinides 1966; Friedman 1971; Falk 1983). An important

mechanism appears to be the production of matrix degrading enzymes including the previously discussed MMPs, which played an important role in atherogenesis also. Activated macrophages within the fibrous cap produce a variety of MMPs and in vitro studies have confirmed the ability of these enzymes to degrade fibrous caps (Shah et al. 1995). Although many of this group of enzymes have been implicated, only gelatinase B (MMP-9) has been associated with rupture prone areas in human atherectomy specimens (Brown et al. 1995). T-cells are present in increased numbers at these rupture prone sites also, and are able to stimulate macrophages to produce MMP-9 (Malik et al. 1996).

Continuous, repetitive stress on the fibrous cap may weaken it and ultimately lead to a sudden fracture in it, a concept called cap fatigue (MacIsaac et al. 1993). By lowering the frequency (heart rate) and magnitude (flow- and pressure-related) of the loading conditions, a reduction in risk of plaque disruption should ensue (Fitzgerald 1987). This is one of the mechanisms by which β-blockers may help to reduce the risk of acute coronary syndromes.

1. 4. 2. Extrinsic Factors

Atherosclerotic lesions within the coronary arterial system are subject to a number of mechanical and haemodynamic forces that may trigger disruption of atherosclerotic plaques (MacIsaac et al. 1993; Lee et al. 1994). Various forces act on the vessel wall throughout the cardiac cycle and it is worthwhile reviewing these briefly.

Cap tension refers to the circumferential wall tension that is exerted on the vessel due to the blood pressure. This force is governed by Laplace's law, which simply implies that the higher the blood pressure and the larger the luminal diameter, the more

tension that develops in the wall (Lee et al. 1994). The soft atheromatous core is unable to bear these forces well and the tension is redistributed to adjacent structures such as the fibrous cap (Richardson et al. 1989). Thus we can appreciate that mild-moderately stenotic lesions will be subject to greater circumferential stresses under Laplace's law than would severely stenotic lesions, and thus at greater risk of rupture. Further forces that the coronary artery wall and thus atherosclerotic lesions are subject to include longitudinal flexion and circumferential bending associated with the motion of the heart and the propagating pulse wave of systole. It appears that part of the mechanism by which β-blockers exert their favorable effect on reducing re-infarction is by attenuating these forces. It is finally worth mentioning that vasospasm or plaque haemorrhage could potentially enhance plaque rupture by compressing the atheromatous core and causing a "blow out" of the plaque into the vessel lumen (Friedman 1971; Lin et al. 1988). However, it is there is little data to confirm the significance of this mechanism in plaque rupture.

Studies of the relative thrombogenicity of the various components of atherosclerotic plaques has demonstrated that lipid-rich plaques are up to 6 times more thrombogenic than all other components (Fernandez-Ortiz et al. 1994). The exact mechanisms for the thrombogenicity of the lipid core are uncertain. However, it has been shown that lipid cores have a high tissue factor content (Toschi et al. 1997), and this may account for some or most of the thrombogenicity. The origin of this tissue factor appears to be from macrophage derived foam calls (Wilcox et al. 1989; Thiruvikraman et al. 1996). Studies with directional atherectomy specimens from patients with unstable coronary syndromes showed a higher population of macrophage rich areas than specimens from stable angina patients. Moreover, there was a significant correlation between these macrophage rich areas and tissue factor positive staining in the atherectomy samples from the patients with unstable coronary

syndromes (Moreno et al. 1994; Annex et al. 1995; Moreno et al. 1996). Despite this evidence, tissue factor in the lipid core may potentially be derived from other sources also (smooth muscle cells, endothelial cells etc.).

1. 4. 3. Systemic Thrombogenicity

There is substantial experimental and clinical evidence that a primary hypercoagulable or thrombogenic state may exist in the circulation that promotes focal thrombus formation. This is of particular importance when considering the risk of complicating thrombosis after plaque rupture and confirms that factors beyond the atherosclerotic plaque are of great importance in predicting thrombotic risk. Systemic factors, including alterations in lipid and hormonal metabolism, haemostasis, fibrinolysis, and platelet and leukocyte function, are known to be associated with increased blood reactivity and thrombogenicity.

Increased plasma levels of catecholamines may favor platelet reactivity. Platelet aggregation and the generation of thrombin has been documented experimentally by circulating catecholamines (Rowsell et al. 1966; Goto et al. 1996; Spalding et al. 1998), and it seems probable that this association helps to explain the link between emotional stress (Krantz et al. 1996) and circadian variation (i.e. early morning clustering of events) (Muller et al. 1985; Willich et al. 1989; Johnstone et al. 1996) with myocardial infarction. There has been increasing evidence of enhanced platelet reactivity in cigarette smokers (Fuster et al. 1981; Winniford et al. 1986; Blann et al. 1998), that may or may not be related to catecholamine levels (Powell 1998). The enhanced thrombogenicity of smoking is further confirmed by the finding that there is a sharp decline in acute vascular events most often associated with thrombosis when smoking is ceased (Buhler et al. 1988; Paul 1989).

Hypercholesterolaemia has been linked with hypercoagulability (Hunt 1990; Thompson et al. 1995) and enhanced platelet reactivity (Carvalho et al. 1974; Badimon et al. 1991; Henry et al. 1995) in numerous studies. Certainly young patients with a strong family history of coronary artery disease seem to have increased platelet reactivity. Importantly, this hypercoagulable state associated with hypercholesterolaemia is reduced with the normalisation of lipid levels with lipid-lowering therapy (Lacoste et al. 1995).

Homocysteine has also been shown to be associated with arterial thrombosis as well as atherosclerosis. It increases tissue factor activity of the endothelial cells [possibly in conjunction with lipoprotein (a)], it inhibits the expression of endothelial cell surface thrombomodulin (the substance central to the activation of protein C), and it inhibits the binding activity of antithrombin III to the endothelial heparan sulphate. Thus, homocysteine, through these various mechanisms, acts to reduce the natural anticoagulant properties of the normal endothelium (Boers et al. 1985; Boers 1997; de Jong et al. 1998; Prasad 1999).

Lipoprotein (a) has been documented as an independent risk factor for coronary artery disease (Dahlen et al. 1986; Seed et al. 1990; Djurovic et al. 1997; Hopkins et al. 1998). Apolipoprotein (a), the major apoprotein found in lipoprotein (a), has close structural homology with plasminogen (McLean et al. 1987). There is evidence that high levels of lipoprotein (a) result in competitive inhibition of the fibrinolytic activity of plasminogen (Scanu 1998). Thus the haemostatic balance is tilted in favor of thrombosis, predisposing patients to thrombotic complications. Both lipoprotein (a) and LDL compete with plasminogen binding to extracellular matrix. However, since endothelial damage with a subsequent proliferative response has been observed

experimentally (Allen et al. 1998), this metabolic condition appears more important in atherogenesis than thrombogenesis.

Thus it seems clear that defects within the fibrinolytic pathways lead to an increased thrombogenic risk in patients with coronary artery disease (Olofsson et al. 1989; Geppert et al. 1998; Vaughan 1998). A correlation between high levels of plasminogen activator inhibitor-1 (PAI-1), tissue-type plasminogen activator (tPA) and cross-linked fibrin with the progression of atherosclerotic disease has been documented (Salomaa et al. 1995). Furthermore, it has been shown that in patients with angina pectoris, plasma levels of fibrinogen, von Willebrand factor (vWF) and tPA are independent predictors of subsequent myocardial infarction or sudden death (Thompson et al. 1995). In patients with some types of dyslipidaemia, high levels of PAI-1 correlated with the cholesterol levels. Whilst this suggests a potential mechanism by which hypercholesterolaemia is associated with increased thrombogenicity, the association between PAI-1 and coronary artery disease and acute myocardial infarction is unclear, with conflicting reports in the literature (Hamsten et al. 1985; Thompson et al. 1995).

Other haemostatic proteins have also been investigated regarding their role as thrombogenic risk factors. Several prospective studies have indicated that high plasma fibrinogen concentrations are independent risk factors for coronary artery disease and myocardial infarction (Meade 1997). The mechanism by which fibrinogen contributes to atherogenesis is not well understood. Hypotheses include increased fibrin formation, increased viscosity, platelet aggregation and stimulation of smooth muscle cell proliferation. It is, however, also important to recall that high plasma fibrinogen levels are correlated with age, degree of obesity, hyperlipidaemia,

diabetes, smoking, and emotional stress; all conditions that are themselves associated with atherosclerosis.

Platelet aggregation and coagulation are increased in diabetes mellitus. Platelets from diabetic patients have shown enhanced adhesiveness and hyperaggregability in response to a wide range of agonists (Winocour 1992; Aronson et al. 1997). Elevated thromboxane A2 synthesis occurs in diabetic patients, facilitating platelet aggregation and thrombus formation (Davi et al. 1990). The primary reason for altered platelet behavior in diabetes is not well understood, but there is evidence that the derangement may start with the megakaryocyte. Other abnormalities in the coagulation system of diabetic patients that could also be implicated in platelet reactivity include increased fibrinogen and vWF levels and decreased antithrombin III activity in response to hyperglycaemia. In addition, a typical feature of insulin resistance and hyperinsulinaemia is an increased PAI-1 activity resulting in reduced plasma fibrinolytic activity (McGill et al. 1994).

Diabetes is also associated with a severely dysfunctional endothelium. Impaired endothelium dependent relaxation is the best characterised of these abnormalities, and can be induced by short exposure to high glucose concentrations. Diabetes may impair endothelium dependent relaxation by an increased generation of advanced glycosylation end products and increased oxygen free radicals in the arterial wall (Chappey et al. 1997). The loss of endothelium derived relaxing factor (NO) has a profound effect on arterial vasomotion and leads to vasospasm and increased platelet aggregation by increasing the local shear rate. Furthermore, diabetes seems to reduce the prostacyclin production by the endothelial cells, possibly resulting in higher levels of platelet activation and endothelial adhesion. High glucose levels have also

been shown to impair endothelial regeneration (Winocour 1992; Aronson et al. 1997).

1. 5. CLINICAL MANIFESTATIONS OF ATHEROTHROMBOSIS

The significance of acute thrombosis complicating a disrupted atherosclerotic plaque was postulated over 40 years. The statement by Jens Dedichen, a Norwegian physician, in 1956 that "man lives with arteriosclerosis and dies of the complicating thrombosis" (Dedichen 1956) shows incredible insight into a process that was not generally accepted until as late as 20 years ago.

The clinical manifestations of atherosclerotic plaques depend on several factors, including the following;

1. Degree and abruptness of blood flow obstruction.
2. Duration of decreased myocardial perfusion.
3. Myocardial oxygen demand at the time of the blood flow obstruction.
4. Extent of the thrombotic response to plaque disruption.

Plaque rupture is generally accompanied by haemorrhage into the plaque and with a variable amount of luminal thrombosis. If the thrombus is small, plaque rupture probably proceeds unnoticed. If the thrombus is large enough to compromise blood flow through the coronary artery, however, the individual may experience an acute ischaemic syndrome.

Disruption of an atherosclerotic plaque in the coronary arteries, whether ruptured or fissured, plays a fundamental role in the development of the acute coronary

syndromes (including unstable angina pectoris, acute myocardial infarction or sudden cardiac death) (Fuster et al. 1992; Fuster et al. 1992; Falk et al. 1995; Ross 1999). Coronary thrombosis almost exclusively occurs in the setting of underlying atherosclerosis, with disruption of the underlying plaque triggering thrombosis (Theroux et al. 1998). Angioscopic studies have documented the presence of intraluminal thrombi both in unstable angina (Sherman et al. 1986; Mizuno et al. 1992; de Feyter et al. 1995; Silva et al. 1995; Nesto et al. 1998) and acute myocardial infarction (Mizuno et al. 1992; Van Belle et al. 1998). The incidence of thrombi in unstable angina varied significantly among different studies largely related to the time interval between anginal symptoms and the angiographic study (Sherman et al. 1986; Uchida et al. 1987; Rehr et al. 1989; Uchida et al. 1995). The shorter the interval between the two, generally the higher the likelihood of finding occlusive thrombi.

It is likely that when injury to the vessel wall is mild, the thrombogenic stimulus is relatively limited and the resulting thrombotic occlusion transient as occurs in unstable angina (Fuster et al. 1992; Fuster et al. 1992). On the other hand, deep vessel injury as is seen with plaque rupture results in the exposure of collagen, lipids and other intravascular components, leading to more persistent thrombotic occlusion and acute myocardial infarction (Theroux et al. 1998).

Plaque fissuring or rupture with subsequent thrombosis accounts for many of the episodes of unstable angina or acute myocardial infarction. However, it is important to consider other mechanisms in the aetiology of acute coronary syndromes. Coronary vasospasm may play an important role in the pathogenesis of acute coronary syndromes, as documented through electrocardiographic and angiographic studies (Maseri et al. 1978). In the setting of a minor plaque disruption with a small

thrombotic response, there can still be the release of vasoactive substances by both the platelet and the arterial wall, leading to further compromise of coronary blood flow (Willerson et al. 1989). Coronary artery vasospasm was found to be an important contributor to the phenomenon of intermittent coronary artery occlusion in patients with acute myocardial infarction (Gasser et al. 1986).

In patients with stable coronary artery disease, symptoms often result from increases in myocardial oxygen demand beyond the availability of stenotic coronary arteries to increase its delivery. Unstable angina, non-Q-wave and Q-wave myocardial infarction represent a continuum of the same disease process and, in contrast to the setting of stable angina, are usually characterised by an abrupt reduction in coronary artery blood flow (Theroux et al. 1998). In the case of unstable angina, the thrombotic vessel occlusion tends to be transient and episodic, leading to anginal symptoms at rest. In addition to plaque disruption, other mechanisms may contribute to the reduction in coronary flow. As mentioned earlier, platelets that have attached to the disrupted plaque release vasoactive substances including thromboxane A2 and serotonin, promoting the aggregation of further platelets to the area and inducing vasoconstriction (Willerson et al. 1989). Alterations in perfusion probably account for 60-70% of cases of unstable angina. The remainder appears to be mainly due to transient increases in myocardial oxygen demand (Braunwald et al. 1994).

In non-Q-wave myocardial infarction, the angiographic morphology of the responsible lesion is similar to that seen in unstable angina, confirming that plaque disruption is common to both syndromes. However, about 25% of patients with non-Q-wave myocardial infarction have a totally occluded infarct related artery at early angiography, with the distal myocardium supplied by collateral vessels (Theroux et al. 1998). The presence of ST-segment elevation in the electrocardiogram, early peak

in the plasma creatine kinase and high angiographic patency rate of the infarct related artery all suggest that complete coronary occlusion followed by early reperfusion (< 2 hours) due to resolution (partial or total) of the thrombus and/or of the vasospasm is important in the pathogenesis of most non-Q-wave myocardial infarctions. Thus, by limiting the duration of myocardial ischaemia, spontaneous thrombus lysis, vasospasm resolution or a well-developed collateral circulation can prevent the formation of Q-wave myocardial infarction (Theroux et al. 1998).

Deep arterial injury or ulceration results in the formation of a fixed and persistent thrombus leading to the abrupt cessation of myocardial perfusion and necrosis of Q-wave myocardial infarction (Fuster et al. 1992; Fuster et al. 1992). The coronary artery lesion responsible for the infarction is frequently only mild to moderately stenotic, suggesting that plaque rupture with subsequent thrombosis is the primary source of the occlusion rather than the severity of the underlying lesion (Falk et al. 1995). Although an individual severe stenosis has been shown to occlude more frequently than less severe stenoses, the lesser stenoses account for more coronary artery occlusions due to their much greater number (Alderman et al. 1993). Furthermore, the less severe stenoses are much less likely to be associated with a protective collateral circulation, and thus occlusion is more likely to lead to an acute clinical event (Danchin 1993). In approximately 25% of patients with Q-wave infarction, coronary thrombosis results from superficial intimal injury in association with a high-grade stenosis (Fuster et al. 1992; Fuster et al. 1992).

The acute onset of malignant ventricular dysrhythmias (ventricular tachycardia and ventricular fibrillation) appear to account for the syndrome of sudden cardiac death (Mehta et al. 1997). However, two distinct mechanisms play a role in the pathogenesis of these dysrhythmias. First, in patients with a substrate for the

generation and maintenance of malignant ventricular dysrhythmias (such as extensive myocardial infarction or cardiomyopathy), a fatal episode of such dysrhythmias can lead to sudden cardiac death (Mehta et al. 1997). Second, a rapidly progressive coronary artery lesion in which plaque rupture and subsequent thrombosis leads to acute myocardial hypoperfusion in the absence of collateral flow may also induce malignant ventricular dysrhythmias and sudden cardiac death (Mehta et al. 1997).

1. 6. ATHEROSCLEROTIC PLAQUE IMAGING

What is clear from the review of the pathogenic mechanisms behind atherosclerosis and the acute coronary syndromes, is that we are currently extremely limited in our ability to accurately identify patients at risk for an acute coronary event. The armamentarium of diagnostic investigations, both non-invasive and invasive, currently clinically available is only able to provide us with data related to the stenotic severity of a coronary artery. The non-invasive testing includes stress–induced (exercise or pharmacologic) ischaemic changes in electrical repolarisation, wall motion or myocardial radioactive-tracer uptake. The invasive test of coronary angiography, although the current gold standard for the detection of coronary atherosclerotic disease, provides us with no data about the composition of the atherosclerotic lesion (Fuster et al. 1995; Topol et al. 1995). However, the vast majority of acute coronary events involve a non-critically stenosed atherosclerotic lesion (Falk et al. 1995), and thus with currently available means of identification, these lesions would be undetected by stress testing/imaging techniques. Thus, given the critical role that atherosclerotic lesion composition has been shown to play in the risk of both plaque rupture and subsequent thrombogenicity, and thus consequently an acute coronary event, new detection techniques need to be investigated for the task of documenting atherosclerotic lesion composition (Fuster 1998).

The imaging of such vulnerable plaques would need to provide information about composition as well as degree of encroachment on the vessel lumen by the atherosclerotic plaque. The ideal imaging modality would need to be safe, noninvasive, accurate and reproducible, thus allowing longitudinal studies in the same patient (Celermajer 1998). There are currently several imaging modalities

under investigation for this purpose, and it is worth to explore the strengths and limitations of each of them.

1. 6. 1. Ultrasonography

Intravascular ultrasound (IVUS) examination utilises a miniaturised ultrasound transducer placed on the distal end of a flexible catheter. By advancing this structure through a coronary catheter and into a coronary artery, cross-sectional images of the vessel wall and atherosclerotic plaque have been obtained for the study of atherosclerosis and percutaneous coronary interventions. Thus, it is by definition an invasive technique, limiting its potential future use for screening or in minimally symptomatic patients. This technique has provided substantial information about the role of remodelling in early atherosclerotic plaque growth (Hermiller et al. 1993), and lesions of up to 40% stenosis of the vessel can be accommodated by this process, leading to no discernible loss of lumen area (Glagov et al. 1987). These lesions are not detectable by coronary angiographic techniques, however, are still potentially able to rupture and thrombose and thus lead to acute coronary syndromes (Falk et al. 1995). For the purpose of atherosclerotic lesion characterisation, numerous studies have been performed with high-frequency (20-30MHz) probes both ex vivo and in vivo in order to validate the technique (Nishimura et al. 1990; Keren et al. 1991; Linker et al. 1991; Tobis et al. 1991). In general, ultrasonic tissue character is determined by the amount and reflectivity of small macromolecules, such as collagen, that scatter the ultrasound beam, some of which is back toward the transducer, and thus is detected (Kimura et al. 1995). "Hard" plaques are highly reflective and thus produce bright echoes (Kimura et al. 1995). They are composed mainly of fibrous tissue and calcium (Kimura et al. 1995). "Soft" plaques are more

echolucent and may represent lipid, thrombus or loose connective tissue (figure 1. 4) (Gussenhoven et al. 1989; Hodgson et al. 1993).

Figure 1. 4

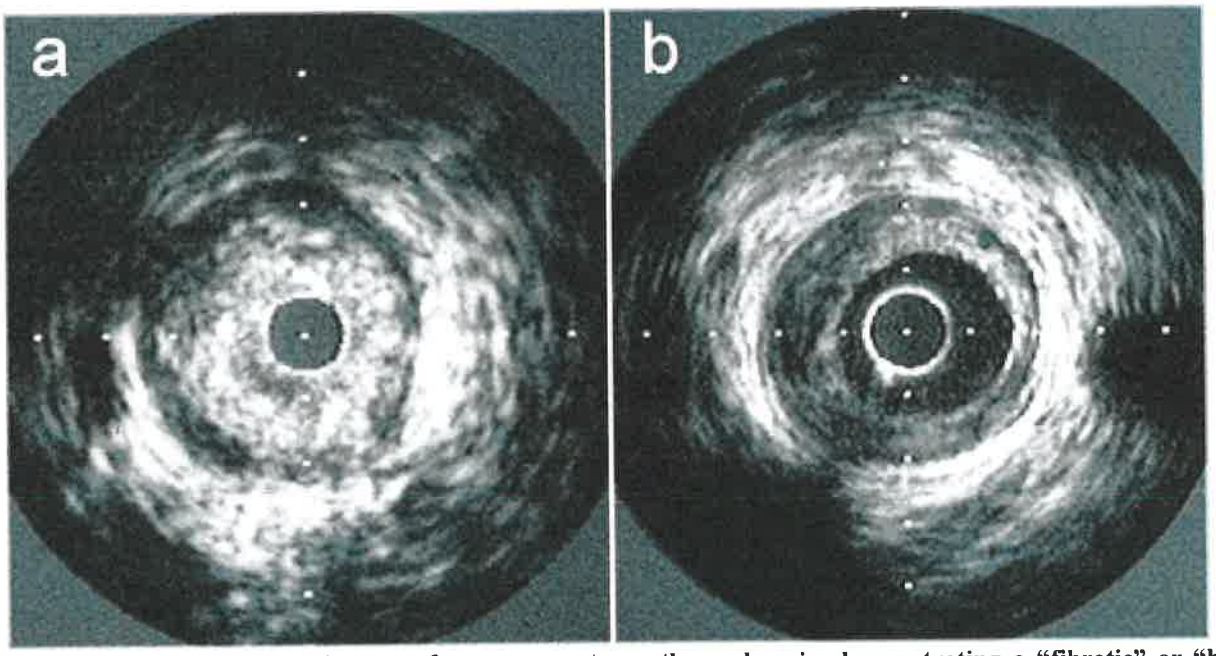

Intravascular ultrasound images of coronary artery atherosclerosis, demonstrating a "fibrotic" or "hard" echogenic lesion (a) and "lipid rich" or "soft" echolucent lesion (b).

Calcification is easily identified by ultrasound imaging because of its high echogenicity (Gussenhoven et al. 1989). Despite this ease of identification on intravascular images, proof that a bright signal with shadowing on IVUS specifically represents calcium is mostly inferred (Kimura et al. 1995). A post-mortem histological validation study in coronary arteries revealed sensitivities of only 89% for dense calcification and 64% for micro-calcifications (Friedrich et al. 1994). Further limitations are that dense fibrous tissue bordering zones of calcification may appear indistinguishable from calcium using imaging criteria (Kimura et al. 1995). Furthermore, IVUS is unable to quantify the total amount of vessel calcification as deeper structures (which may or may not be calcified) are hidden in the shadow of the superficial calcified region (Kimura et al. 1995).

The differentiation of "hard" from "soft" plaques relies on the analysis of echo reflectance (brightness) of the tissues (Kimura et al. 1995). Despite efforts to standardise this analysis (Hodgson et al. 1993), it is often a subjective measure that is further dependent on the transmit gain, attenuation by intervening tissues and the time-gain compensation settings (Kimura et al. 1995). Thus, analysis of plaque brightness for the discrimination of fibrous tissue content is difficult to quantify because of its dependence on gain.

Echolucent plaques with IVUS imaging, initially thought solely due to "lipid lakes", may also represent areas of intraplaque and/or luminal thrombosis (Kimura et al. 1995). Despite the use of higher frequency IVUS probes, it remains difficult to differentiate acute thrombus from surrounding soft plaque on IVUS images (Kimura et al. 1995); a differentiation that may have significant implications for the evaluation and treatment of the patient.

Thus, although IVUS has the potential to discriminate some of the components of the atherosclerotic plaque, especially calcification, the differentiation of thrombus, soft plaque and hard plaque can be problematic (Kimura et al. 1995). Furthermore, it is an invasive procedure, and therefore intrinsically limited in its use.

It is worth mentioning that transthoracic (Ross et al. 1990; Caiati et al. 1999; Caiati et al. 1999) and transoesophageal (Taams et al. 1988; Yoshida et al. 1990; Redberg et al. 1995) echocardiography have been reported to visualise the proximal coronary arteries, and thus potentially provide data about the vessel wall without the invasive aspects of IVUS. However, the intrinsic limitations of ultrasonographic discrimination of plaque components discussed above are still factors with these modalities.

1. 6. 2. Ultrafast Electron Beam Computerised Tomography

This imaging modality has been prominent in the literature recently, and although associated with the exposure of the patient to some, relatively minimal radiation (generally <600mrad per scan) (Detrano et al. 1999), it is a non-invasive procedure, and thus potentially able to be utilised for the purpose of risk stratification in an asymptomatic or minimally symptomatic population.

Ultrafast electron beam computerised tomography (ultrafast EBCT) requires a specific CT scanning machine, and is not a modification of currently available CT machines. Ultrafast EBCT machines are relatively specialised scanners, in that they allow the rapid acquisition of imaging data (100msec per image slice) which can be gated to the more quiescent cardiac phase of diastole. However, the image quality for these scanners for non-cardiovascular scans (i.e. brain imaging) is considered less than for the conventional CT scanners. Current research is underway validating the ability of helical CT scanners to quantify coronary artery calcium (CAC), and thus make the technique more obtainable at a clinical level. However to date, no significant data has been published using helical CT scanners, although a recent comparison between conventional CT and ultrafast EBCT assessment of CAC showed similar results.

Ultrafast EBCT has been shown able to quantify relatively accurately and reproducibly CAC using a validated scoring method (figure 1. 5) (Detrano et al. 1994; Mahaisavariya et al. 1994; Mautner et al. 1994).

Figure 1. 5

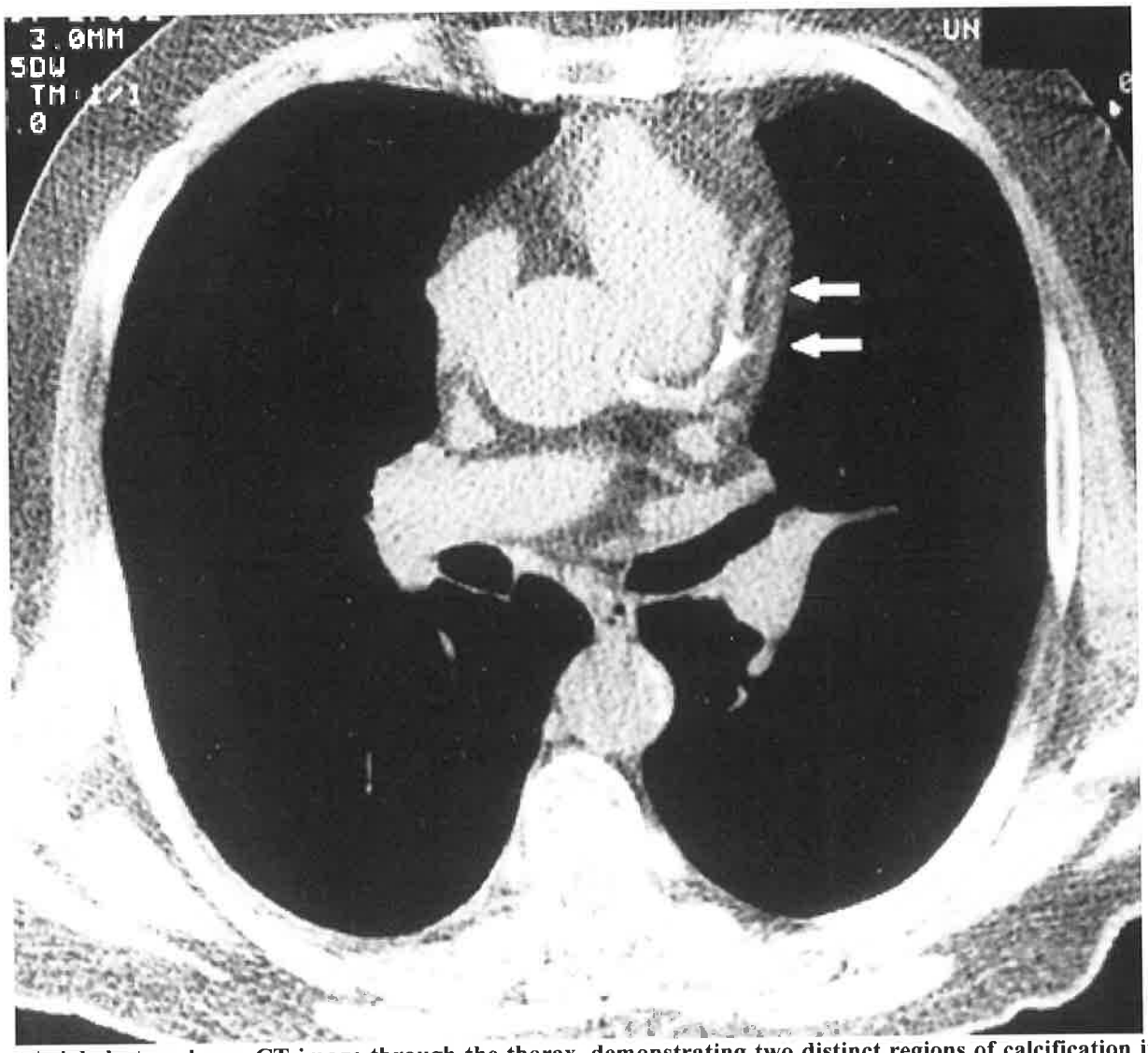

Axial electron beam CT image through the thorax, demonstrating two distinct regions of calcification in the left anterior descending artery (white arrows) which appear bright. There is a third region of calcification at the origin of the left main artery (no arrow) (image courtesy of Dr. William Stanford)

As we discussed earlier, CAC seems to be a marker of atherosclerotic burden within the coronary arterial system (Simons et al. 1992; Fallavollita et al. 1994; Mautner et al. 1994; Rumberger et al. 1994; Detrano et al. 1996; Kennedy et al. 1998) and subsequent prognosis (Arad et al. 1996; Detrano et al. 1996; Secci et al. 1997). It is equally true, however, that CAC has also been shown associated with a decreased risk of individual plaque rupture and vulnerability (Johnson et al. 1985; Kragel et al. 1989). There is extensive data from animal atherosclerotic models that atherosclerotic regression is associated with more calcium than atherosclerotic progression (St Clair 1983; Strong et al. 1994). Paradoxically, a recent study

suggested that CAC scores increased in a patient population after treatment with lipid-lowering therapy and therefore theoretically inducing atherosclerotic regression (Callister et al. 1998). Racial variances have also been noted regarding the correlation between CAC and coronary atherosclerosis (Tang et al. 1995; Doherty et al. 1997). In particular, African-American subjects had a significantly lower prevalence of coronary calcific deposits when compared with Caucasian or Asian Americans, even after controlling for risk factors (Tang et al. 1995; Doherty et al. 1997). Thus, the overall role of calcium in deposits in atherosclerotic lesions remains somewhat unclear.

Certainly, the conclusion from recent studies is that in symptomatic patients, ultrafast EBCT appears to be moderately useful in predicting the severity of coronary artery disease (Doherty et al. 1999). Furthermore, prognostic data is available from these studies. In one study using cinefluoroscopy, the 5-year survival rate of patients with CAC was 58% compared with 87% in patients without CAC (Margolis et al. 1980). The results for ultrafast EBCT assessment of CAC and prognosis appear similar to this (Doherty et al. 1999). Thus, a significant correlation between CAC as quantified by ultrafast EBCT and the occurrence of subsequent coronary events exists. However, another study, in asymptomatic patients showed that ultrafast EBCT, although able to predict risk of future coronary events, was in fact no better than standard risk factor assessment (Detrano et al. 1999). Other studies in asymptomatic patients have shown that >45% of patients with death or myocardial infarction had a CAC score of <152 Hounsfield units (HU) considered to represent a low CAC score (Detrano et al. 1999). Thus, it seems that a negative calcium score does not rule out the presence of atherosclerosis and more importantly, a vulnerable atherosclerotic lesion may exist in the absence of calcium in the coronary arteries (Wexler et al. 1996).

It is clear that estimating only one component of the atherosclerotic lesion, namely the calcium content, which appears to provide limited information anyway, is inadequate in assessing risk of plaque vulnerability at a given site. Ultrafast EBCT is unable to provide any data about any of the other plaque components (i.e. lipid-core, fibrous cap, and thrombus).

It is worth mentioning that ultrafast EBCT has been studied for use in coronary angiography. A recent study showed excellent correlation with coronary angiography obtained by EBCT when compared with traditional coronary angiography (Achenbach et al. 1998). However, images of all three coronary arteries could be obtained in only 63% of patients, due to inadequate image quality (Achenbach et al. 1998). Thus above and beyond the intrinsic limitations of coronary angiography techniques, this non-invasive imaging modality has a long way to go before being potentially clinically relevant as an alternative to traditional coronary angiography.

1. 6. 3. Coronary Angioscopy

The angioscopy technique reveals the characteristics of the vessel and atherosclerotic plaque surface, information not provided by conventional coronary angiography (den Heijer et al. 1994; Uchida et al. 1995). The colour of the material in the artery (red, white and yellow) can provide information about the predominant contents of the lesion (thrombotic, lipidic and fibrotic respectively), however, this technique does not provide accurate information about the internal heterogeneity of the lesion. Recent clinical trials have shown that yellow plaque colour was closely related to degenerated plaques or atheroma and was associated with acute coronary syndromes (Thieme et al. 1996) and that angioscopic identification of plaque rupture and

thrombus were independently associated with adverse outcome in patients with complex lesions after interventional procedures (Feld et al. 1996). This technique, due to its intrinsically invasive nature, and the limitations with the data it can provide about the atherosclerotic lesion, remains a research tool.

1. 6. 4. Nuclear Imaging of Atherosclerosis

Nuclear imaging techniques have been extensively researched and are frequently used in clinical practice for the investigation of patients with proven or suspected coronary artery disease. However, the data provided depends on perfusion limitations and or myocardial injury and no information is provided about the atherosclerotic lesion per se. As such the role of nuclear imaging is limited in assisting with the characterisation of atherosclerotic lesions, however, it is worth briefly mentioning some recent research in this field.

Given the role of LDL in atherosclerotic development and progression, investigators have studied the uptake and distribution of radiolabelled LDL in both animal models (Vallabhajosula et al. 1988; Rosen et al. 1990; Sinzinger et al. 1990) and humans (Lees et al. 1983; Lees et al. 1988; Ginsberg et al. 1990; Vallabhajosula et al. 1990; Virgolini et al. 1991; Pirich et al. 1995) with atherosclerotic disease. Not only did it localise to the atherosclerotic regions, but was correlated with the macrophage content of the lesions (Lees et al. 1988; Virgolini et al. 1991). However, limitations with the resolution, relatively low uptake and high blood-pool activity have hindered the utility of this technique (Vallabhajosula et al. 1997).

More promising has been the radiolabelling of platelets with indium 111 or technetium-99m, for the detection of thrombus (Vallabhajosula et al. 1997). The role

of thrombosis and platelets in the pathogenesis of atherosclerosis and especially in the acute coronary syndromes has been described earlier. Thus, the potential to be able to detect this complication of plaque rupture would potentially provide important prognostic information with therapeutic implications. However to date, studies of its clinical utility in carotid atherosclerosis have shown poor results in predicting risk of subsequent plaque ulceration and clinical events (Minar et al. 1989; Moriwaki et al. 1995). Furthermore, like radiolabelled LDL, high blood pool activity and inadequate radiotracer concentrations at the site of interest have limited this technique (Vallabhajosula et al. 1997).

Other substrates have also been radiolabelled in order to image atherosclerotic lesions (endothelin derivatives (Dinkelborg et al. 1998) and several immunoglobulins to plaque components including macrophages (Sinzinger et al. 1996) and fibrin derivatives (Knight 1993)). The results have been of varying success, but to date, none appears any more successful than those discussed above in identifying atherosclerotic plaque components.

1. 6. 5. Positron Emission Tomography

This advanced form of nuclear imaging, positron emission tomography (PET), utilises positron emitting isotopes, such as C-11, O-15, N-13 and F-18, labeled with naturally found compounds in the body (i.e. F-18 and glucose). In conjunction with the advances in image acquisition, PET imaging has been able to quantify many physiological and metabolic processes in humans (Beanlands 1996). Its most studied cardiovascular application has been as a noninvasive means of diagnosing critical coronary artery lesions, using myocardial perfusion tracers (Go et al. 1990; Stewart et al. 1991). Furthermore, F-18 FDG PET, by quantifying myocardial metabolism,

has become the gold standard for defining viable myocardium in patients with compromised left ventricular function being considered for a revascularisation procedure (Tillisch et al. 1986; Maddahi et al. 1994).

Beyond its cardiovascular applications, F-18 FDG PET has been utilised for many years in the diagnosis and prognosis of various malignancies (Strauss et al. 1991). The avidity of the malignant tissues for the F-18 FDG tracer is felt related to the high metabolic rate of the malignant cells (Strauss et al. 1991). Interestingly, recent data studying the relative avidity of the cellular components of malignancies for the F-18 FDG tracer showed that macrophages were the cell type with the highest affinity for the tracer (Kubota et al. 1994). This was felt to be due to the enhanced rate of glucose utilisation by macrophages (Kubota et al. 1994).

We have previously examined in detail the critical role of the macrophages in plaque vulnerability, risk of rupture and subsequent thrombogenicity. Indeed, the density of macrophages, on pathological and post-mortem studies, correlates highly with plaque instability and risk for acute coronary syndromes. Thus, a non-invasive imaging technique that was able to provide quantitative information about the macrophage density within a given atherosclerotic site could potentially allow risk stratification for subsequent acute coronary events. Moreover, the potential for longitudinal studies exists whereby progression and/or regression of this risk could be monitored by quantifying changes in macrophage content of the atherosclerotic plaque. This remains an unconfirmed postulate however.

1. 6. 6. Novel Imaging Methods and Atherosclerosis

New imaging modalities are just emerging, as research tools only at this stage, but with future potential uses, and we should be aware of their potential uses.

Infrared light has been used to detect the vessel wall structures (Fujimoto et al. 1999). Optical coherence tomography was able to define the ultrastructure of the normal arterial vessel wall in rabbit aortas using infrared light with an invasive imaging catheter in a recent study (Fujimoto et al. 1999). In a different study, infrared thermal images were able to reveal heterogeneity in temperature among atherosclerotic plaques taken at carotid endarterectomy, which correlated with cell density, most of which were macrophages (Casscells et al. 1996). Of course, this data is recent and very preliminary and whether or not this technique may play a role in the future of atherosclerotic plaque characterisation remains to be seen.

1. 6. 7. Magnetic Resonance Imaging

Magnetic resonance (MR) imaging is a unique technology that allows the noninvasive visualisation of cardiovascular anatomy (Kaufman et al. 1983). Of all imaging modalities currently available in all fields, MR imaging provides the greatest intrinsic contrast between soft tissue structures. Thus, it is a powerful tool for defining pathoanatomical processes of the visceral organs, including the heart and vascular structures. Furthermore, the absence of ionising radiation the free choice of tomographic planes enhances the potential of this technique for the future. However, it does have limitations, including relatively long imaging time, relative isolation of the patient from medical care from medical care during image acquisition, and contraindication in patients with certain metallic implants (i.e. permanent

pacemakers). Imaging time and quality is rapidly improving with technological advances in the field, and the information that MR can provide in the cardiovascular field is rapidly growing. MR has the potential to provide information about cardiac anatomy, function (myocardial and valvular), perfusion and metabolism. More recently, application to the coronary arteries suggests that MR may supply information about coronary angiography, flow velocity and even the characterisation of the atherosclerotic lesions themselves within the coronary artery wall. Although we are still a long way from this "one stop shop" of cardiac imaging with MR, it is an exciting field that will surely play a significant role in cardiovascular imaging in the future.

1. 6. 7. 1. MR Basics

Current MR imaging techniques have evolved to a highly specialised degree and the understanding of the processes involved is extremely complex. However, it is worth exploring the concept of MR imaging on a simplistic level. Central to the basics of MR imaging is that a person, when placed within an external magnetic field, is able to become partially magnetised although this is orders of magnitude less than the strength of the external magnetic field. Much of this effect is associated with hydrogen ions (protons) within the body; the largest source of which is water. By subjecting the person to subsequent and different magnetic fields perpendicular to the first magnetic field, the vector of magnetisation within the person changes. A physical principle of changing magnetic fields is that they emit radiofrequency waves, and it is the collection of this information that can be translated into the MR image we finally analyze. The characteristics of these radiofrequency waves are determined by many factors, including the parameters of MR techniques but

importantly, the various tissues themselves, and this allows for the accurate differentiation between the soft tissue components of the body.

Two main imaging sequences or techniques form the basis for much of the MR imaging performed today.

Spin-echo imaging can provide excellent discrimination between various components of the heart and has flexible contrast characteristics, depending on the programmed parameters of the imaging sequence (i.e. T1 weighted – T1W, proton density weighted - PDW and T2 weighted – T2W imaging). With this technique, blood within the vascular compartment appears black (so-called "black blood imaging"). Due to the often-longer imaging times, this imaging sequence has traditionally been used for the imaging of static phenomena, including myocardial wall thickness, cardiac chamber volumes and intracardiac thrombus.

Gradient-echo imaging is especially useful for vascular lumen angiography and the flowing blood appears white (so-called "bright blood imaging"). This form of imaging sequence may be acquired rapidly allowing cine imaging of the heart and thus the assessment of myocardial function. The advent of extremely rapid image acquisition (10-15 images per second) with this technique allows for real-time imaging and with further improvements in the resolution and image quality, the potential for performing interventional vascular procedures with MR real-time imaging exists. This technique of imaging is less able to provide varying tissue contrast compared with spin-echo imaging, although images with T1 and T2 weighting can be obtained.

1. 6. 7. 2. Myocardial Imaging

Myocardial ischaemia and infarction are associated with changes in the tissue relaxation times (including T1 and T2 relaxation - concepts beyond this discussion) and this manifests as an increase in the signal intensity of these regions on T2W images (Williams et al. 1980; Higgins et al. 1983; Scholz et al. 1992). Furthermore, by using a paramagnetic contrast agent, such as gadolinium chelated with DTPA (Gd-DTPA), there has been enhancement of the signal intensity of these ischaemic regions with T1W imaging (McNamara et al. 1984; Wesbey et al. 1984; Runge et al. 1985; Peshock et al. 1986; Tscholakoff et al. 1986; Johnston et al. 1987; Nishimura et al. 1987; Matheijssen et al. 1991). These paramagnetic agents cause the relaxation times to shorten. The significance of this is that on T1W images, depending on the intrinsic characteristics of the tissue and the local concentration of the paramagnetic agent, the signal intensity will be brighter on a T1W image. Numerous studies have shown the ability of Gd-DTPA contrast enhanced MR imaging to identify changes in myocardial segments during ischaemia (McNamara et al. 1984; Runge et al. 1985; Johnston et al. 1987), infarction (Wesbey et al. 1984; Matheijssen et al. 1991) and reperfusion (Peshock et al. 1986; Tscholakoff et al. 1986) in research settings. The role of these techniques in the clinical setting, however, is yet to be established.

Visual evaluation of global and regional wall motion can be obtained by cinematic viewing of MR images throughout the cardiac cycle. This so-called cine MR imaging technique provides accurate information about bi-ventricular function, and is an accurate technique for the noninvasive assessment of right ventricular volumes and function (Pattynama et al. 1992; Pattynama et al. 1995).

The above techniques for myocardial imaging have been modified somewhat to allow for the detection of patients with significant coronary artery stenoses. Cine MR imaging, by visualising the myocardial motion and contractility, can be used to monitor wall motion abnormalities under conditions of stress such as dobutamine infusion (Pennell et al. 1992; van Rugge et al. 1993; Baer et al. 1994). Studies to date have shown high sensitivity and specificity for this technique in the diagnosis of severe coronary artery disease, at least as good as that of nuclear stress imaging(Baer et al. 1994) or dobutamine stress echo (Nagel et al. 1999). Alternatively, myocardial perfusion abnormalities can be detected in patients with chest pain (Manning et al. 1991) or under conditions of stress (i.e. dipyridamole) (Eichenberger et al. 1994) after the administration of Gd-DTPA. Lower peak signal intensity and lower rate of signal increase than the myocardial segments perfused by non-stenotic coronary arteries identified areas of regional myocardial hypoperfusion.

Recently, techniques have been described for the determination of the thickening and torsion of specific myocardial segments. This relies on the ability of MR to perform "myocardial tagging" (Zerhouni et al. 1988; Axel et al. 1989; Axel et al. 1989; Bolster et al. 1990). This in effect allows a grid to be applied to a MR image of the heart in diastole using specialised MR techniques, and these grids will distort through systole (Buchalter et al. 1990). The myocardial thickening and rotational torsion can be quantified. This method allows information about myocardial strain to be obtained and future studies about its role in clinical settings is awaited with interest (Clark et al. 1991; Beyar et al. 1993; Lima et al. 1993).

MR spectroscopy is a unique tool that allows the evaluation of cardiac metabolism by direct measurement of high-energy phosphates and the in vivo pH in animal models (Stamper et al. 1992). The potential for this technique to provide information

about metabolic changes in the myocardium in various disease states (i.e. myocardial ischaemia and infarction, cardiomyopathy etc.) is very exciting and could further our understanding of the pathogenesis of such processes. To date, however, data with this technique is restricted to research settings with limitations due to the size of the region of interest required for analysis (Bottomley 1994).

1. 6. 7. 3. Valvular Function and MR

Using the cine MR techniques described earlier, which show normal blood flowing the cardiac chambers as bright, one can detect valvular lesions by the turbulence in blood creating signal loss and thus appearing black within the otherwise bright blood signal (Sechtem et al. 1987). Using the amount of signal loss as an indicator of severity of the valvular lesion (either stenosis or regurgitation) similar to the way one might use colour doppler information on echocardiography (echo), one can semi-quantitatively assess valvular lesions (Mitchell et al. 1989). This allows for valvular regurgitation assessment with comparable accuracy to echo, however, does not provide numerical severity of the gradient across the valve in conditions of a valvular stenosis.

Recently, a technique called velocity encoded cine MR (VEC MR) imaging (also called phase contrast cine MR imaging), has allowed for the accurate quantification of the velocity of flow across cardiac valves (Kilner et al. 1991). This technique (also conceptually beyond the scope of this discussion) has been shown to be highly correlated with doppler echo estimations of velocity of flow across cardiac valves (Eichenberger et al. 1993; Kilner et al. 1993), and thus able to estimate the pressure gradient across stenotic valves, using the modified Bernoulli equation. In addition to the described estimations of flow, cardiac MR imaging provides information about

the cardiac chambers (size and function) as well as structural data about the valves themselves (although not with the resolution of echo), thereby providing additional information of importance in the assessment of valvular cardiac disease.

1. 6. 7. 4. Coronary Artery MR

The noninvasive visualisation by MR imaging of coronary arteries is an exciting area. Technical difficulties exist, related to motion (both cardiac and respiratory), the small size of the coronary arteries and their tortuous, nonlinear course (van der Wall et al. 1995). The best results have been reported using ultrafast breath-hold techniques, in conjunction with cardiac gating that allow the acquisition of one image in approximately 15-18 seconds (Edelman et al. 1991). Using the bright blood imaging sequences, in conjunction with an MR imaging technique that removes any signal from the epicardial fat (thus improving the definition of the epicardial coronary arteries) image quality of the coronary arteries is continually improving. Although MR coronary angiography has been shown to compare favorably with conventional coronary angiography for the detection of stenoses >50% (Manning et al. 1993), the resolution currently obtainable (approximately 1mm) is inadequate for routine clinical use at this stage. Recent improvements in MR coronary angiography techniques, including the use of "navigator echo" which attempts to reduce artifacts from motion by analyzing only the data obtained when the diaphragm or heart is in a small range of positions, have been reported (Botnar et al. 1999). In addition, MR angiography of coronary artery bypass grafts has been reported using these techniques (White et al. 1987; White et al. 1988; Aurigemma et al. 1989). The role of MR coronary angiography in clinical practice is unclear, although the future may show it to be of use for the screening the major epicardial coronary arteries for significant stenoses.

Using VEC MR imaging as described earlier, flow within the coronary arteries has recently been reported (Hundley et al. 1999), and potentially will allow the assessment of coronary flow noninvasively. Thus coronary lesions may not only be assessed by the percent stenosis, but a physiological analysis of the limitation to flow may be undertaken. This may be useful in not only assessing significance of coronary lesions, but also in documenting responses to percutaneous coronary interventions. This currently is still an investigational tool at this stage.

1. 6. 7. 5. Coronary Artery Plaque Characterisation

As has been extensively reviewed earlier, the ability to accurately define the components of a complex coronary atherosclerotic lesion (i.e. fibrous cap, lipid core, calcium and haemorrhage) would potentially allow the risk stratification of patients for future acute coronary syndromes. Given the excellent soft tissue contrast provided by MR imaging techniques, the ability of MR to differentiate between these plaque components has been investigated recently (Skinner et al. 1995; Toussaint et al. 1995; Toussaint et al. 1996; Toussaint et al. 1997; Fayad et al. 1998; Yuan et al. 1998). Experimental data has shown that MR is effective in identifying both the normal vessel wall components and atherosclerotic plaque in research conditions, often using high-field MR systems and performing imaging ex vivo, to improve the resolution obtainable (Toussaint et al. 1995; Toussaint et al. 1997). In animal models recently, MR has been shown able to characterise the components of atherosclerotic lesions in rabbits but also using specialised MR systems (Skinner et al. 1995; Fayad et al. 1998). Very recently, using spin-echo sequences, atherosclerotic lesions in humans have been investigated in the carotid system with very promising results (Toussaint et al. 1996; Yuan et al. 1998). However, the ability to translate these

techniques to the coronary arteries in vivo has the same limitations that initially faced MR coronary angiography, namely motion (cardiac and respiratory), small vessel size and tortuosity of the vessels. However, in order to visualise the component of coronary atherosclerotic lesion, sub-millimeter resolution will be required. Thus despite the incredible potential for MR characterisation of coronary atherosclerotic lesions, it has yet to been shown that this is feasible.

1. 6. 7. 6. Other Cardiovascular Uses of MR

For completeness, it is worth mentioning that cardiovascular MR has also been of great use for imaging patients with congenital heart disease (Hirsch et al. 1994; Hoppe et al. 1996). It has also been used for aortic imaging with great success, especially in diseases of the aortic wall (including aortic dissection (Nienaber et al. 1993; Deutsch et al. 1994; Laissy et al. 1995) and aneurysm (Moore et al. 1984; Dinsmore et al. 1986)).

1. 7. AIMS OF THE THESIS

The aims of the thesis are to investigate the ability of high resolution MR imaging to both characterise and quantify atherosclerotic lesions in both porcine and rabbit models, and explore whether MR could be used to monitor serially changes in arterial wall parameters.

1. 7. 1. Specific Aims of the Thesis

1. To validate that MR imaging is able to accurately quantify and characterise coronary and aortic atherosclerotic lesions, including calcified, lipid-rich, fibro-cellular and haemorrhagic regions in a porcine model of complex atherosclerosis ex vivo in a clinical 1.5T MR system using routine clinical radiofrequency (RF) coils.

2. That MR imaging techniques are able to account for the significant motion of the coronary arteries in vivo by performing a comparison between in vivo and ex vivo MR imaging using the exact techniques in a clinical 1.5T MR system usually routine clinical RF coils.

3. Using a new noninvasive MR imaging technique in a clinical 1.5 T MR system, to confirm that experimental coronary artery lesions can be visualised, quantified and characterised in vivo in an experimental porcine model using standard RF coils by comparison with histopathological specimens.

4. To document that MR imaging techniques in a clinical 1.5 T MR system with a standard noninvasive phased array RF coil can accurately define experimental aortic atherosclerotic lesions in a New Zealand White rabbit model. To explore which MR sequence has the greatest contrast between lipidic and fibrotic components of the plaques in this model, and confirm that MR can in fact accurately quantify the lipidic and fibrotic components of the plaques.

5. Validate MR imaging as a tool for the serial monitoring of atherosclerotic plaque composition in the New Zealand White rabbit model described above under conditions of dietary atherosclerotic progression and regression.

6. To investigate the ability of MR imaging to noninvasively and serially monitor the arterial remodelling process in the Watanabe Heritable Hyperlipidaemic (WHHL) rabbit model of atherosclerosis.

Chapter 2

METHODS

TABLE OF CONTENTS

2. 1. ANIMAL MODELS OF ATHEROSCLEROSIS

2. 1. 1. Porcine Aortic Atherosclerosis

Yucatan mini-swine (initial weight 28-33 kg) were fed an atherogenic diet (2% cholesterol) for 6 months. The mini-swine had free access to water and were able to move around freely within their pens. To localise and accelerate the development of atherosclerotic lesions, balloon denudation of the abdominal aorta was performed on two occasions, at time 0 and 3 months. The mini-swine were pre-medicated with ketamine (15mg/kg IM), deeply anaesthetised with pentobarbital (25mg/kg IV) via an auricular vein, intubated and ventilated mechanically. Anaesthesia was maintained with inhalation of isoflurane and continuous ECG monitoring was performed. The right femoral artery (or the left femoral artery, if the right had been previously used) was exposed via a cut-down technique and an 8 French introducer sheath inserted into the vessel. Heparin was administered via the intra-arterial sheath (100 units/kg) 15 minutes prior to the interventions.

A 4 French Fogarty embolectomy catheter was introduced into the abdominal aorta and advanced under fluoroscopic guidance to the level of the renal arteries. The balloon was then inflated with 0.5-0.7 mL of dilute contrast and the catheter withdrawn to the iliac bifurcation with the balloon inflated to maintain moderate resistance as determined by the operator under fluoroscopic guidance. This procedure was repeated four times. The femoral artery was then tied and thereafter the animals were recovered and returned to their pens.

2. 1. 2. Porcine Coronary Artery Atherosclerosis

Two models of experimental coronary artery atherosclerosis were used for the purposes of this thesis. Anaesthesia was performed as described above.

Firstly, as for the porcine aortic atherosclerotic model described above, Yucatan mini-swine were used, by feeding an atherogenic diet (2% cholesterol) for 6 months and performing coronary angioplasty 3 months after commencing the diet. The left main coronary artery was selectively engaged with an appropriate coronary catheter under fluoroscopic guidance (Phillips BV-24). Coronary angioplasty was performed in both the left anterior descending (LAD) and circumflex (LCx) arteries by 3 inflations of a 4.0 X 20-mm angioplasty balloon (Cordis Corp). The first inflation was at 6 atmospheres, the second and third inflations at 8 atmospheres. Each inflation lasted 15 seconds, with an interval of 60 seconds between inflations. Pre- and post-intervention angiograms were performed. The femoral artery was tied after the procedure and thereafter the animals were recovered and returned to their pens.

Secondly, Yorkshire albino swine were used without using an atherogenic diet. Coronary lesions were induced in these animals (weight 30-35 kg) in all three major epicardial coronary arteries (LAD, LCx and RCA) by balloon angioplasty. The proximal segments of the three major epicardial coronary arteries were injured with a 4.5 X 20 mm angioplasty balloon (Titan, Cordis Corp), using inflations of up to 14 atmospheres. Each inflation lasted 15 seconds, separated by a 60 second interval. Post-procedure management was as previously reported above.

2. 1. 3. Rabbit Aortic Atherosclerosis

Two models of rabbit aortic atherosclerosis were used for the thesis.

Firstly, cholesterol fed New Zealand White rabbits were used. Complex atherosclerotic aortic lesions were induced in New Zealand white rabbits (3.0 to 3.5 kg) by a combination of atherogenic diet (0.2% cholesterol) and sequential balloon denudation, one week and thirteen weeks after initiation of the atherogenic diet. Aortic denudation of the aorta from the aortic arch to the iliac bifurcation was performed by four withdrawals, with moderate resistance, of a 4Fr Fogarty embolectomy catheter introduced through the iliac artery. All procedures were performed under general anaesthesia by intramuscular injection of ketamine (Fort Dodge Animal Health, Fort Dodge, IA) (20mg/kg) and xylazine (Bayer Corporation, Shawnee Mission, KA) (10mg/kg).

Secondly, the Watanabe Heritable Hyperlipidaemic (WHHL) rabbit was used. The WHHL rabbit has an intrinsic deficiency in LDL receptors, thus more closely approximating humans with atherosclerosis than the cholesterol fed rabbit models. WHHL rabbits (weight=3.0 kg) underwent aortic denudation of the aorta from the renal arteries to the iliac bifurcation, one week after arrival to the institution as described above.

2. 2. MAGNETIC RESONANCE (MR) SYSTEM AND IMAGING SEQUENCES

Nuclear magnetic resonance (NMR) is based on the absorption of radio-frequency energy by the magnetic moments of atomic nuclei in samples placed in a strong magnetic field. The sensitivity of NMR parameters to the local chemical milieu and

molecular mobilities has allowed NMR to be utilised for compound identification and chemical compositional studies for many years. However, in 1973, Lauterbur added an entirely new aspect to the growing array of emerging NMR uses, namely image formation based on NMR principles. This achievement has led to the highly successful application of NMR imaging (or "MRI") to clinical medicine.

The General Electric (GE) Signa CV/i system is a high resolution, whole body imaging system operating at 1.5 Tesla, and all MR imaging for the purposes of this thesis was performed with this system. As described in the introduction, Cardiovascular MR imaging sequences are generally classified as bright (white) blood or dark (black) blood imaging techniques.

2. 2. 1. Black Blood Imaging Sequences

The black blood MR imaging techniques used in this thesis were standard Fast spin echo (FSE) and double inversion recovery fast spin echo (2IRFSE).

Standard FSE MR techniques were used to provide high resolution images of rabbit aortic atherosclerotic lesions and the ex vivo porcine atherosclerotic lesions. The animals were fully anaesthetised with ketamine and xylazine as described above and placed supine in the 1.5 Tesla MRI system (Signa, General Electric), using a conventional phased-array volume coil. Fast gradient-echo coronal images were used to localise the abdominal aorta. Sequential axial images (3-mm thickness) of the abdominal aorta from the renal arteries to the iliac bifurcation were obtained using a fast spin-echo sequence with an in plane resolution of 350 x 350 μm (PDW: TR/TE: 2300/17 msec; T2w: TR/TE: 2300/60 msec, field of view (FOV)=9 x 9 cm, matrix 256 x 256, echo train length=8, signal averages=4). Inferior and superior radio

frequency saturation pulses were used to null signal from flowing blood in the inferior vena cava and aorta. Fat suppression was used to null the signal from the peri-adventitial fat, in order to minimise chemical shift artifacts.

The 2IRFSE imaging sequence was used to image the experimental porcine coronary artery lesions in vivo. Four weeks after the coronary interventions, the pigs were again pre-medicated with ketamine (15mg/kg IM) and anaesthesia induced with intravenous propofol (Zeneca Pharmaceuticals, Wilmington, Delaware) (10mg/kg). The pigs were then intubated and mechanically ventilated with a MR compatible ventilator (pneuPAC, Broomall, PA.). Anaesthesia was maintained with a continuous intravenous infusion of propofol (10-15 mg/kg/hr.) and intermittent intravenous boluses of doxacurium (Catalytica Pharmaceuticals, Grenville, NC.) (150μg/kg). The animals were placed supine in the magnet, MR compatible ECG leads were positioned and a cardiac phased-array surface coil applied to the anterior chest wall. Magnetic resonance imaging was performed in a Signa clinical 1.5 Tesla magnet (GE Medical Systems). After initial gradient echo series to localise the heart all subsequent imaging used the double inversion recovery fast spin echo sequence (2IRFSE). Non-selective and selective preparatory inversion pulses, long echo train imaging and short radio frequency pulses, maximising blood flow suppression and minimising vessel motion artifacts, characterise this sequence. This allows for proton density and T2 weighted imaging through direct manipulation of the echo time (TE), using a constant repetition time (TR) of twice the R-R' interval (2RR') whilst maintaining cardiac gating of the sequence to end-diastole. The 2IRFSE permits the acquisition of single images within a time period (less than 30 seconds) that makes breath hold imaging possible and thus feasible in humans. Image slices were obtained perpendicular to the long axis of the coronary artery. The inversion time (TI) was determined close to the null point of the blood signal and is based on the

longitudinal relaxation (T1) value of the blood and the TR interval. A TE of 42 msec was chosen for T2W images on the basis of prior work estimating the T2 values for various atherosclerotic lesion components. The following imaging parameters were used; T2W: TR / TE : 2RR' / 42 msec; PDW: TR / TE : 2 X RR' / 17 msec; receiver bandwidth ± 62.5 Hz; echo train length (ETL) 32; echo spacing (ESP) 4.4 msec; field of view (FOV) 10 X 10cm (or 12 X 12cm for fat suppressed images); matrix 256 X 256; slice thickness 5 mm; 2 signal averages. A saturation pulse was used to eliminate the epicardial fat signal and thus enhance the definition of the outer boundary of the vessel in some images. The in-plane resolution obtained was therefore 390-470 X 390-470 microns.

2. 2. 2. White Blood Imaging Sequence

The white blood imaging sequence used for this thesis was a 2D-time of flight (TOF) technique for the purpose of localisation of the anatomical structures of the aorta in order to assist with MR image and histopathological co-registration. After fasting the previous night, the rabbits were anaesthetised as described above. After initial gradient echo scout images to identify the thoracic aorta, 2D-time of flight MR imaging was performed (field of view: 18X11.25cm; matrix 256X160; TR/TE: 46/4.4msec, slice thickness 2mm; flip angle: 45^0).

2. 3. EUTHANASIA AND SPECIMEN FIXATION

Rabbits were euthanased by intravenous injection of "Sleepaway" 5 mL IV (Fort Dodge Animal Health, Fort Dodge, IA) after receiving heparin (100 U/kg) to prevent post-mortem blood clotting. The aortas were immediately flushed with 250ml of physiological buffer (0.1mol/L PBS, pH 7.4) followed by perfusion fixation with

250ml cold (4^0C) 4% paraformaldehyde in 0.1% PBS at 100mmHg. After perfusion fixation, all specimens were immersed in fresh fixative and stored at 4^0C.

Pigs were euthanased by pre-medication with ketamine and subsequent deep anaesthesia with pentobarbital as described earlier. Heparin was administered (100 units/kg) and the aorta and heart exposed via an extensive median incision. "Sleepaway" (a proprietary substance containing propyl alcohol and pentobarbital) 10 mL IV (Fort Dodge Animal Health, Fort Dodge, IA) was administered for euthanasia. The heart was immediately excised and large bore catheters inserted into the ascending aorta to perfuse the rest of the aorta antegradely and the aortic root to perfuse the coronary arteries retrogradely. The coronary arteries were flushed with 1 L of physiological buffer (0.1 mol/L PBS, pH 7.4), followed by perfusion fixation with 1 L cold (4^0C) 4% paraformaldehyde in 0.1% PBS, pH 7.4 and removed "en bloc" with surrounding epicardial fat and myocardium before sectioning. The entire aorta from the aortic root to the iliac arteries was excised and flushed and perfusion fixed in the above manner. All perfusions were performed at 100 mmHg. After perfusion fixation, specimens were immersed in fresh fixative and stored at 4^0C.

2. 4. HISTOPATHOLOGY PREPARATION

The coronary artery and aortic atherosclerotic specimens for both porcine and rabbit models were matched with corresponding MR images using distance from known landmark structures such as arterial branches or external fiducial markers. Specimens that were to be prepared for morphometric analysis and comparison with MR images were embedded in paraffin and sections 5-micron thick were cut and stained with a combined Masson's trichrome elastin stain. Specimens for determination of lipidic

atherosclerotic plaque components and comparison with MR images were kept at -80^{0}C for specific lipid staining with Oil Red O.

2. 5. IMAGE AND DATA ANALYSIS

Histopathological sections were digitised to a Macintosh computer from a Sony 3CCD video camera attached to a Zeiss Axioskop light microscope. The MR images were transferred to the same Macintosh computer and matched with the corresponding histopathological sections. Cross-sectional areas of the lumen and outer boundary of each section (coronary or aortic) were determined for both MR images and histopathology by manual tracing with Image-Pro Plus (Media Cybernetics). From these measurements, mean wall thickness (MWT - a computer generated value), vessel wall area (VWA) could be calculated. Areas containing lipidic and fibrotic material were also measured in the rabbit aortic atherosclerotic model using the above described image software package, Image-Pro Plus. With T2W MR imaging, lipidic regions are low signal and fibrotic regions are high signal, thus allowing differentiation. Histopathological measurements of mean wall thickness and vessel wall area were analyzed with sections stained by combined Masson elastin stain (CME); lipidic and fibrotic areas were analyzed with Oil Red O staining.

2. 6. STATISTICAL ANALYSES

Both simple linear regression and Bland-Altman techniques (Bland et al. 1986) were used to compare correlations between MR imaging and histopathological parameters.

Correlations between measurements of mean wall thickness (MWT), vessel wall area (VWA), lipidic and fibrotic area by MR and histopathology were analysed by simple linear regression with 95% confidence intervals (Statview, SAS Institute Inc). All values are expressed as mean ± SEM. A p value < 0.05 was used to indicate statistical significance.

The comparability between MR imaging and histopathologically derived parameters was performed using the Bland-Altman technique (Bland et al. 1986). By plotting the difference (i.e. subtraction) between the measurements by both techniques (y-axis) against the mean of the measurements (x-axis) an appreciation for the level of agreement between histopathology and MR imaging at different values can be obtained. The value for twice the standard deviation of the difference between measurements allowed an objective assessment of level of agreement.

To define intra-observer and inter-observer variability, a subset of coronary segment MR images and corresponding histopathology sections were re-analyzed and the intraclass correlation coefficients determined.

The accuracy of MR imaging for the identification of atherosclerotic plaque components was tested using a table formulated by our group (i.e. T1W, T2W and PDW - see Table 1). One investigator, blinded to the results of the histopathology and the number of atherosclerotic plaque components present, analyzed the MR images. In the initial porcine ex vivo study (Chapter 3), complex plaques with 3 or greater components were analysed. In the subsequent in vivo study (Chapter 4) the presence of vessel wall haematoma was analysed.

Chapter 3

HIGH RESOLUTION EX VIVO MAGNETIC RESONANCE IMAGING OF IN SITU CORONARY AND AORTIC ATHEROSCLEROTIC PLAQUE IN A PORCINE MODEL

TABLE OF CONTENTS

3. 1. INTRODUCTION

As reviewed previously, coronary artery disease is the single leading cause of mortality in the Western world (Fuster et al. 1992; Fuster et al. 1992; Ross 1993). The acute clinical complications of coronary artery disease are associated with atherosclerotic plaque disruption and thrombosis (Fuster et al. 1992; Fuster et al. 1992; Ross 1993; Burke et al. 1997; Fuster et al. 1997; Libby et al. 1997; Ross 1999). Atherosclerotic plaque composition rather than stenotic severity predicts the risk of plaque rupture and its thrombogenicity (Fuster et al. 1992; Fuster et al. 1992; Ross 1993; Fernandez-Ortiz et al. 1994; Toschi et al. 1997; Ross 1999). Thus imaging techniques that can characterise the plaque and its components will potentially allow risk stratification in asymptomatic, as well as symptomatic, patients with coronary artery disease and potentially select the most appropriate therapies to help attenuate this risk.

Magnetic resonance (MR) imaging has been shown in ex vivo models of atherosclerosis to be effective in identifying both normal vessel wall components (Toussaint et al. 1995) and atherosclerotic plaque composition (Toussaint et al. 1995; Toussaint et al. 1997). These studies have usually required high field research MR systems (Toussaint et al. 1995; Toussaint et al. 1997). Recently, in vivo MR imaging in animal models of atherosclerosis including mice (Fayad et al. 1998), rats (Chandra et al. 1998), rabbits (Skinner et al. 1995) and pigs (Lin et al. 1997), has been demonstrated. However, to date, only linear arteries have been successfully imaged. The in-plane resolution in 1.5 T clinical systems using standard surface coils has generally been greater than 300 X 300 microns, in both in and ex vivo studies (Skinner et al. 1995; Toussaint et al. 1996). Imaging the coronary artery wall with magnetic resonance techniques in vivo provides added levels of difficulty due to

cardiac and respiratory motion, as well as its curvi-linear course (Post et al. 1994; van der Wall et al. 1995). Given the predilection of coronary atherosclerotic lesions for more tortuous sites in the vessel, associated with lower shear stress (Traub et al. 1998), it is important to confirm that MR imaging can accurately identify and characterise atherosclerotic lesions in the curved coronary arteries. Additional data, confirming the unique response of the coronary arterial system to injury, in comparison to other arterial beds (Badimon et al. 1998), highlight the importance of being able to serially and noninvasively characterise atherosclerotic lesions within the coronary system. The ability to accurately identify and quantify the coronary wall components ex vivo on the intact heart in an atherosclerotic model has yet to be documented.

Despite the many animal models of atherosclerosis available, there is no perfect model of human coronary atherosclerosis (Fuster et al. 1991). Cholesterol feeding with balloon denudation of the proximal coronary arteries in pigs inducing such lesions has been associated with high mortality (Lee et al. 1975). Balloon angioplasty in normal porcine vessels, in the absence of an atherogenic diet leads to intimal hyperplasia and occasionally vessel haematoma, but no other components of complex atherosclerotic plaque (i.e. lipid cores, fibrous caps, calcification) (Steele et al. 1985; Fuster et al. 1991). We investigated the use of Yucatan mini-swine fed an atherogenic diet combined with balloon injury of the coronary arteries and abdominal aorta as a potential new experimental model for complex atherosclerotic lesions.

Our data show that MR imaging of coronary atherosclerotic lesions is not limited by the architectural curvature of the arteries. We have been able to characterise the composition of coronary and aortic atherosclerotic lesions. This suggests the possible

future use of MR imaging for noninvasive serial studies of atherosclerotic plaque in an in vivo setting.

3. 2. METHODS

3. 2. 1. Animal Species

Yucatan mini-swine (n=4, initial weight 28-33 kg) were selected as an animal model for this study. They were fed an atherogenic diet (2% cholesterol) for 6 months. To localise and accelerate the development of atherosclerotic lesions, balloon denudation of the abdominal aorta was performed on two occasions, at time 0 and 3 months, and coronary angioplasty was performed at 3 months after commencing diet.

3. 2. 2. Anaesthesia and Balloon Interventions

The mini-swine were pre-medicated with ketamine (15mg/kg IM), deeply anaesthetised with pentobarbital (25mg/kg IV) via an auricular vein, intubated and ventilated mechanically. Anaesthesia was maintained with inhalation of isoflurane as described previously.

Coronary angioplasty was performed in both the left anterior descending (LAD) and circumflex (LCx) arteries by 3 inflations of a 4.0 X 20 mm angioplasty balloon (Cordis Corp) as described. A 4 French Fogarty embolectomy catheter was introduced into the abdominal aorta and advanced under fluoroscopic guidance to the level of the renal arteries and the catheter withdrawn to the iliac bifurcation with the balloon inflated to maintain moderate resistance as determined by the operator under fluoroscopic guidance as described.

3. 2. 3. Blood Sampling

In 2 of the 4 mini-swine studied (random selection) blood samples were drawn at the time of surgery, 3 months post diet commencement, for full lipid profile and routine biochemical analysis.

3. 2. 4. Euthanasia and Specimen Fixation

Six months after commencement of the atherogenic diet, the mini-swine were euthanased. This was achieved by pre-medication with ketamine and subsequent deep anaesthesia with pentobarbital as described under "anaesthesia and preparation." Heparin was administered (100 units/kg) and the aorta and heart exposed via an extensive median incision. "Sleepaway" 10 mL IV (Fort Dodge Animal Health, Fort Dodge, IA) was administered for euthanasia. The heart was immediately excised and large bore catheters inserted into the ascending aorta to perfuse the rest of the aorta antegradely and the aortic root to perfuse the coronary arteries retrogradely. After perfusion fixation, specimens were immersed in fresh fixative and stored at 4^0C.

3. 2. 5. Specimen Preparation

On the evening before imaging, the specimens were removed from the fixative bath and washed overnight with water. The following morning, the samples were placed in commercially available zip-lock bags, allowing direct application of a conventional 7.6-cm surface coil to the specimen. MR imaging was performed in a Signa clinical 1.5 Tesla magnet (GE Medical Systems).

3. 2. 6. Imaging Parameters

The entire excised heart was placed inside the scanner, and a conventional 7.6-cm circular receive-only surface coil applied over the coronary artery to be imaged. After initial gradient echo series to locate the coronary artery, high resolution, 2-dimensional fast spin echo imaging was performed, with an echo train length of 8.

T1 weighted (T1w): repetition time (TR) / echo time (TE) : 600 / 13 msec; T2 weighted (T2w): TR / TE : 2300 / 55 msec; proton density weighted (PDW): TR / TE : 2300 / 19 msec; field of view (FOV) 4 X 4 cm; matrix 256 X 256; slice thickness 2 mm; 4 signal averages. A saturation pulse was used to eliminate the epicardial fat signal and thus enhance the definition of the outer boundary of the vessel. The in-plane resolution obtained was 156 X 156 microns.

The aortic specimens were also imaged with the same conventional 7.6-cm surface coil. Fast spin echo imaging (echo train length of 8) with T1w: TR / TE : 600 / 14 msec; T2w: TR / TE : 2300 / 80 msec; PDW: TR / TE : 2300 / 16 msec; FOV 6 X 6 cm; matrix 256 X 256; slice thickness 3 mm; 4 signal averages. In-plane resolution was 234 X 234 microns.

3. 2. 7. Histopathology

Serial sections of the coronary arteries were cut at 2-mm intervals matching corresponding MR images. Co-registration was carefully performed by utilising one or more landmark structures external to the coronary arteries, including arterial branches. The aortic specimens were decalcified and cut at 3-mm intervals to also match MR imaging. Coronary and aortic specimens were first embedded in paraffin and thereafter sections 5-micron thick were cut and stained with a combined Masson's trichrome elastin stain.

3. 2. 8. Image and Data analysis

The MR images were transferred to a Macintosh computer for analysis. The histopathological sections were digitised to the same computer from a camera (Sony,

3CCD Video Camera) attached to a Zeiss Axioskop light microscope. The MR images were then matched with corresponding histopathological sections for both the coronary (n=54) and aortic (n=43) specimens.

Cross-sectional areas of the lumen and outer boundary of the vessels were determined for both MR images and histopathology by manual tracing with Image-Pro Plus (Media Cybernetics). From these measurements, mean and maximal wall thicknesses were calculated for all sections. In addition, for the aortic specimens, atherosclerotic plaque area was calculated by tracing the inner surface of the media (readily identifiable on both MR and histopathology), and subtracting the luminal area. Separate investigators, blinded to the results of others, performed each analysis. The data were then analyzed by simple linear regression with 95% CIs (Statview, Abacus Corp).

To facilitate the analysis by MR imaging of atherosclerotic plaque components, we formulated criteria based on a visual assessment of the signal intensity of the different areas of the atherosclerotic lesion for each of the imaging sequences used (ie. T1W, T2W and PDW - see Table 3. 1).

Table 3. 1

ATHEROSCLEROTIC PLAQUE COMPONENT CHARACTERISTICS WITH MR IMAGING

	MR SIGNAL INTENSITY			
Imaging sequence	Dense fibro-cellular	Lipid-rich	Haematoma	Calcification
PDW	High	intermediate	Intermediate	Nil
T1W	High	intermediate	High	Nil
T2W	High	Low	Low	Nil

This table extends the information gained from previous work in this field. One investigator, blinded to the results of the histopathology and the number of atherosclerotic plaque components present, analyzed all MR images of complex plaques with 3 or greater components using this table in order to validate its diagnostic accuracy.

3. 3. RESULTS

The MR images of the coronary artery specimens that were matched with histopathology (n=54) included segments from all 3 coronary arteries. Both atherosclerotic and non-atherosclerotic segments were included in the analysis. The MR images from the aortic specimens that were histopathology matched (n=43) included sections from the renal arteries to the iliac trifurcation. Some of these had no significant plaque while others had extensive complex atherosclerotic disease.

On the cholesterol-enriched diet, there was an elevation of the total serum cholesterol (serum total cholesterol 466.5±17.5 mg/dL).

3. 3. 1. Coronary Atherosclerosis

Of the 54 matched coronary segments, there were 22 sections from the left anterior descending (LAD), 10 from the left circumflex (LCx) and 22 from the right coronary artery (RCA). In order to maximise the number of segments from the proximal LAD, some segments from the origin of the LCx were sacrificed. The correlation between the measurements of mean artery wall thickness by MR and histopathology ($r=0.94$, slope=0.81) was highly significant ($p<0.0001$) (Figure 3. 1). This correlation ($p<0.0001$) was independent of vessel site including the LAD (interventricular course : $r=0.94$, slope=0.87) and the RCA / LCx collectively (atrio-ventricular course : $r=0.94$, slope=0.77).

Figure 3. 1

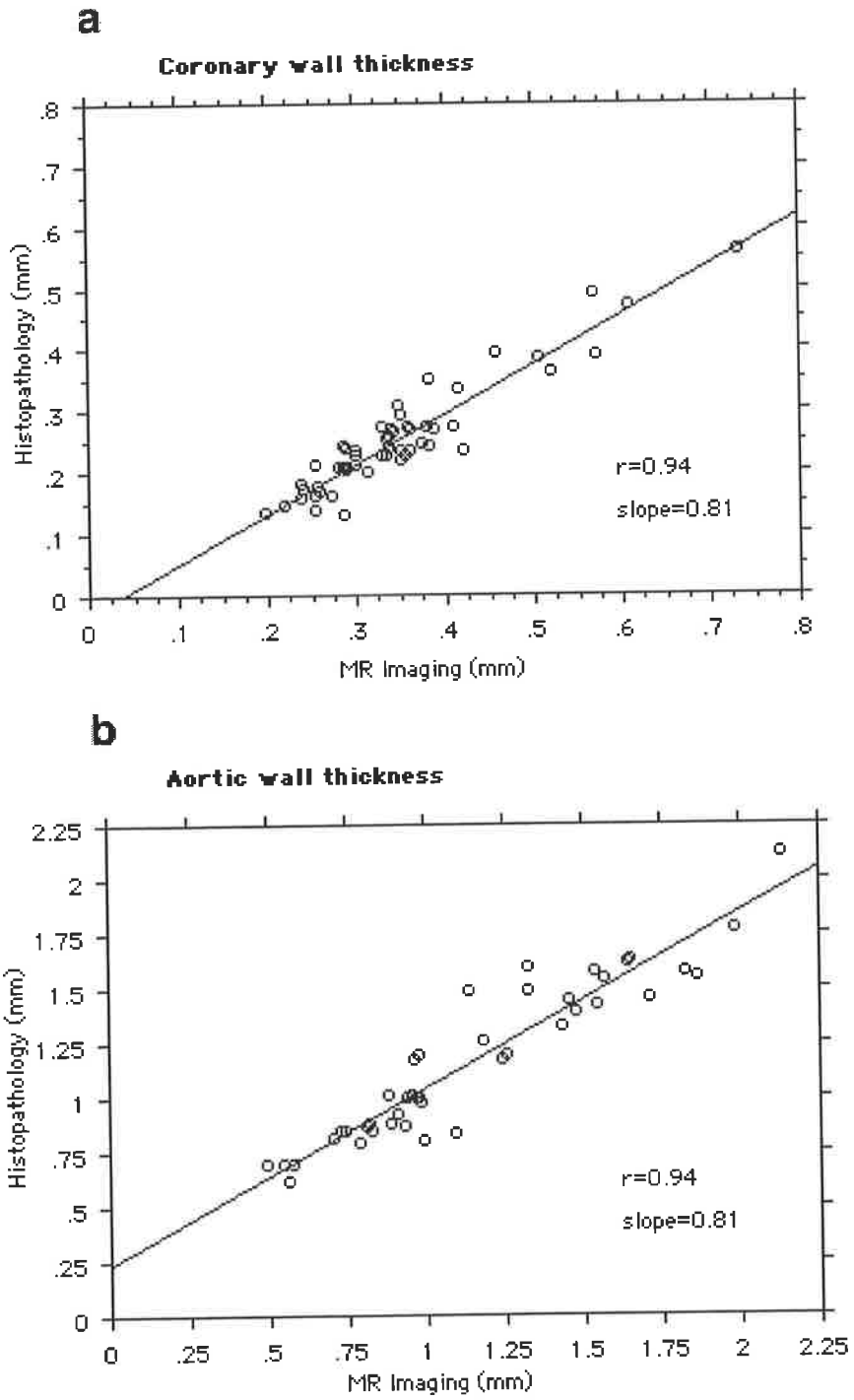

Linear regression analyses showing excellent correlation of the wall thickness as measured by MR and matched histopathology in the a. coronary arteries and b. aortas.

Coronary atherosclerotic lesions were well defined by all MR imaging sequences and appeared as a homogeneous bright (high signal) structure consistent with a fibrocellular composition (Figure 3. 2). This was confirmed with histopathology. With T2W imaging the normal components of the vessel wall could be readily

distinguished. The dense adventitia appeared dark and the media appeared bright (Figure 3. 3) as previously described (Toussaint et al. 1995).

Figure 3. 2

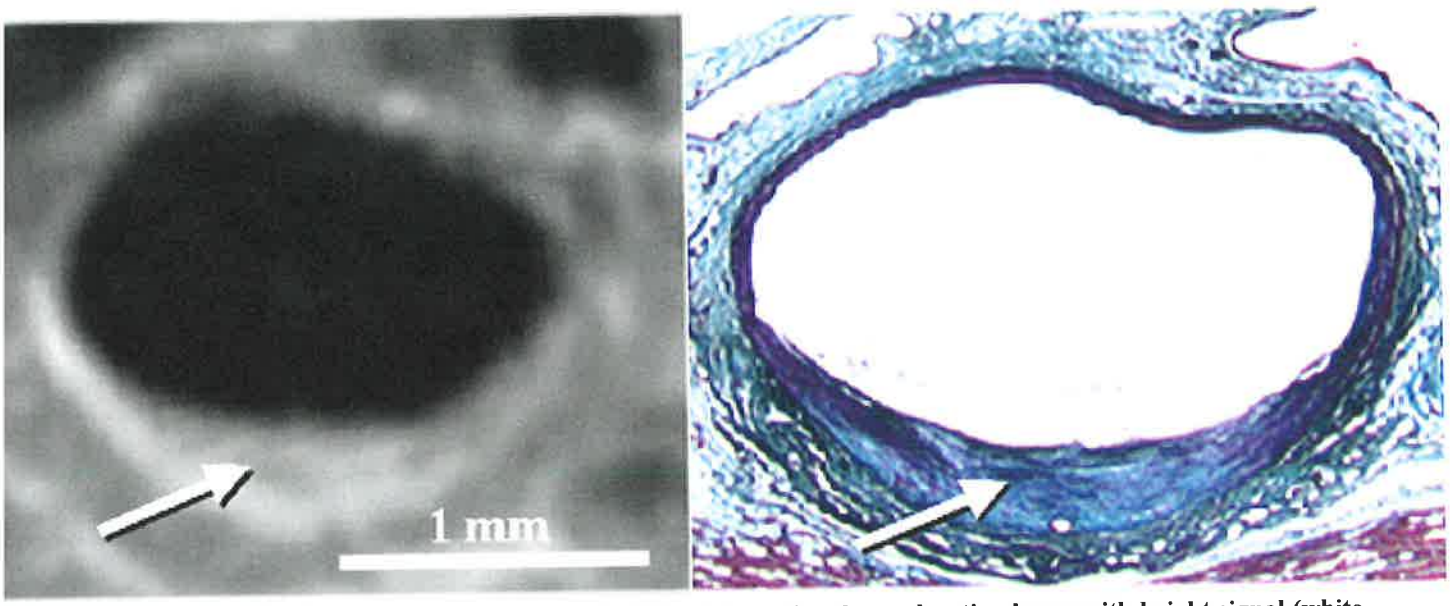

MR image (PDW) of the LAD showing an inferior crescentic atherosclerotic plaque with bright signal (white arrow) indicative of fibrocellular composition. The accompanying histopathology section confirms this (with the fibrous structures staining green on the Masson's trichrome and elastin stain).

Figure 3. 3

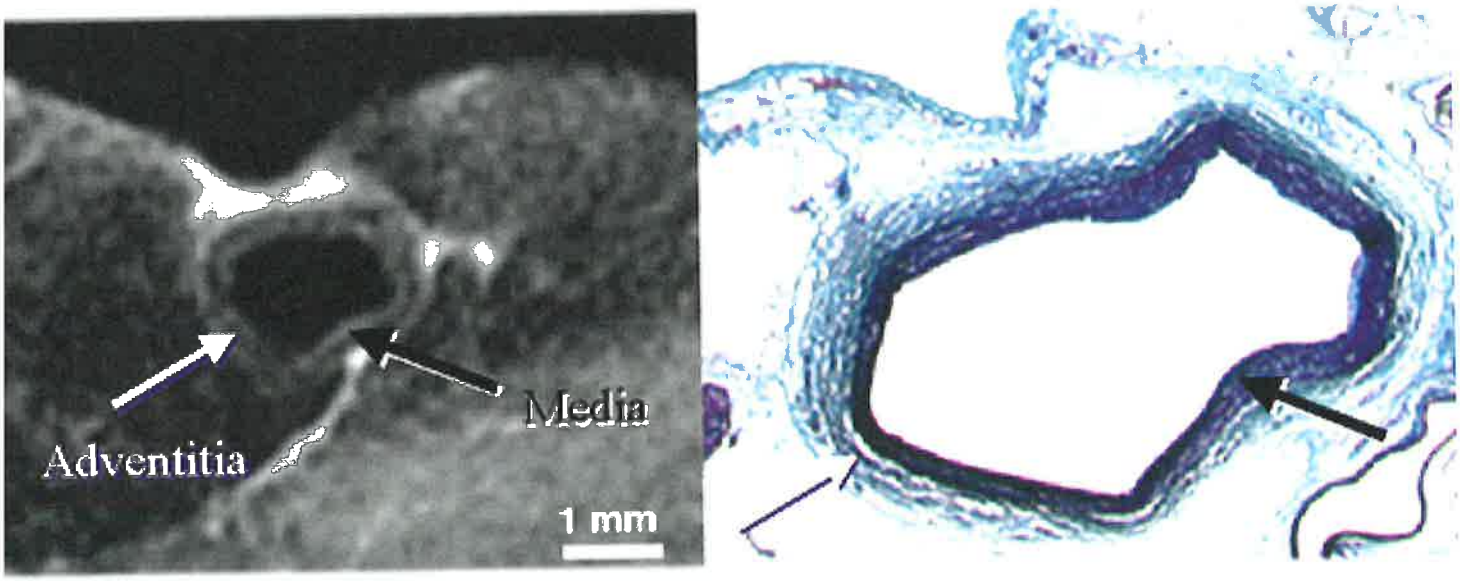

MR image (T2w) of the RCA showing no obvious atherosclerotic plaque but defining the media (high signal – white) with a black arrow from the dense adventitia (low signal – black) with a white arrow. The corresponding histopathology section confirms the accurate identification of the vessel wall. Surrounding the vessel wall is another high signal structure on the T2w image representing connective tissue.

3. 3. 2. Aortic Atherosclerosis

There was a highly significant correlation ($P<0.0001$) between mean wall thickness of the MR images and matched histopathological sections ($r=0.94$, slope=0.81) for the aortic specimens (Figure 3. 1). Total atherosclerotic plaque area per section was measured and was also significantly correlated ($P<0.0001$) between MR imaging and matched histopathology ($r=0.97$, slope=0.90).

The experimental model of atherosclerosis used induced complex atherosclerotic lesions characterised by lipid rich, dense fibrocellular, calcified and haemorrhagic regions. These regions were accurately identified with the imaging sequences performed (Figures 3. 4 and 3. 5). With T1W imaging, the calcifications were well defined by signal loss, due to the low mobile proton density within the calcified area, but there was less contrast between the other regions within the atherosclerotic plaque. The calcifications were also well visualised with T2W and PDW imaging. The dense fibrocellular cap was well distinguished from the less dense body of the plaque containing regions of extracellular lipid deposition on T2w imaging (as previously reported(Toussaint et al. 1995; Toussaint et al. 1996)) but also on PDW imaging. Plaque haematoma was also well visualised with both T2W and PDW imaging. However, there was less tissue contrast between the lipid rich areas and the haematoma with the PDW and T2W images, than for either of these two atherosclerotic plaque components and the dense fibrocellular regions.

Of the complex atherosclerotic lesions with 3 or more plaque components (n=13), using the criteria in table 1 we were able to accurately identify dense fibrocellular (13 of 13), lipid rich (13 of 13) and calcification (13 of 13). However, haematoma

was accurately identified in only 2 of 3 cases (66% sensitivity), and one specimen was falsely characterised as having haematoma (92% specificity).

Figure 3. 4

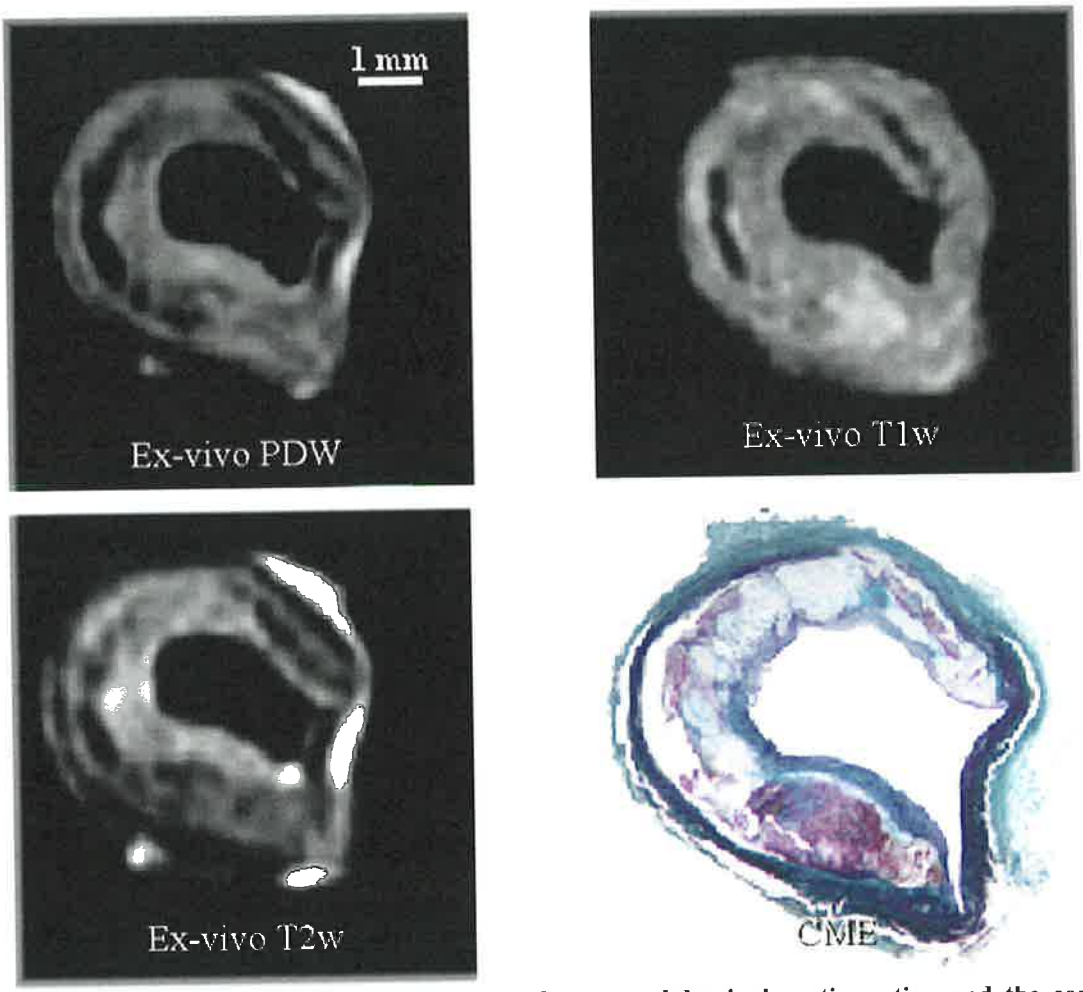

Series of 3 different MR imaging sequences of the same abdominal aortic section and the corresponding histopathology section, highlighting the various signal intensities for each atherosclerotic plaque component with the different MR imaging sequences.

Figure 3. 5

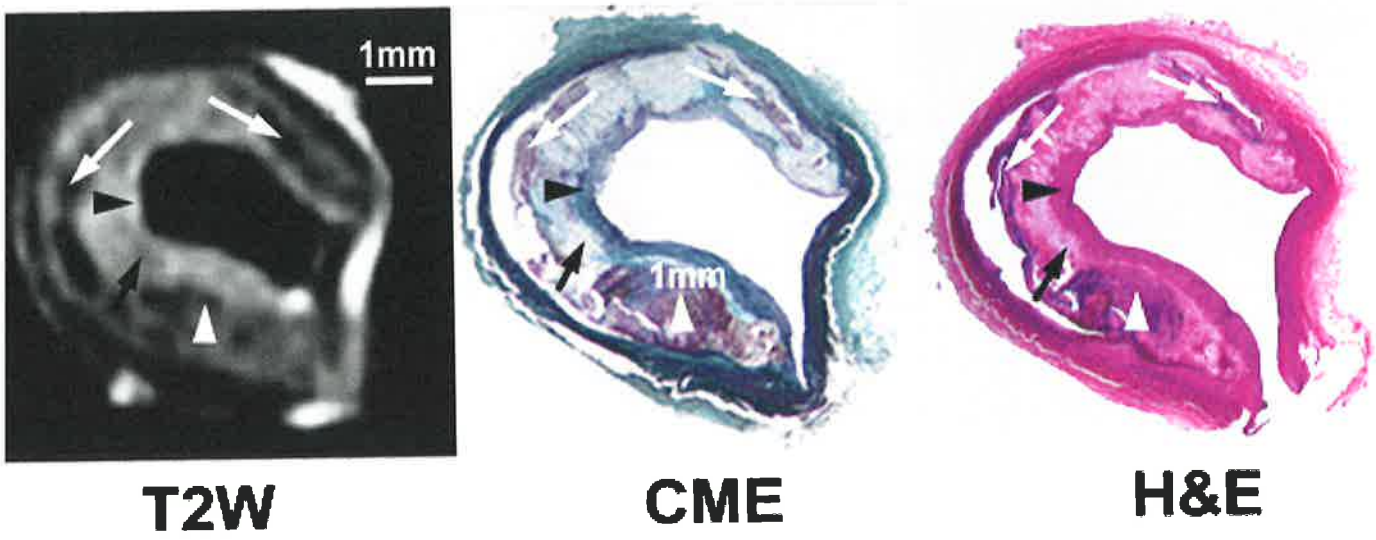

A higher magnification of the T2w image and the histopathology section from Figure 3. 4 with confirmation of the accurate identification of calcified (white arrows), dense fibrocellular (black arrowheads), lipid rich (black arrows) and haemorrhagic (white arrowheads) regions.

3. 4. DISCUSSION

High resolution MR imaging is able to identify, quantify and characterise atherosclerotic plaques within the coronary arteries in the intact heart and the aorta in this model of experimental atherosclerosis. The combination of cholesterol feeding and balloon injury induces the formation of complex atherosclerotic lesions within the coronary and aortic arterial systems that may be able to be used for future in vivo experimentation. Although ex vivo study of atherosclerotic plaque has been recently reported (Toussaint et al. 1997; Raynaud et al. 1998; Toussaint et al. 1998), our work adds new important information to the field of atherosclerosis and its imaging.

Previous reports of MR imaging studies of the vessel wall and atherosclerotic plaque (ex vivo and in vivo) were only focused on straight vascular segments (Carpenter et al. 1991; Skinner et al. 1995; Toussaint et al. 1995; Toussaint et al. 1996; Lin et al. 1997; Toussaint et al. 1997; Chandra et al. 1998; Fayad et al. 1998; Raynaud et al. 1998; Toussaint et al. 1998). Although it is reported that with cardiac gating and respiratory motion compensation techniques it should be possible to perform MR imaging of the coronary arteries in vivo (van der Wall et al. 1995; Steffans et al. 1996), no-one has addressed the ability of MR to accurately quantify the vessel wall of the coronary arteries given their tortuous course in the heart. By imaging the coronary arteries within the intact heart, we have been able to determine the accuracy of MR imaging when carefully applied to ensure perpendicularity of the image slices to the vessel wall. Even though the course of the proximal LAD is often straighter than the other major epicardial coronary arteries, we have shown that the atrio-ventricular vessels (RCA and LCx) had the same correlation between MR imaging and matched histopathology as the LAD for mean wall thickness measurements ($r=0.94$ for both). Given recent data highlighting the unique response to injury of the

coronary arterial system in comparison to other arterial beds (Badimon et al. 1998), it has become more important to be able to characterise serially and noninvasively atherosclerosis within the coronary arteries. Also reports outlining the role of shear stress on atherosclerotic pathogenesis confirm that the sites of predilection for atherosclerosis within the coronary arteries are commonly in the most curved aspects of the arteries (Traub et al. 1998). Thus the ability to perform MR imaging within the curved coronary arteries remains crucial to future studies of atherosclerosis pertaining to this arterial system.

With a combination of MR imaging sequences, we were able to accurately identify dense fibrocellular, lipid rich and calcified regions of the atherosclerotic plaque. Plaque haematoma was less accurately identified and other investigators (Toussaint et al. 1997) have noted this. The signal from intra-plaque haematoma is dependent upon its age and, given the problems of its identification, further techniques such as diffusion imaging (Toussaint et al. 1997) may be required to readily differentiate haematoma from other plaque components, in particular the lipid rich areas.

Many of the ex vivo and in vivo atherosclerotic imaging studies have used high field research MR imaging systems (Carpenter et al. 1991; Toussaint et al. 1995; Toussaint et al. 1996; Toussaint et al. 1997; Chandra et al. 1998; Fayad et al. 1998; Raynaud et al. 1998; Toussaint et al. 1998). By performing our study in a clinical 1.5 T system using a conventional surface coil, we are closer to simulating the parameters that will be used in the in vivo application of MR imaging.

By MR imaging, the measurements of mean vessel wall thickness were approximately 10-20% larger than by histopathology. This was a consistent finding and is to be expected. Firstly, even though the arteries were perfusion-fixed,

specimen shrinkage occurs with paraffin embedding during the histopathological preparation. Secondly, there may be some volume averaging given that the MR images are significantly thicker than the 5-micron histopathology sections. However, given that there was not a significant difference in the level of over-estimation for the coronary arteries or the aortas by MR imaging, a major component of volume averaging in the coronary arteries contributing to this phenomenon is less likely.

The ex vivo nature of our study obviously limits its direct applicability to human atherosclerotic imaging. The imaging was performed at room temperature (25^0C). However, despite the fact that temperature is an important variable in the lipid signal on MR imaging (Booth et al. 1990; Yuan et al. 1997), it has been shown that at varying temperatures the contrast between the lipid signal and the vessel wall remains significant (Altbach et al. 1991; Yuan et al. 1997). Despite these limitations we were able to discern the various atherosclerotic plaque components in our study.

There is no perfect animal model of complex atherosclerosis, as evidenced by the many animal models currently in use for atherosclerosis research (Fuster et al. 1991; Schwartz 1994). The anatomy and response to injury of the pig coronary arteries is most like that of the human coronary arteries (Fuster et al. 1991) and thus they have been favored for atherosclerosis research (Steele et al. 1985; Badimon et al. 1998; Gallo et al. 1998). Miniature (Post et al. 1994) or young swine (Gallo et al. 1998) are often used because of the large size of the mature pig. The most commonly used technique for inducing atherosclerosis in the coronary arteries of these pigs is by balloon (Steele et al. 1985; Badimon et al. 1998; Gallo et al. 1998). However, this induces an intimal hyperplastic response with occasional vessel wall haemorrhage but no lipid rich regions or calcification characteristic of complex human atherosclerosis (Steele et al. 1985; Fuster et al. 1991). Feeding an atherogenic diet

can lead to excessive rapid weight gain, making the animal more difficult to handle. By limiting the duration of cholesterol feeding, it may be possible to limit this problem. There have been previous descriptions of balloon pullback injury in the coronary arteries of pigs fed an atherogenic diet, but not using standard balloon angioplasty catheters and techniques (Lee et al. 1975). Indeed there was a high mortality (Lee et al. 1975). We believe that this is the first report describing this combination of balloon injury types involving the aorta and coronary arteries in cholesterol fed mini-swine.

The histological verification of the accuracy of MR imaging of non-linear (coronary) arteries for the identification, quantification and characterisation of the vessel wall and atherosclerotic plaque is an important step toward the ultimate goal of in vivo MR imaging of human coronary atherosclerosis. The ability of MR imaging of atherosclerosis to stratify risk and to direct therapeutic approaches in patients with coronary atherosclerosis requires further study. This model of complex atherosclerosis in pigs, with all the components of complex human atherosclerotic plaques, may be useful for future studies. Ongoing improvements in MR image resolution and decreases in acquisition time, together with new MR imaging techniques including navigator echo, contrast enhancing agents and diffusion weighting should lead to further improvements in atherosclerotic plaque characterisation. The difficulties in performing MR imaging of the coronary arteries when compared with other arterial areas (such as the carotid system) are well recognised. Recent data confirming different responses to injury of these systems in comparison with the coronary arteries (Badimon et al. 1998) and the predilection of coronary atherosclerotic lesions for curved sites (Krams et al. 1997; Traub et al. 1998) reinforce the need to directly image the curved coronary artery wall. The results of our study clearly define the feasibility of future in vivo coronary artery

atherosclerosis identification and characterisation in this unique model of coronary and aortic atherosclerosis and thus the possibility for serially monitoring atherosclerotic plaque in studies of progression and/or regression.

Chapter 4

CARDIAC GATED BREATH-HOLD BLOOD BLACK MRI OF THE CORONARY ARTERY WALL: AN IN VIVO AND EX VIVO COMPARISON

TABLE OF CONTENTS

4. 1. INTRODUCTION

Magnetic resonance (MR) imaging has been shown to accurately characterise and quantify atherosclerotic lesions in various arterial systems (Skinner et al. 1995; Toussaint et al. 1996; Fayad et al. 1998; Yuan et al. 1998; McConnell et al. 1999; Worthley et al. 2000). Before MR imaging of coronary atherosclerosis can be routinely performed, a number of obstacles need to be overcome. This includes accounting for the combination of cardiac and respiratory motion artifacts, and the problems with obtaining adequate signal-to-noise from the relatively small coronary arteries that are situated deep within the thoracic cavity. Cardiac gating and limiting image acquisition to a small diastolic window has helped to minimise artifacts related to cardiac motion. Navigator echo and limited breath-holding have been the two techniques used to date to account for respiratory motion (Manning et al. 1993; McConnell et al. 1997; Botnar et al. 1999). Both allow MR imaging of cardiac structures with adequate suppression of respiratory motion. However, in order to image the coronary artery wall in vivo, higher resolution is required and it is unclear whether currently used motion suppression techniques will be adequate for this purpose.

Double inversion recovery fast spin echo MR imaging is able to obtain high resolution imaging of anatomical structures whilst allowing flexible image contrast (Edelman et al. 1991). Recent reports of its ability to suppress blood flow artifacts for the imaging of cardiac structures in conjunction with breath-holding and cardiac gating (Campos et al. 1999), suggest this sequence may be ideal for coronary artery wall imaging in vivo.

The porcine model has been extensively used for the purposes of atherosclerosis research (Fuster et al. 1991). The pig coronary anatomy closely resembles that of humans and the diameter of the coronary arteries is comparable (Fuster et al. 1991). Thus, it is a useful model for testing MR imaging sequences, as the results could be translated to humans.

We undertook a comparative study of in vivo and ex vivo black blood MR imaging of coronary artery lesions in a porcine model, in order to evaluate the ability of cardiac gating and limited breath-holding to adequately limit motion artifacts.

4. 2. METHODS

4. 2. 1. Animal Model

Coronary lesions were induced in Yorkshire albino swine (n=6, weight 30-35 kg) in all three major epicardial coronary arteries (LAD, LCx and RCA) by balloon angioplasty. The coronary angioplasty was performed as has been previously described (Gallo et al. 1998; Worthley et al. 2000). The proximal segments of the three major epicardial coronary arteries were injured with a 4.5 X 20 mm angioplasty balloon (Titan, Cordis Corp), using inflations of up to 14 atmospheres. Each inflation lasted 15 seconds, separated by a 60 second interval. Post-procedure management was as previously reported (Gallo et al. 1998; Worthley et al. 2000). The Mount Sinai School of Medicine animal management program, under accreditation from the American Association for the Accreditation of Laboratory Animal Care (AALAC), approved all procedures.

4. 2. 2. In vivo MR Imaging

Four weeks after the coronary interventions, the pigs were again pre-medicated with ketamine (15mg/kg IM) and anaesthesia induced with intravenous propofol (Diprivan®, Zeneca Pharmaceuticals, Wilmington, DE) (10mg/kg). Intubation of the pigs was performed and mechanical ventilation undertaken with a MR compatible ventilator (pneuPAC, Broomall, PA.). Anaesthesia was maintained with a continuous intravenous infusion of propofol (10-15mg/kg/hr.) and intermittent intravenous boluses of doxacurium (Catalytica Pharmaceuticals, Grenville, NC.) (150μg/kg). MR imaging was performed with the animals supine in a 1.5 T clinical MR system (Signa, GE Medical Systems). MR compatible ECG leads were positioned and a cardiac phased-array surface coil applied to the anterior chest wall.

Gradient echo series were used to localise the heart. Thereafter, all subsequent imaging was with the double inversion recovery fast spin echo sequence (2IRFSE). Non-selective and selective preparatory inversion pulses, long echo train imaging and short radio frequency pulses, maximising blood flow suppression and minimising vessel motion artifacts, characterise this sequence. Flexible image contrast could be obtained, allowing proton density and T2 weighted imaging through direct manipulation of the echo time (TE), using a constant repetition time (TR) of twice the R-R' interval (2RR'). The 2IRFSE allows the acquisition of single images within a time period (less than 25 seconds) that makes breath hold imaging possible. Image slices were obtained perpendicular to the long axis of the proximal segments of the coronary arteries.

The inversion time (TI) was determined close to the null point of the blood signal and is based on the longitudinal relaxation (T1) value of the blood and the TR interval. The following imaging parameters were used; T2W: TR / TE : 2RR' / 42 msec; PDW: TR / TE : 2 X RR' / 17 msec; receiver bandwidth ± 62.5 Hz; echo train length (ETL) 32; echo spacing (ESP) 4.4 msec; field of view (FOV) 10 X 10cm (or 12 X 12cm for fat suppressed images); matrix 256 X 256; slice thickness 5 mm; 2 signal averages. A saturation pulse was used to eliminate the epicardial fat signal and thus enhance the definition of the outer boundary of the vessel in some images. The in-plane resolution obtained was therefore 390-470 X 390-470 microns.

4. 2. 3. Euthanasia and Specimen Fixation

The animals were recovered after MR imaging. The following day euthanasia and subsequent coronary artery fixation were performed as previously reported (Gallo et

al. 1998; Worthley et al. 2000). One animal was euthanased in the magnet, and immediate post-mortem MR imaging performed in order to compare these images with in vivo images for motion suppression.

4. 2. 4. Ex vivo MR Imaging

On the evening before imaging, the hearts were removed from the fixative bath and washed overnight with water. The following morning, the samples were placed in resealable plastic bags, allowing direct application of a conventional 7.6-cm diameter surface coil to the specimen. Magnetic resonance images were obtained using the same parameters as for in vivo imaging. The TR was fixed at 2000ms (equivalent to an in vivo heart rate of 60 beats per minute) for both the PDW and T2W images.

4. 2. 5. Image and Data Analysis

The MR images were transferred to a Macintosh computer for analysis. The in vivo and corresponding ex vivo MR images were then matched (n=26).

Cross-sectional areas of the lumen and outer boundary of the vessels were determined for both the in vivo and ex vivo MR images by manual tracing with Image-Pro Plus (Media Cybernetics). From these measurements, vessel wall area and maximal wall thickness was calculated for all sections. Separate investigators, blinded to the results of others, performed each analysis.

4. 2. 6. Statistical Analysis

Comparison between in vivo and ex vivo measurements of vessel wall area and maximal wall thickness with MR is made by simple linear regression analysis and Bland-Altman analysis (Bland et al. 1986), presented as mean difference ± SD. A p value of <0.05 was used to indicate statistical significance.

4. 3. RESULTS

Using the double inversion recovery fast spin echo MR imaging sequence in conjunction with the motion suppression techniques described, high quality in vivo MR imaging of the coronary artery wall from all three major epicardial coronary arteries was able to obtained in all 6 pigs. The adequate suppression of respiratory and cardiac motion artifacts could be appreciated by comparing in vivo and immediate ex vivo imaging with the animal still inside the MR system (figure 4. 1).

Figure 4. 1

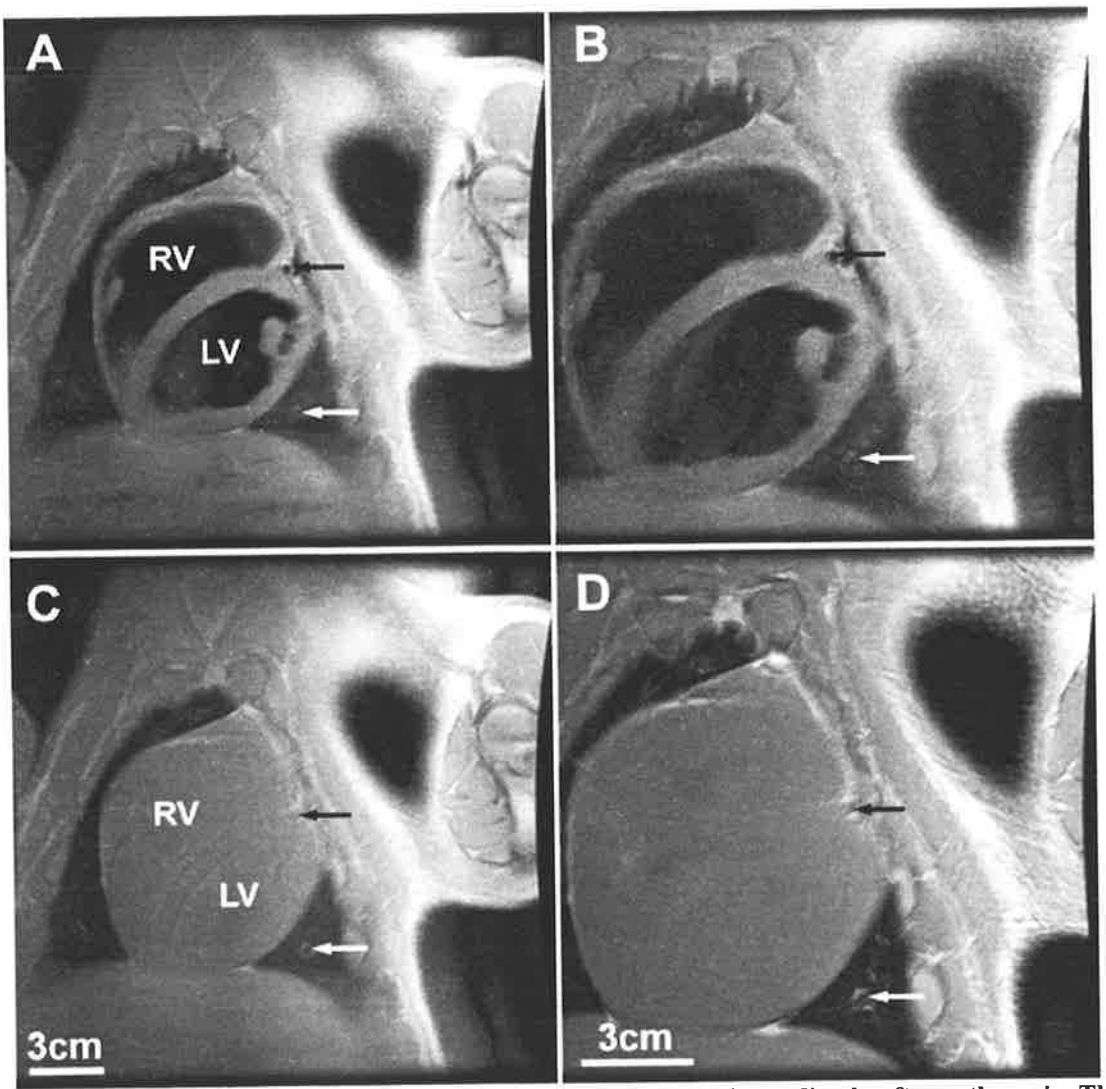

Montage of MR images (PDW) from the same site taken in vivo and immediately after euthanasia. The heart appears in a short axis view with good motion suppression in vivo as evidenced by the crisp contours of the cardiac chambers in both the 16 X 16cm (A) and 12 X 12cm (B) field of views. The corresponding post-mortem images (C for A, D for B) showing the good agreement between the images. Post-mortem there is no flowing blood and thus the blood within the cardiac chambers appears bright. The left anterior descending artery can be identified (black arrow). Further evidence of motion suppression is in the visualisation of a broncho-vascular structure in all images (white arrow).

Furthermore, the comparability of the in vivo and ex vivo MR imaging of the coronary artery wall allowed a visual confirmation between the images obtained (figures 4. 2 and 4. 3).

Figure 4. 2

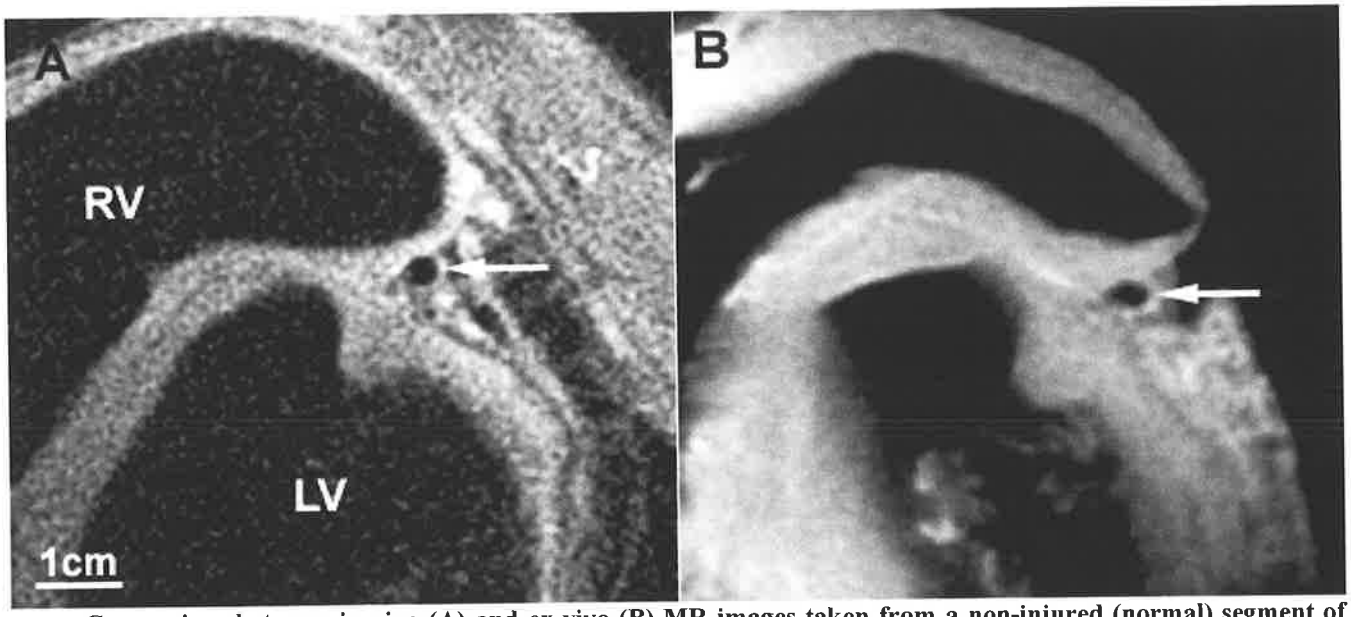

Comparison between in vivo (A) and ex vivo (B) MR images taken from a non-injured (normal) segment of the left anterior descending artery. The normal artery wall (white arrow) can be appreciated.

Figure 4. 3

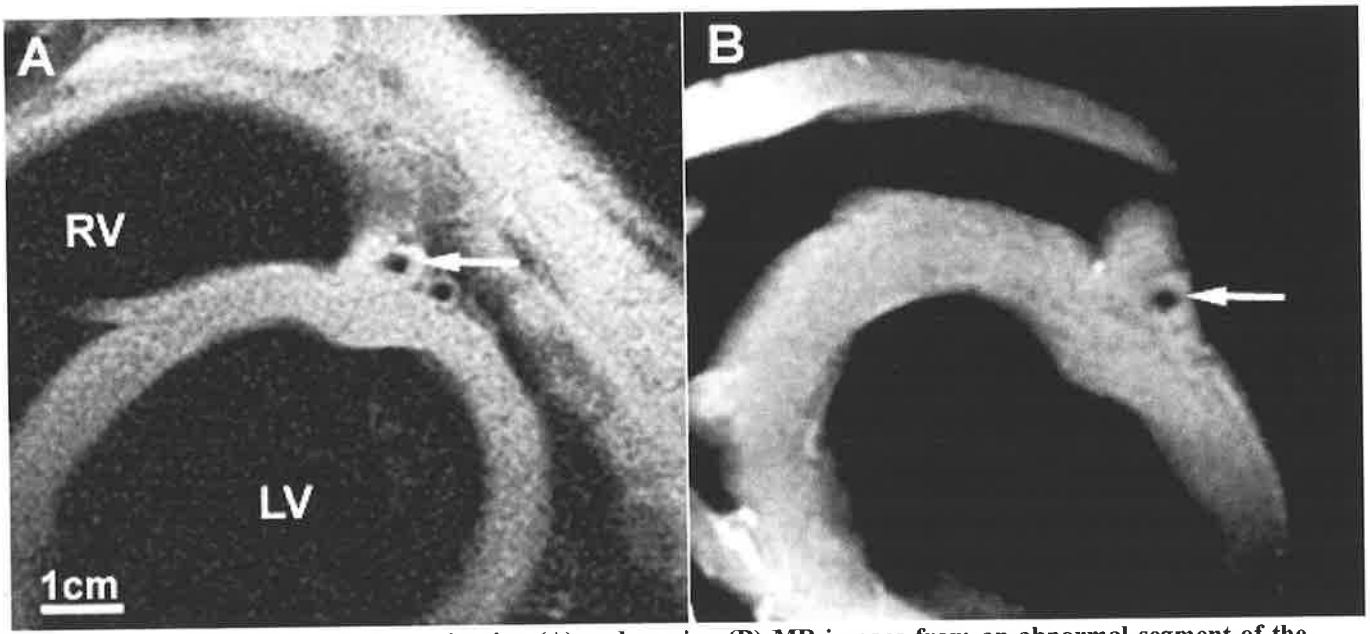

Comparison between in vivo (A) and ex vivo (B) MR images from an abnormal segment of the left anterior descending artery. The clearly thickened vessel wall (white arrow) can be seen in both images.

The analysis of coronary artery vessel wall area allowed a more objective assessment of the agreement between the in vivo and ex vivo imaging protocols, and thus the quality of the motion suppression achieved. There was a statistically significant ($p<0.0001$) correlation between measurements of vessel wall area ($r=0.87$, slope=0.87) and maximal wall thickness ($r=0.84$, slope=0.88) obtained with in vivo and ex vivo MR imaging (figure 4. 4).

Figure 4. 4

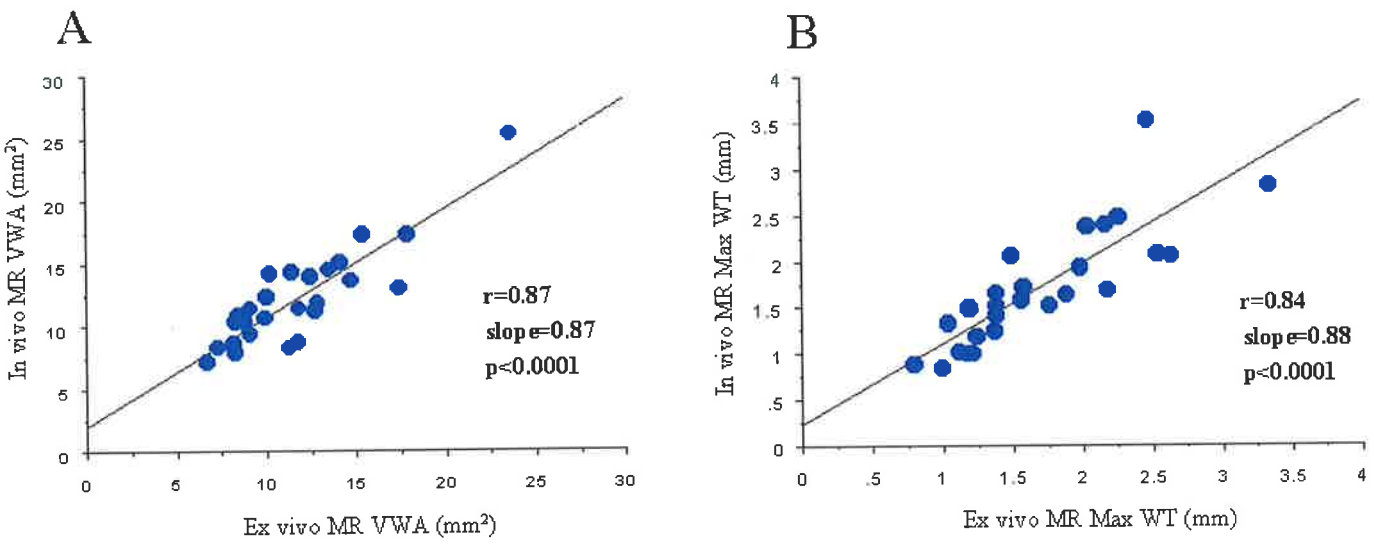

Simple linear regression analysis confirming the significant agreement between in vivo and ex vivo MR measurements for both vessel wall area (A) and maximal wall thickness (B).

The agreement between in vivo and ex vivo measurements was confirmed by Bland-Altman analysis, with mean differences between in vivo and ex vivo MR measurements of 0.56 ± 1.98 mm^2 and 0.02 ± 0.36 mm for vessel wall area and maximal wall thickness respectively (figure 4. 5).

Figure 4. 5

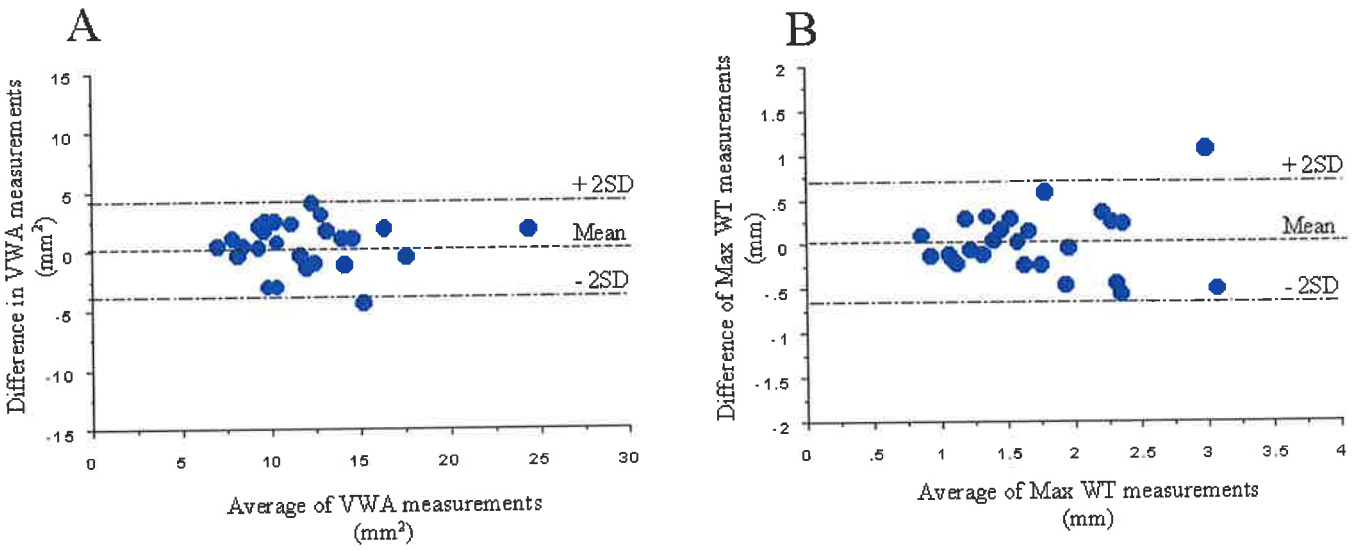

Bland-Altman analyses confirming the good agreement between in vivo and ex vivo MR measurements as evidenced by the small standard deviations for both vessel wall area (A) and maximal wall thickness (B).

4. 4. DISCUSSION

The results of this study, confirm that using short breath holding and cardiac gating, with a double inversion recovery fast spin echo MR imaging sequence, adequate suppression of motion and flow artifacts can be achieved to allow visualisation of the coronary artery wall. Clearly further studies are required to validate these observations with other imaging modalities (such as intravascular ultrasound) and pathological findings in both animal models of coronary artery lesions and humans. However, the feasibility and potential of this technique is demonstrated by the results of this study.

Magnetic resonance imaging has been shown to characterise the components of complex atherosclerotic lesions in animal models and humans in both the in vivo and ex vivo setting (Skinner et al. 1995; Toussaint et al. 1996; Fayad et al. 1998; Yuan et al. 1998; McConnell et al. 1999; Worthley et al. 2000). However, further studies will be required to determine if MR can perform this in the coronary arteries of humans in vivo. The MR imaging sequence we used provided adequate resolution for the evaluation of in vivo vessel wall thickness when compared to ex vivo imaging, as shown by the linear regression analysis. However, further improvements in resolution may be required to adequately characterise these lesions. Allowing for the comparable anatomical characteristics of the porcine and human coronary artery system (Fuster et al. 1991), this imaging technique could be translated to human coronary arteries.

We have shown the feasibility of MR for the noninvasive imaging of coronary artery lesions. Thus, studies to compare other methods of motion suppression (such as navigator echo) are warranted. Further improvements in MR imaging techniques may be required before MR imaging can noninvasively characterise coronary artery atherosclerosis in vivo.

Chapter 5

NONINVASIVE IN VIVO MAGNETIC RESONANCE IMAGING OF EXPERIMENTAL CORONARY ARTERY LESIONS IN A PORCINE MODEL

TABLE OF CONTENTS

5. 1. INTRODUCTION

Despite advances in our understanding of the cellular and molecular mechanisms in the pathogenesis of atherosclerosis, coronary artery disease remains the single largest cause of mortality in Western society (Libby et al. 1997; Ross 1999). The composition of the atherosclerotic plaque, rather than the degree of vessel stenosis, is known to modulate both risk of rupture and subsequent thrombogenicity (Fuster et al. 1997; Toschi et al. 1997; Gronholdt et al. 1998). Magnetic resonance (MR) imaging has been shown to accurately characterise and quantify atherosclerotic lesions in various arterial systems (Skinner et al. 1995; Toussaint et al. 1996; Fayad et al. 1998; Yuan et al. 1998; Worthley et al. 2000). The critical limitation of MR imaging has been the inability to translate these techniques to the coronary artery system in vivo, due to the combination of cardiac and respiratory motion artifacts, non-linear course and relatively small size of the coronary arteries. Using a double inversion recovery fast spin echo MR imaging sequence in a clinical whole-body 1.5 Tesla MR system, we are able to visualise coronary lesions in vivo in an experimental porcine model. The ability to noninvasively characterise and quantify coronary artery atherosclerotic lesions may allow stratification of risk for future acute coronary syndromes. Moreover, it could permit tailoring of therapeutic approaches based on atherosclerotic plaque characteristics and sequential assessment of their efficacy.

The process of atherogenesis is often unpredictable, as it is well documented that mild coronary lesions may be associated with significant progression to severe stenosis or total occlusion (Davies 1996; Burke et al. 1997; Fuster et al. 1997; Gronholdt et al. 1998). Plaque disruption with subsequent thrombosis appears to be the main cause of this non-linear and episodic progression, accounting for the processes of both intermittent plaque growth and acute occlusive coronary

syndromes (Fuster et al. 1997; Gronholdt et al. 1998). Post-mortem studies have greatly improved our understanding of which coronary atherosclerotic lesions are associated with these complications of plaque disruption (Davies et al. 1985; Burke et al. 1997). In many patients who die from coronary artery disease, the culprit lesion is a plaque occupying less than 50% of the vessel lumen associated with thrombosis (Davies et al. 1985; Burke et al. 1997). A large necrotic lipid core and a thin fibrous cap characterise these culprit or vulnerable plaques (Fuster et al. 1997; Gronholdt et al. 1998). Disruption of the fibrous cap exposes the highly thrombogenic lipid core to flowing blood, thus promoting thrombus formation (Toschi et al. 1997). Therefore, the ability to identify patients with vulnerable plaques within the coronary arteries could provide a useful tool for stratification of risk for cardiovascular events.

The imaging of vulnerable plaques needs to provide information about composition as well as degree of encroachment on the vessel lumen by the atherosclerotic plaque. The ideal imaging modality would need to be safe, noninvasive, accurate and reproducible, thus allowing longitudinal studies in the same patient (Celermajer 1998). Many currently available imaging techniques for the assessment of coronary artery disease are invasive (i.e. coronary angiography and intravascular ultrasound). Coronary angiography provides information about the residual lumen and no information about plaque composition. Apart from invasive intravascular probes, B-mode ultrasound is limited to superficial arteries. Furthermore, it has yet to be proven that ultrasound can accurately and reproducibly distinguish between lipid-rich and fibrous regions (Arnold et al. 1999). Ultrafast electron beam computerised tomography, whilst potentially able to provide angiographic data (Achenbach et al. 1998), has mainly been used to supply information about the calcium composition of atherosclerotic lesions (Fiorino 1998). Magnetic resonance imaging is unique in that it is the only potentially noninvasive imaging modality currently available that is able

to identify all components of complex atherosclerotic lesions, including lipid-rich, fibrous, calcified and haemorrhagic components (Toussaint et al. 1996; Worthley et al. 2000).

The porcine model has been extensively used for the purposes of atherosclerosis research. The pig coronary anatomy closely resembles that of humans and the size of the coronary arteries is similar (Gallo et al. 1998). Consequently, the MR imaging sequences and resolution required to accurately image coronary artery lesions would be comparable for pigs and humans. Using a double inversion recovery fast spin echo MR imaging sequence in a clinical MR system, we are able to perform high resolution in vivo MR imaging of coronary artery lesions.

5. 2. METHODS

5. 2. 1. Animal Species and Interventions

Yorkshire albino swine (n=6, weight 30-35 kg) were selected for this study. Coronary lesions were induced in all three major epicardial coronary arteries (LAD, LCx and RCA) by balloon angioplasty. The Mount Sinai School of Medicine animal management program, under accreditation from the American Association approved all interventional procedures for the Accreditation of Laboratory Animal Care (AALAC).

Anaesthetic and surgical preparation for the coronary angioplasty was performed as previously described (Gallo et al. 1998). Coronary angioplasty was performed in the proximal segments of the three major epicardial coronary arteries by 5 inflations of a 4.5 X 20 mm angioplasty balloon (Titan, Cordis Corp) to 14 atmospheres. Each inflation lasted 15 seconds, separated by a 60 second interval. Post-procedure management was as previously reported (Gallo et al. 1998).

5. 2. 2. In vivo MR Imaging

Four weeks after the coronary interventions, the pigs were again pre-medicated with ketamine (15mg/kg IM) and anaesthesia induced with intravenous propofol (Zeneca Pharmaceuticals, Wilmington, Delaware) (10mg/kg). The pigs were then intubated and mechanically ventilated with a MR compatible ventilator (pneuPAC, Broomall, PA.). Anaesthesia was maintained with a continuous intravenous infusion of propofol (10-15 mg/kg/hr.) and intermittent intravenous boluses of doxacurium (Catalytica Pharmaceuticals, Grenville, NC.) (150μg/kg). The animals were placed

supine in the magnet, MR compatible ECG leads were positioned and a cardiac phased-array surface coil applied to the anterior chest wall.

Magnetic resonance imaging was performed in a Signa clinical 1.5 Tesla magnet (GE Medical Systems). After initial gradient echo series to localise the heart all subsequent imaging used the double inversion recovery fast spin echo sequence (2IRFSE). Non-selective and selective preparatory inversion pulses (Edelman et al. 1991), long echo train imaging and short radio frequency pulses, maximising blood flow suppression and minimising vessel motion artifacts, characterise this sequence. This allows for proton density and T2 weighted imaging through direct manipulation of the echo time (TE), using a constant repetition time (TR) of twice the R-R' interval (2RR') whilst maintaining cardiac gating of the sequence to end-diastole. The 2IRFSE permits the acquisition of single images within a time period (less than 30 seconds) that makes breath hold imaging possible and thus feasible in humans. Image slices were obtained perpendicular to the long axis of the coronary artery.

The inversion time (TI) was determined close to the null point of the blood signal and is based on the longitudinal relaxation (T1) value of the blood and the TR interval. A TE of 42 msec was chosen for T2W images on the basis of prior work estimating the T2 values for various atherosclerotic lesion components (Toussaint et al. 1996). Even though this was not essential for our model, which does not have lipid rich lesions, it showed that this technique could be transferred to humans. Thus, the parameters determining the contrast-to-noise ratio (CNR) were pre-determined on the basis of previously published work. MR imaging of 3 normal pigs was performed prior to commencing the study in order to assist the selection of MR parameters. However, a formal study for sequence optimisation was not performed. The following imaging parameters were used; T2W: TR / TE : 2RR' / 42 msec; PDW: TR

/ TE : 2 X RR' / 17 msec; receiver bandwidth ± 62.5 Hz; echo train length (ETL) 32; echo spacing (ESP) 4.4 msec; field of view (FOV) 10 X 10cm (or 12 X 12cm for fat suppressed images); matrix 256 X 256; slice thickness 5 mm; 2 signal averages. A saturation pulse was used to eliminate the epicardial fat signal and thus enhance the definition of the outer boundary of the vessel in some images. The in-plane resolution obtained was therefore 390-470 X 390-470 microns.

5. 2. 3. Euthanasia and Specimen Fixation

The animals were recovered after MR imaging. The following day euthanasia and subsequent coronary artery fixation were performed as previously reported (Gallo et al. 1998).

5. 2. 4. Ex vivo MR Imaging

On the evening before imaging, the specimens were removed from the fixative bath and washed overnight with water. The following morning, the samples were placed in resealable plastic bags, allowing direct application of a conventional 7.6-cm diameter surface coil to the specimen. Magnetic resonance images were obtained using the same parameters as for in vivo imaging. The TR was fixed at 2000ms (equivalent to an in vivo heart rate of 60 beats per minute) for both the PDW and T2W images.

5. 2. 5. Histopathology

Serial sections of the coronary arteries were cut at 5-mm intervals matching corresponding MR images. Co-registration was carefully performed by utilising one

or more landmark structures external to the coronary arteries, including arterial branches. Surrounding epicardial fat and myocardium were included in the section for arterial support during fixation and to enhance co-registration through the use of fiducial markers. Coronary specimens were first embedded in paraffin and thereafter sections 5-micron thick were cut and stained with a combined Masson's trichrome elastin stain.

5. 2. 6. Image and Data analysis

The MR images were transferred to a Macintosh computer for analysis. The histopathological sections were digitised to the same computer from a camera (Sony, 3CCD Video Camera) attached to a Zeiss Axioskop light microscope. The MR images were then matched with corresponding histopathological sections for the coronary (n=43) specimens.

Cross-sectional areas of the lumen and outer boundary of the vessels were determined for both MR images and histopathology by manual tracing with Image-Pro Plus (Media Cybernetics). For the in vivo MR images, the outer vessel boundary was defined as the vessel wall-epicardial fat interface; for histopathology, the outer boundary was defined as the dense adventitia-epicardial fat interface. From these measurements, mean wall thickness and vessel wall area was calculated for all sections. Separate investigators, blinded to the results of others, performed each analysis. This data was then analyzed as described by Bland and Altman (Bland et al. 1986). To define intra-observer and inter-observer variability, a random subset of coronary segment MR images (n=12) and corresponding histopathology sections were re-analyzed and the intraclass correlation coefficients determined.

All MR images obtained were analyzed for the presence or absence of vessel wall haematoma. On the basis of prior work on atherosclerotic plaque characterisation, we defined the presence of low signal (dark) regions within the otherwise high signal (bright) vessel wall on T2W images as indicating vessel wall haematoma (Toussaint et al. 1996; Worthley et al. 2000). Using the presence of vessel wall haematoma as identified by histopathology as the gold standard, the sensitivity and specificity of MR imaging to detect vessel wall haematoma in this study was determined.

5. 3. RESULTS

High resolution in vivo MR images of all three coronary arteries were obtained, with an in-plane resolution of 390-470 X 390-470 microns, including non-injured and injured segments, with consistent suppression of potential motion artifacts. Cardiac motion was minimised by gating the imaging acquisition to short periods during diastole, when myocardial motion is least. The use of propofol to maintain anaesthesia with mechanical ventilation provided stable anaesthesia of the pigs, maintaining the heart rate between 60 and 90 beats per minute, and we believe this assisted in obtaining good cardiac gating.

Ex vivo MR images of the same coronary segments were obtained from the intact heart and there was good correlation with the corresponding in vivo MR images (figure 5. 1), confirming the effectiveness of the motion suppression techniques used for the in vivo imaging.

Figure 5. 1

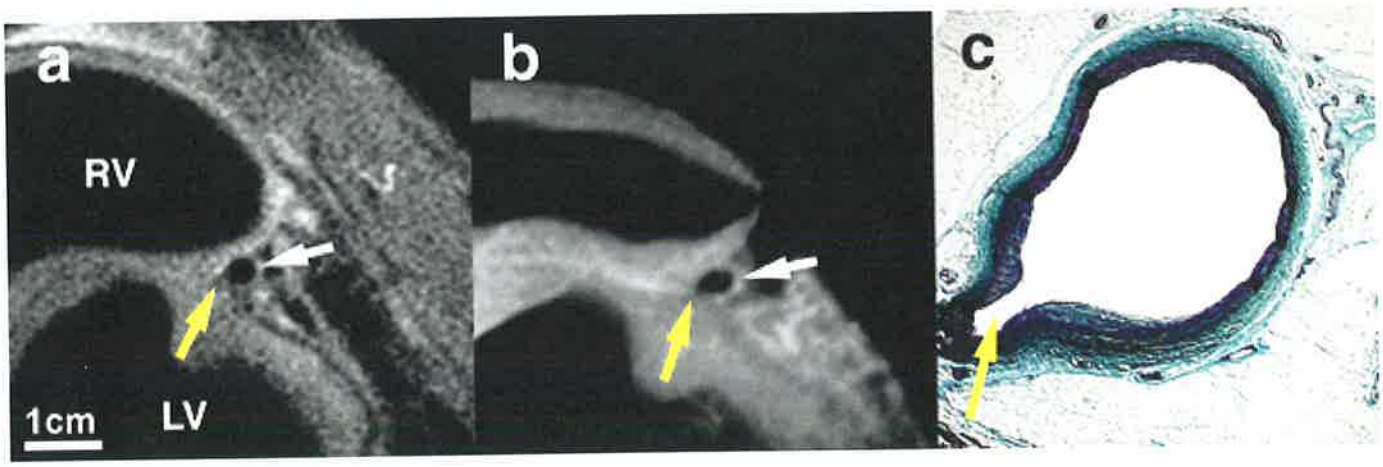

Magnetic resonance imaging of a non-injured coronary arterial segment (LAD). The MR images (a and b) are PDW fat suppressed images from the same position as evidenced by the same appearance of the left ventricular contours and the presence of the origin of the first septal perforator artery (yellow arrow). The thin vessel wall of the non-injured LAD (white arrow) is readily discerned from the surrounding epicardial fat in these images. The comparable appearance of the two MR images demonstrates the ability of the motion suppression as the in vivo image (a) has the same appearance as the ex vivo image (b). The corresponding histopathology section (c) confirms the vessel wall is thin. The presence of the first septal perforator from the histopathology section aids in the co-registration with the MR images.

Image slices were obtained perpendicular to the long axis of the coronary artery to be imaged providing cross-sectional images of the coronary arteries despite their non-linear course (figures 5. 2, 5. 3 and 5. 4).

Figure 5. 2

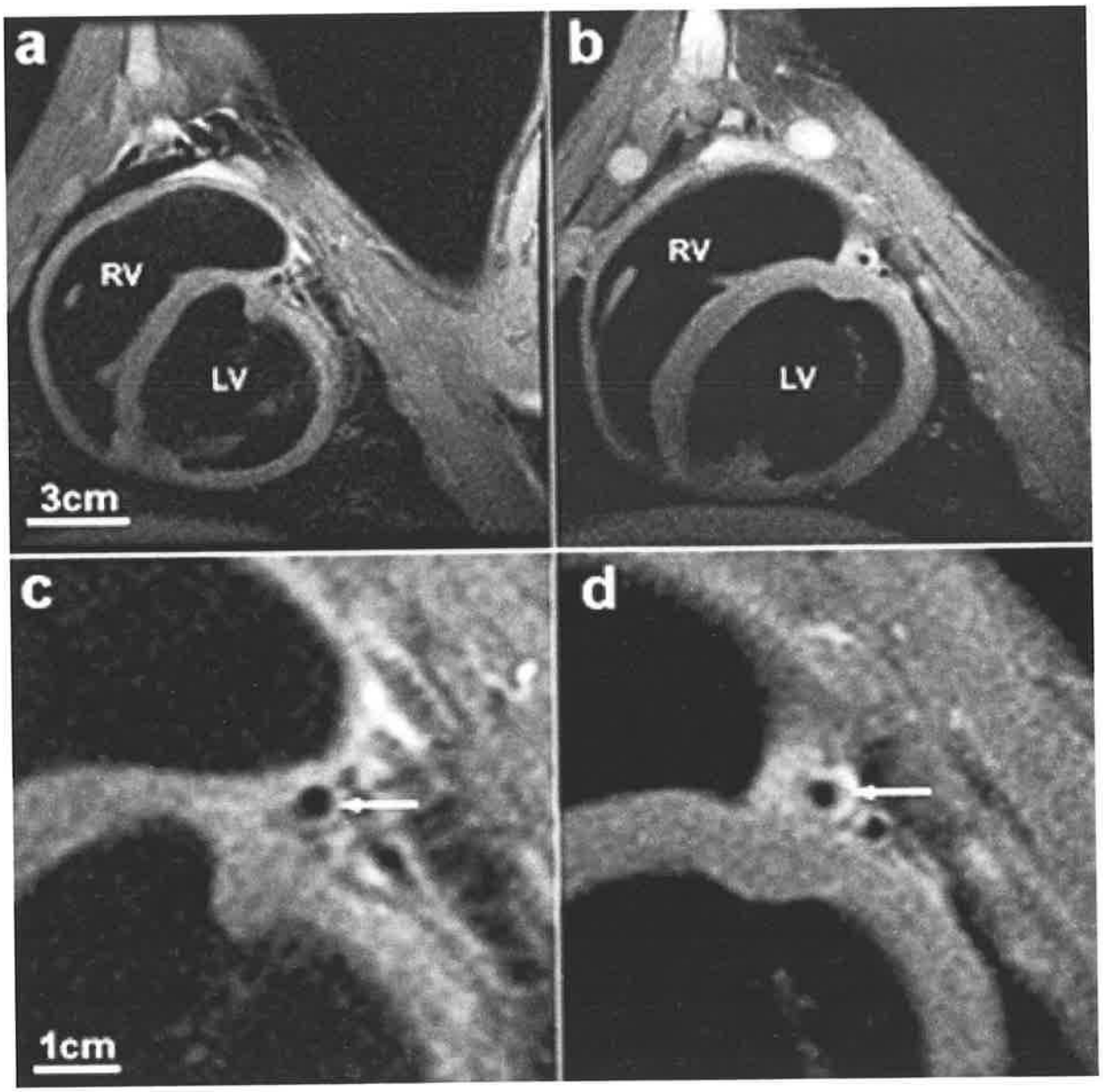

Detection of coronary artery lesions with magnetic resonance imaging. Unmagnified axial MR images showing short axis views through the heart from animals without (a) and with (b) balloon angioplasty. Magnifications of a and b (c and d respectively) showing the thin wall of the uninjured left anterior descending artery (white arrow, panel c) in comparison the eccentric thickening of the left anterior descending wall after balloon angioplasty (white arrow, panel d).

Figure 5. 3

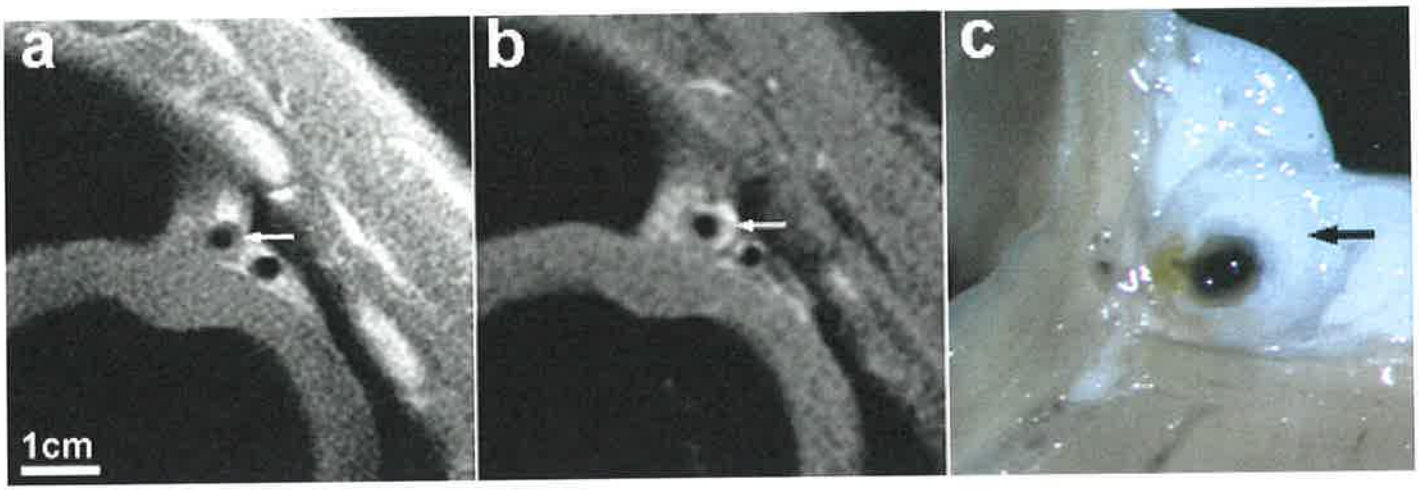

MRI and gross pathology from an injured LAD artery. The magnified MR images that are transverse to the left anterior descending artery after balloon injury are taken without (a) and with (b) fat suppression. Thus we can appreciate that suppression of the perivascular fat allows a clearer definition of the outer vessel wall. A good agreement between MR images and the corresponding gross pathological specimen (c) can be seen, as indicated by the eccentric coronary plaque which is mainly fibrocellular (white arrows in a and b, black arrow in c).

Figure 5. 4

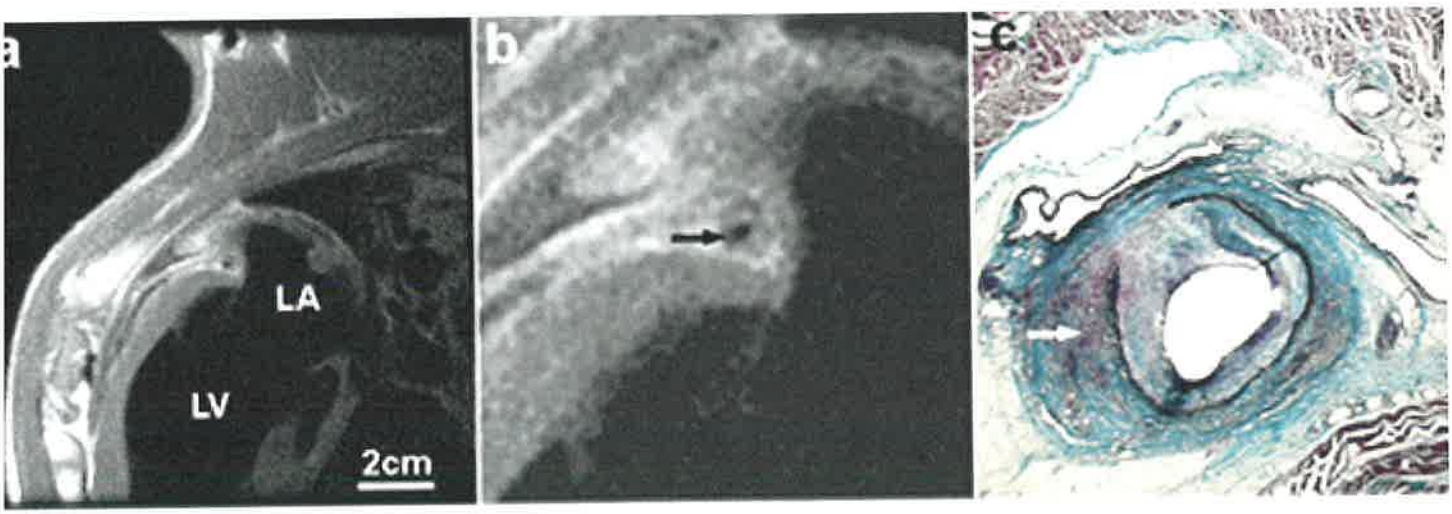

Identification of haematoma/thrombus. a, Unmagnified MR image (T2W) transverse to the long-axis of the LCx artery. b, Magnification of a showing a region of decreased signal intensity (black arrow) that appears to correlate with an area of haematoma/thrombus on the corresponding histopathology (white arrow, c). However, it is perhaps difficult to discern the region of lower intensity in the wall of the left circumflex from the artery lumen and the arterial adventitia that also appears dark. Clearly improvements in resolution and more than a single image weighting (i.e. T2W, T1W, and/or PDW) may be needed in order to accurately characterise coronary artery lesions in vivo.

Histological validation of the in vivo MR images from the coronary arteries was performed by careful matching of the MR images with the corresponding histopathology sections (n=43). This included sections from the LAD (n=18), LCx (n=13) and RCA (n=12). There was a good agreement between MR imaging and histopathological analysis for estimation of mean wall thickness and vessel wall area using Bland-Altman analyses, and this is summarised in figure 5. 5. The mean difference (MR imaging minus histopathology ± SD) for mean wall thickness was 0.26 ± 0.18mm (figure 5. 5a) and for vessel wall area was 5.65 ± 3.51mm^2 (figure 5. 5b). Thus, there was a tendency for measurements by MR imaging to be slightly larger than by histopathology. However, the reasonable standard deviations for paired measurements of both mean wall thickness and vessel wall area confirms agreement between MR imaging and histopathology.

Figure 5. 5a

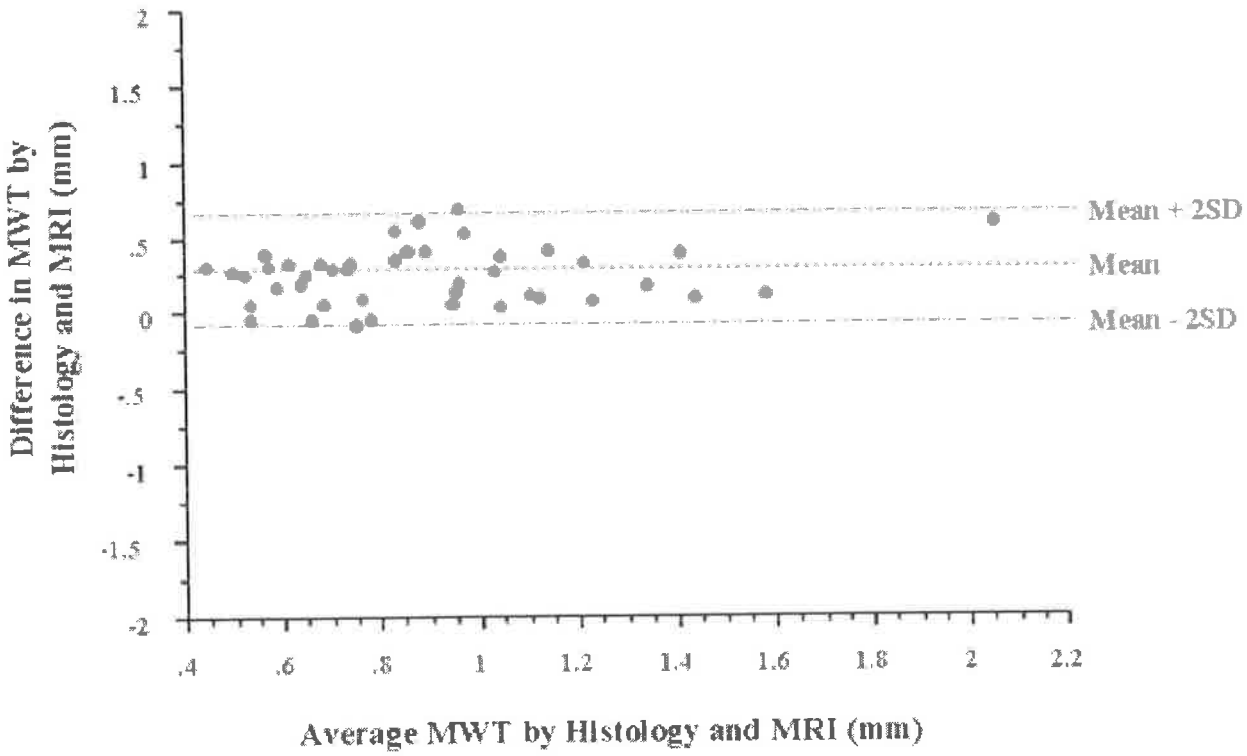

Figure 5. 5b

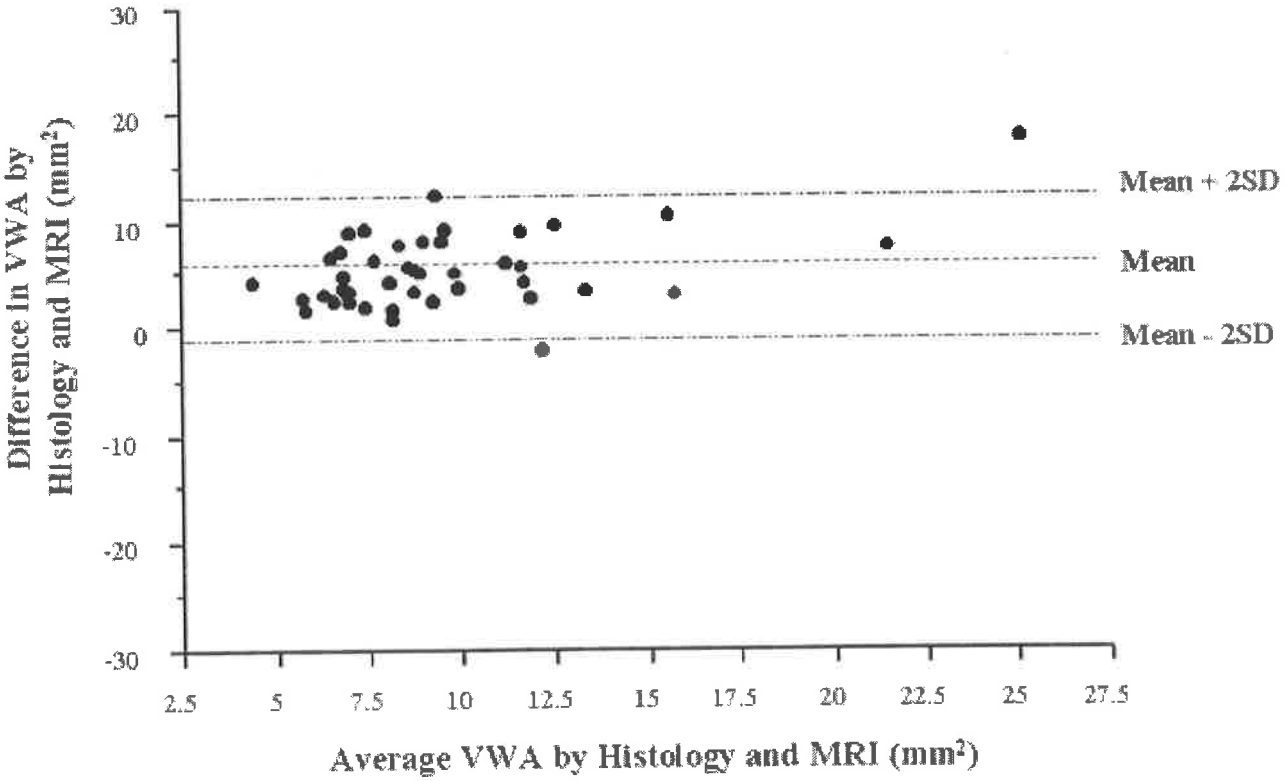

Bland-Altman analyses comparing the a. mean wall thickness and b. vessel wall area by MR imaging and histopathology.

T2W MR imaging was often able to identify intralesion haematoma/thrombus. A total of 11 of the 43 coronary segments analyzed had vessel wall haematoma/thrombus on histopathology. Using the criteria previously defined for MR detection of haematoma in the vessel wall, MR correctly identified 9 of the 11 coronary segments with vessel wall haematoma (specificity 82%) and correctly identified its absence in 27 of the 32 coronary segments without vessel wall haematoma (specificity 84%), (figure 4). Fibrocellular components of the coronary lesions were noted to appear as bright (high signal) structures in images where the epicardial fat signal was suppressed, but less bright than the surrounding epicardial fat in non-fat suppressed images (figure 3). However, in this study we were not able to test the ability of MR imaging to characterise atherosclerotic components in vivo.

Intra- and inter-observer variability assessment by intraclass correlation for both MR imaging and histopathology showed good reproducibility, with the intraclass correlation co-efficient ranging from 0.96 to 0.99 (table 5. 1).

Table 5. 1

Intraclass Correlation Coefficient for Intraobserver and Interobserver Variability for MR Imaging and Histopathology.

	Intraclass Correlation Coefficient	
	Mean Wall Thickness	**Vessel Wall Area**
Intraobserver		
MR Imaging	0.98	0.96
Histopathology	0.99	0.98
Interobserver		
MR Imaging	0.99	0.99
Histopathology	0.99	0.97

5. 4. DISCUSSION

In vivo noninvasive MR is able to provide high resolution images of coronary artery lesions in this porcine model. This study documents the feasibility of MR for coronary lesion imaging in vivo, but further studies are required to confirm the ability of MR to quantify accurately and characterise atherosclerotic lesions. Given that the size and anatomy of coronary arteries in the pig are comparable to the human, it may be possible to extrapolate this technique to humans.

We, as well as others, have recently demonstrated in vivo MR imaging of non-coronary atherosclerotic lesions in animals (Skinner et al. 1995; Fayad et al. 1998) and humans (Toussaint et al. 1996; Yuan et al. 1998). However, it is acknowledged that substantial improvements in the signal-to-noise ratio and reductions in the significant motion artifacts would be required before coronary atherosclerosis imaging could be performed. We have achieved this using cardiac gating, limited breath holding and a double inversion recovery fast spin echo imaging sequence, that is nevertheless compatible with currently available clinical 1.5 Tesla MR systems.

The small but consistent overestimation of mean wall thickness and vessel wall area by MR imaging in comparison to histopathology may relate to partial volume effects by MR imaging as well as shrinkage of the histopathology specimens as a consequence of their preparation. The Bland-Altman analyses show that in general there is a good agreement between MR and histopathological measurements, although further work is needed in order to improve the accuracy of MR imaging for the quantification of coronary lesions.

This experimental porcine model produces coronary artery lesions that contain fibrocellular and haemorrhagic regions without lipid deposition. Thus we are unable to test the ability of in vivo MR imaging to characterise coronary atherosclerotic lesions. MR imaging was able to correctly identify intralesion haematoma/thrombus in approximately 4 out of every 5 cases. This was confounded by the difficulty in distinguishing the low signal (dark) regions due to thrombus from the lumen and low signal adventitial structures. Indeed the resolution used both in-plane (390-470 microns) and through-plane (5mm) limit the ability to discern lesion composition. Thus, further improvements will be required in order to accurately characterise and quantify atherosclerotic lesions in human coronary arteries. Although caution should be used before extrapolating experimental studies to humans, given the previously mentioned anatomical characteristics of this model, this imaging technique could be translated to human coronary arteries.

The ability to perform noninvasive coronary artery imaging in humans could lead to the monitoring of potential future management options for patients both at risk of and with coronary artery disease. The noninvasive nature of this imaging could permit the longitudinal analysis of a given coronary atherosclerotic lesion in patients, and thus the potential exists for monitoring lesions over time before and during therapies such as lipid lowering.

Lipid lowering therapies have been shown to reduce cardiovascular mortality by 30-35% (Gould et al. 1998). Modification or stabilisation of vulnerable plaques in the coronary arteries by strengthening the fibrous cap and decreasing the lipid core has been proposed as the mechanism responsible for the observed beneficial clinical effect of these lipid lowering therapies (Archbold et al. 1998). Thus in the future one

might be able sequentially image and monitor such compositional atherosclerotic plaque changes with MR imaging.

We are reporting the feasibility of MR for the noninvasive imaging of coronary artery lesions. Continued improvements in MR imaging techniques and further studies are required however in order to confirm the ability of MR to noninvasively quantify and characterise coronary artery atherosclerosis in vivo.

Chapter 6

ATHEROSCLEROTIC AORTIC COMPONENT QUANTIFICATION BY NONINVASIVE MAGNETIC RESONANCE IMAGING: AN IN VIVO STUDY IN RABBITS.

TABLE OF CONTENTS

6. 1. INTRODUCTION

Atherosclerotic disease is one of the leading causes of morbidity and mortality in Western societies (Fuster et al. 1992; Fuster et al. 1992; Ross 1999). The composition of the atherosclerotic plaque, rather than the degree of stenosis, has emerged as the most important determinant for the thrombus-mediated acute coronary syndromes. Atherosclerotic plaques with a large lipid core surrounded by a thin fibrous cap are considered vulnerable because they are more prone to rupture and their contents more thrombogenic (Falk et al. 1995; Davies 1996). Therapeutic approaches for the prevention of acute coronary syndromes appear to act by stabilising the atheromatous plaque through modification of lesion composition (Libby 1995; Vaughan et al. 1996).

The possibility of an imaging modality able to quantify plaque composition could allow the stratification of patients at high risk for plaque rupture. Different imaging modalities for the assessment of plaque composition include magnetic resonance (MR) imaging, angioscopy, vascular ultrasonography and infrared imaging analysis. These techniques can discriminate wall components in normal and atheromatous arteries (Toussaint et al. 1995; Casscells et al. 1996; Toussaint et al. 1996; Brezinski et al. 1997; Kleber et al. 1998). Magnetic resonance techniques appear to be able to noninvasively identify and discriminate the components of complex atherosclerotic lesions both in ex vivo and in vivo settings (Skinner et al. 1995; Toussaint et al. 1995; Toussaint et al. 1996; Fayad et al. 1998) but have not been shown to allow quantification of the plaque components. The characterisation of atherosclerotic plaque composition, in particular the lipidic and fibrotic components, is important in understanding and predicting which lesions are at risk for disruption; therefore the quantification of different components of atherosclerotic lesions is important.

We report the feasibility of in vivo noninvasive high resolution MR imaging to quantify lipidic and fibrotic components in the aorta. We also demonstrate the utility of T2W images in the differentiation of these components within the plaque. This method provides the basis for the continued development and investigation of the use of MR imaging to noninvasively assess changes in the composition of atherosclerotic lesions.

6. 2. METHODS

6. 2. 1. Animal Model of Experimental Atherosclerosis

The animal model selected for this study was the New Zealand white rabbit (n=5, weight 3.0 to 3.5 kg). Atherosclerotic aortic lesions with fibrotic and lipidic components were induced by a combination of atherogenic diet (0.2% cholesterol) for 9 months and repeat balloon denudation, one week and thirteen weeks after initiation of the atherogenic diet. Aortic denudation of the aorta from the aortic arch to the iliac bifurcation was performed by withdrawal, with moderate resistance, of a 4 French Fogarty embolectomy catheter introduced through the iliac artery and passed into the aortic arch. Catheter insertion and inflation were repeated for four passes, after which the catheter was removed, the femoral artery tied, and the incision closed. All procedures were performed under general anaesthesia by intramuscular injection of ketamine (20mg/kg, Fort Dodge Animal Health, Fort Dodge, IA) and xylazine (10mg/kg, Bayer Corporation, Shawnee Mission, KS). All experiments were approved by the Mount Sinai School of Medicine animal management program, under accreditation from the American Association for the Accreditation of Laboratory Animal Care (AALAC).

6. 2. 2. MR Imaging

Nine months after the initiation of the diet, rabbits were anaesthetised fully with ketamine and xylazine as described above and placed supine in a 1.5 Tesla clinical MRI system (Signa, General Electric), using a conventional phased-array volume coil. Gradient-echo coronal images were used to localise the thoracic and abdominal aorta. Thereafter, sequential axial images (3-mm thickness) of the aorta from the arch

to the iliac bifurcation were obtained using a fast spin-echo sequence (total imaging time - 70 minutes) with an in plane resolution of 350 x 350 microns (PDW:TR/TE: 2300/17 msec; T2W: TR/TE:2300/60 msec, field of view [FOV]=9 x 9 cm, matrix 256 x 256, echo train length=8, signal averages=4). MR images were not cardiac-gated as described by others (Skinner et al. 1995; McConnell et al. 1999) and us (Worthley et al. 2000). Inferior and superior radio frequency saturation pulses were used to null signal from flowing blood in the inferior vena cava and aorta. Fat suppression was used to null the signal from the peri-adventitial fat.

6. 2. 3. Histopathology

Rabbits were euthanased within 48 hours of MR imaging by intravenous injection of "Sleepaway" 5 mL IV (Fort Dodge Animal Health, Fort Dodge, IA) after receiving heparin (100 IU/kg) to prevent post-mortem blood clotting. The aortas were immediately flushed with 250ml of physiological buffer (0.1mol/L PBS, pH 7.4) followed by perfusion fixation with 250ml cold (4^0C) 4% paraformaldehyde in 0.1% PBS. Perfusions were performed at 100mmHg. The entire aorta from the aortic root to the iliac arteries was excised. After perfusion fixation, all specimens were immersed in fresh fixative and stored at 4^0C. Serial sections of the aorta were cut at 3-mm intervals matching corresponding MR images. The total number of sections analyzed was 108, n=53 for the thoracic and supra renal aortic sections, 20 to 25 sections per rabbit. Co-registration was performed carefully by utilising the position of the aortic arch, renal arteries and iliac bifurcation. Aortic specimens were embedded in paraffin and sections 5-micron thick were cut and stained with combined Masson's trichrome elastin stain. A subset of abdominal aortic specimens were kept at -80^0C for specific lipid staining with Oil Red O (n=7).

6. 2. 4. Image and Data Analysis

The MR images were transferred to a Macintosh computer for further analysis. The histopathological sections were digitised to the same computer from a camera (Sony, 3CCD Video Camera) attached to a Zeiss Axioskop light microscope. The MR images were matched with corresponding histopathological sections for the aortic specimens (n=108).

Cross-sectional areas of the lumen and outer boundary of each aortic section were determined for both MR images and histopathology by manual tracing with Image-Pro Plus (Media Cybernetics) as previously reported (Worthley et al. 2000). From these measurements, mean wall thickness (MWT), vessel wall area (VWA) and lumen area were calculated. In those MR images corresponding to the subset of atherosclerotic plaques (n=7) prepared by frozen sectioning and staining with Oil Red O, lipidic and fibrotic areas were measured by manual tracing as described above. Mean wall thickness and vessel wall area were analyzed with CME staining, lipidic and fibrotic areas were analyzed with Oil Red O staining. Two independent investigators, each blinded to the results of the other, performed the analyses.

Aortic sections in which fibrotic and lipidic components could be separately identified on the MR image (n=23) were further analyzed in order to assess the contrast ratios between fibrotic and lipidic components for PDW and T2W images. For each MR image of the complex plaques, signal intensity was measured for PDW and T2W images at two separate points within both the fibrotic (defined as high signal regions) and lipidic (defined as low signal regions) areas as previously reported (Skinner et al. 1995; McConnell et al. 1999). This distinction by MR was confirmed by histopathology using combined Masson elastin staining.

6. 2. 5. Statistical Analysis

The correlations between measurements of mean wall thickness (MWT), vessel wall area (VWA), lumen area, lipidic and fibrotic area by MR and histopathology were analysed by simple linear regression with 95% confidence intervals (Statview, SAS Institute Inc.). The ratios between the signal intensity for fibrotic and lipidic regions were obtained for each image and displayed as the mean ± standard deviation for PDW and T2W images. Comparison between the ratios for PDW and T2W images were made using a Student's paired t test. A p value < 0.05 was considered statistically significant.

To define intra-observer and inter-observer variability for the quantification of lipidic and fibrotic components, the MR images of aortic atherosclerotic plaques used for comparison with Oil Red O staining (n=7) were re-analysed and the intraclass correlation coefficients determined.

6. 3. RESULTS

6. 3. 1. Atherosclerotic Characterisation by Histopathology

The combination of the atherogenic diet for 9 months and repeat balloon denudation of the whole aorta induced a significant thickening of the arterial wall due to the increase in lipid and fibrotic components in both thoracic and abdominal parts of the aorta. However, unlike humans, no calcium or intra-plaque thrombus is associated with this model. The staining clearly allowed the discrimination of lipidic and fibrotic areas. The lipidic areas were mainly located in the deeper part of the wall while the fibrotic areas showed a more luminal distribution (figure 6. 1).

Figure 6. 1

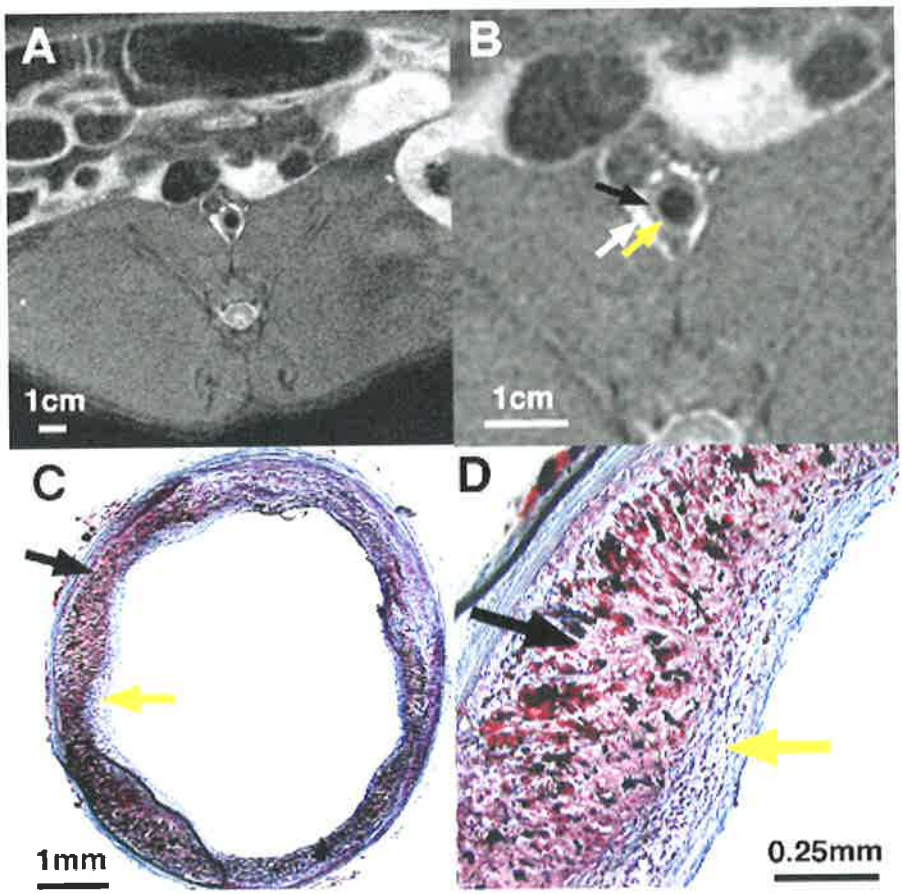

A - In vivo magnetic resonance (MR) image (PDW) of a rabbit abdominal aorta. B - The same section magnified (see scale) showing a concentric atherosclerotic lesion and bright peri-adventitial lymphatics (white arrow). Inside the lesion, one can differentiate a dark area (black arrow) and a white area (yellow arrow). C - The corresponding histopathology section stained with Oil Red O showing the lipidic area (black arrow) and the non lipidic (fibrous) area (yellow arrow). D - Magnification (see scale) of C showing the lipid-laden foam cells staining red.

Histopathology sections were compared with MR imaging for mean wall thickness and vessel wall area (n=108) and atherosclerotic component quantification (n=7), and MR images with both fibrotic and lipidic components of the plaque identifiable (n=23) underwent signal intensity analysis.

6. 3. 2. MR Imaging

The PDW and T2W axial images showed marked wall thickening in the aorta, from the aortic arch to the iliac bifurcation. In these in vivo images, the collagen-rich areas appeared brighter than the foam-cell rich areas, which appeared darker. There was a good correlation between the images obtained in vivo and the histopathological sections of the aorta (figure 6. 1). Co-registration was obtained by utilising the position of the aortic arch, renal arteries and iliac bifurcation (figure 6. 2).

Figure 6. 2

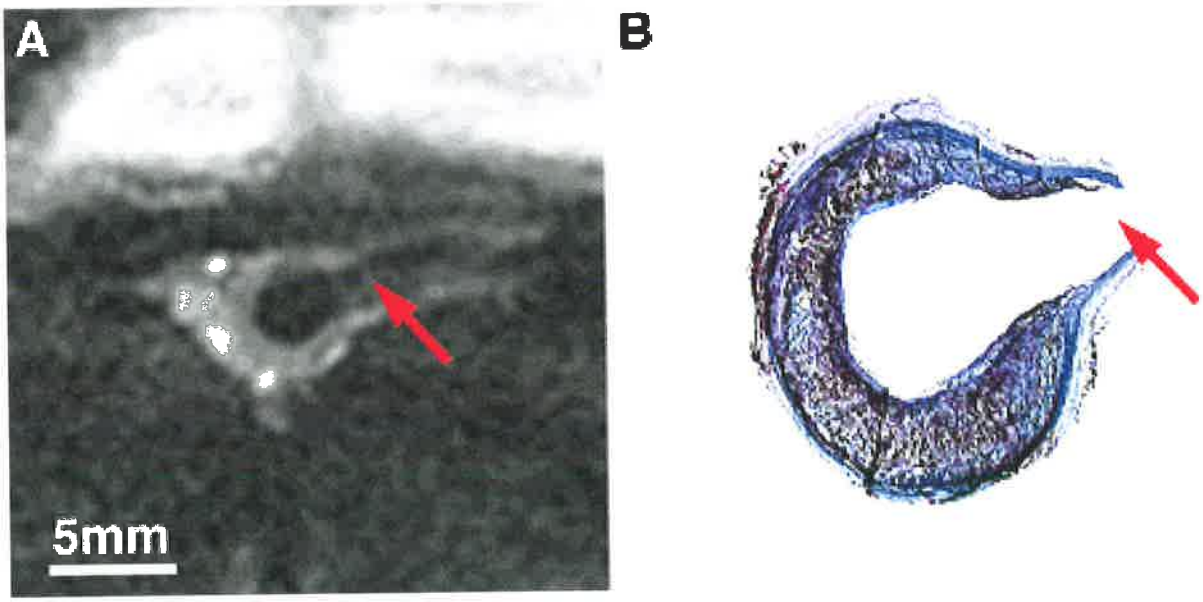

In vivo MR axial image (T2) of abdominal aorta at the level of the left renal artery (red arrow). B - Corresponding histopathological section illustrating the use of left renal artery (red arrow) as anatomical landmark for matching MR imaging and histopathology.

6. 3. 3. Quantification of Plaque Composition

The fast spin-echo images showed different signal intensity areas identifying fibrous and lipidic plaque components. A relatively dark area (low signal intensity both on T2W and PDW images) and a bright area adjacent to the lumen (high signal intensity both on T2W and PDW images) were easily distinguished (figure 6. 3). There was a significant correlation ($p<0.05$) between MRI (T2W images) and histopathology for analysis of lipidic areas ($r=0.81$, y[MR]=1.25+1.02x[histo]). A significant correlation ($p<0.05$) between MRI (T2W images) and histopathology for analysis of fibrous areas ($r=0.86$, y[MR]=0.53+1.35x[histo]) was also observed.

Figure 6. 3

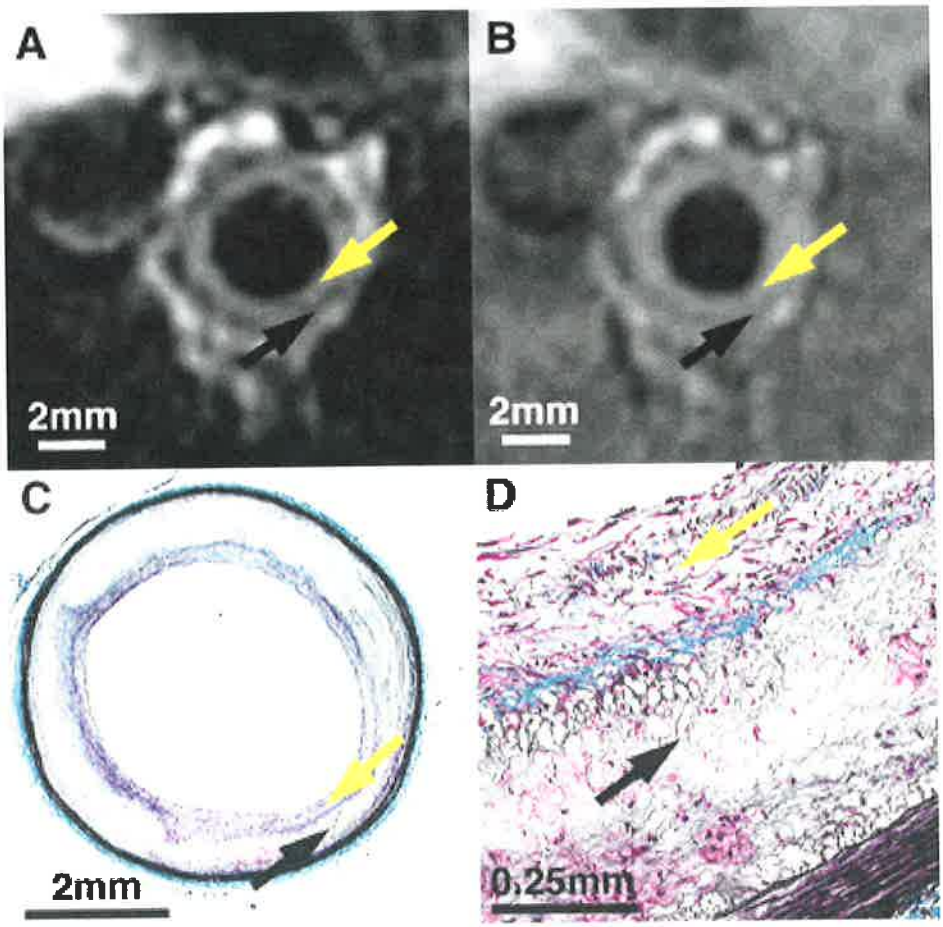

Differentiation of lipidic area (dark arrow) from fibrotic area (yellow area) of abdominal aortic lesions with in vivo (A) T2W image and (B) PDW image. The greater contrast between fibrotic and lipidic components of the atherosclerotic plaque with T2W imaging is evident. C - Corresponding histopathological section stained with a combined Masson's elastin stain. D - Magnification of C showing the lipid-laden foam cells and the fibrotic cap.

6. 3. 4. Signal Intensity Analysis

Signal intensity was measured, in PDW and T2W images, at two separate points within both the fibrotic and lipidic areas. T2W images demonstrated a significantly ($p<0.001$) higher contrast between fibrotic areas and lipidic areas than PDW images as assessed by the ratios of their signal intensities (1.83±0.26 versus 1.36±0.16).

6. 3. 5. Atherosclerotic Wall Measurements

A significant correlation ($p<0.001$) was observed for mean wall thickness (MWT) and vessel wall area (VWA), correlates of atherosclerotic burden, between MR imaging and histopathology ($r=0.87$, y[MR]=0.17+0.83x[histo] and $r=0.85$, y[MR]=0.22+1.50x[histo] respectively) throughout the whole aorta (figure 6. 4). The correlation was still observed considering only the thoracic and upper part of the abdominal aorta susceptible to respiratory motion artifacts ($r=0.83$, y[MR]=0.28+0.65x[histo] for MWT and $r=0.77$, y[MR]=2.03+1.37x[histo] for VWA) (figures 6. 4 and 6. 5).

Figure 6. 4

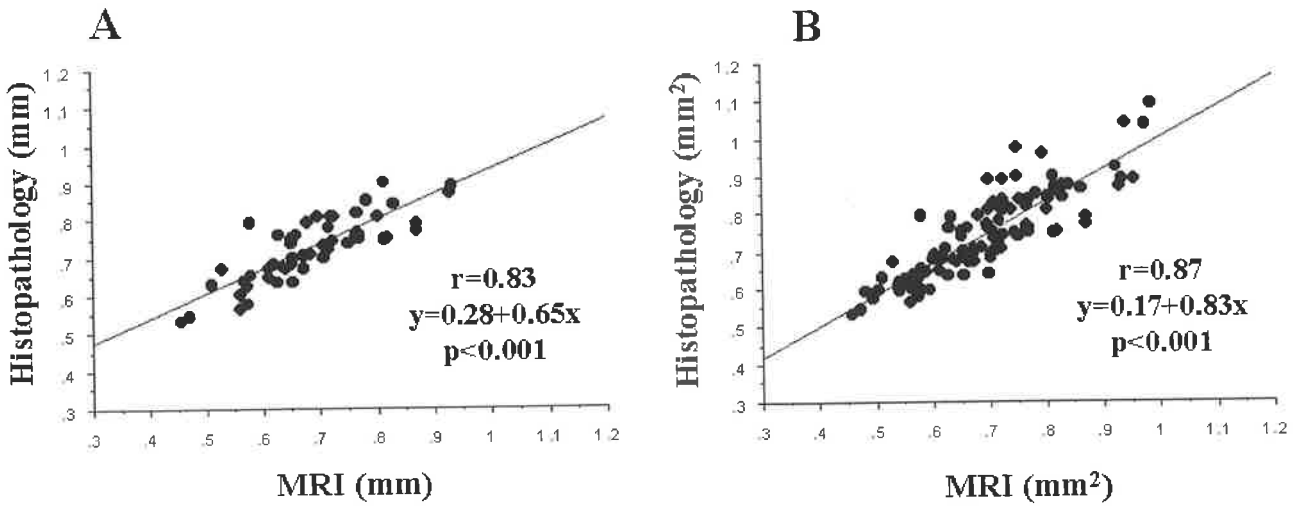

Linear regression analyses showing excellent correlation of the mean wall thickness (MWT) as measured by MR and histopathology A - in the thoracic and upper part of the abdominal aorta ($r=0.83$, $p<0.001$)., and B in the whole aorta ($r=0.87$, $p<0.001$).

Figure 6. 5

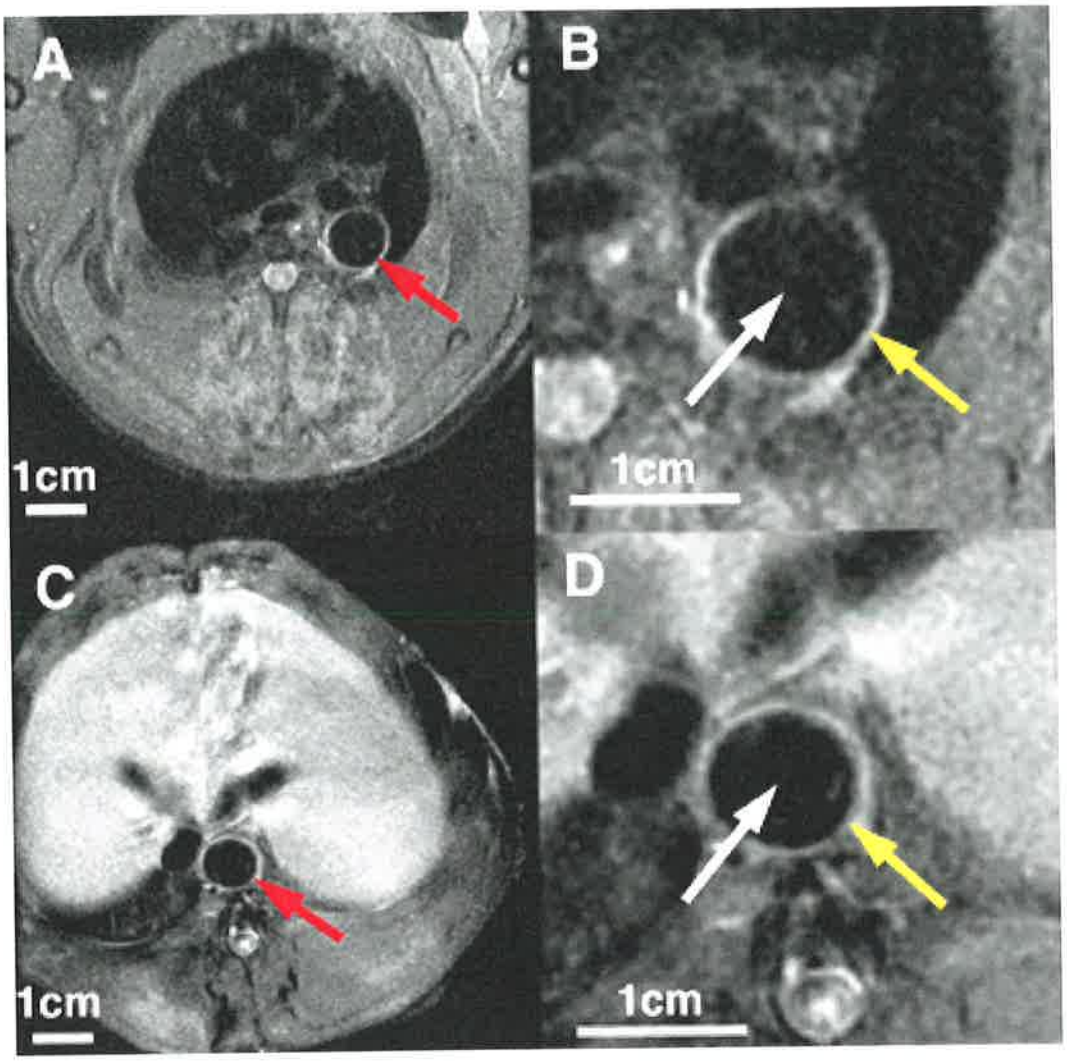

A - In vivo MR image (T2W) of thoracic aorta (red arrow). Despite potential cardiac and respiratory motion, the thoracic aorta, which is adherent to the paraspinal structures, is relatively preserved from such artifacts and is well delineated. B - the same section magnified showing the differentiation between lumen (white arrow) and vessel wall (yellow arrow). C - In vivo MR image (T2W) of the upper part of the abdominal aorta (red arrow), adjacent to the diaphragm, potentially susceptible to respiratory motion, is well delineated. D - the same section magnified showing the differentiation between lumen (white arrow) and vessel wall (yellow arrow).

Intra- and inter-observer variability assessment by intraclass correlation for MR imaging of fibrotic and lipidic components showed good reproducibility, with the intraclass correlation co-efficients ranging from 0.91 to 0.98 (table 6. 1).

Table 6. 1

INTRACLASS CORRELATION COEFFICIENT FOR INTRAOBSERVER AND INTEROBSERVER VARIABLITY FOR MR IMAGING

	Intraclass Correlation Coefficient	
	Fibrotic Area	Lipidic Area
Intraobserver		
MR Imaging	0.98	0.97
Interobserver		
MR Imaging	0.94	0.91

6. 4. DISCUSSION

Our study has demonstrated for the first time that in vivo MR imaging can reliably and noninvasively detect and quantify fibrous and lipid components of aortic atherosclerosis in a rabbit model. We have shown the superiority of T2W over PDW imaging in the discrimination of the different components within the plaques. Despite respiratory and cardiac motions, the thoracic and abdominal aorta was well characterised in this rabbit model.

Given the importance of plaque composition in plaque vulnerability and subsequent thrombogenicity, the possibility of assessing plaque composition could have significant prognostic value (Falk et al. 1995; Davies 1996). The quantification of different components within the plaque is important because the individual makeup of the atherosclerotic plaque has been identified as a dominant prognostic factor. This could allow both the stratification of patients at risk of plaque disruption and the selection of the most appropriate therapeutic strategy based on lesion composition. Studies of coronary disease have shown that its progression is episodic and unpredictable by angiography (Ambrose et al. 1988; Lichtlen et al. 1992). The sites at which the thrombotic lesions occurred are usually of mild to moderate stenotic severity (Haft et al. 1988). The combination of a large core and a thin cap is the major determinant of plaque vulnerability (Falk et al. 1995). These two major determinants of plaque vulnerability, core size and cap thickness, are not statistically related (Mann et al. 1996). A technique that could assess not only the measurements of the wall thickness and vessel wall area but also measurements of different components of the lesions in atherosclerotic arteries is crucial for assessing plaque vulnerability. Therefore, we have focused on the ability of a clinical magnet and a conventional coil to accurately quantify lipidic and fibrotic areas within the plaques.

Currently, as histopathological methods provide the most accurate method of determining atherosclerotic plaque composition, we have compared MR images to histopathological sections. Angiographic techniques can only assess the severity of luminal narrowing. Electron-beam computed tomography (EBCT) is noninvasive, however it only permits the assessment of a calcium score in the arterial wall (Celermajer 1998). Other imaging techniques that have recently improved the observation of the arterial wall, such as intravascular ultrasound and angioscopy, are invasive (Brezinski et al. 1997; Kleber et al. 1998). To date, none of these imaging techniques have demonstrated their ability to measure and quantify the different components of atherosclerotic plaques. Quantitative assessments of atherosclerotic plaque size in vivo using high resolution MR imaging in human carotid arteries have been obtained (Yuan et al. 1998). These authors showed the possibility of in vivo MR imaging for measuring atherosclerotic burden of atherosclerotic carotid arteries but were not able to quantify the plaque composition. Good results for the determination of wall thickness and plaque area were obtained with high resolution intravascular MR imaging in hyperlipidaemic rabbits (Zimmermann-Paul et al. 1999). Using this invasive MR imaging technique, the possibility to assess plaque size and distinguish the components of plaque was shown in isolated thoracic human aortas obtained at autopsy (Correia et al. 1997).

In our study, we were able to assess plaque size, discriminate the fibrotic and lipidic components of plaques, and quantify these components. As in previous reports (Skinner et al. 1995; Yuan et al. 1996), the lipidic areas have a low signal on T2W and PDW images and are very distinctive from the fibrous areas which have a high signal on T2W and PDW images. Proton density weighted imaging (PDW) with an echo time of 17 ms has some T2 character. This could explain the low signal of the lipidic areas with PDW imaging. Analyzing the components of the plaques, we

showed a significant correlation between MR imaging and histopathology with Oil Red O staining for analysis of lipid (r=0.81) and fibrous (r=0.86) areas. The fibrous cap as identified by MRI appears thicker than that by histopathology. However, there is a good correlation between MR and histopathological quantification of the fibrous areas as evidenced by the statistically significant correlation co-efficient (r=0.86, $p<0.05$). The fibrous cap is thin (around 0.25 to 0.5 mm) and with an in-plane resolution of 0.35mm, clearly there will be a tendency to over-estimation with this MR technique; a concept related to "partial volume averaging". The lipidic areas are larger, as indicated by histopathology, and thus less subject to over-estimation by MR with the resolution described. Once again, although there is a tendency to over-estimation with MR, it is less than for the fibrotic areas. Despite these potential limitations, there was a good correlation between the two techniques for both components of the atherosclerotic lesion in this model, and thus the potential for serially documenting changes over-time exists. The quantification of atherosclerotic components is important given therapeutic approaches like lipid lowering appear to exert a beneficial effect by increasing the fibrotic and decreasing the lipidic components of the plaque (Shiomi et al. 1995; Aikawa et al. 1998).

We have shown that in this model the T2W images had greater contrast between the lipidic and fibrotic areas within the plaque than the PDW images. Previous reports have concluded that PDW images are the most useful for demonstrating atherosclerotic plaque components in a rabbit model (Yuan et al. 1996). Our data show that T2W images have the highest contrast between these components of the plaques. We used the same echo time (17 ms) for our PDW imaging as other studies, for comparability (Yuan et al. 1996).

The analysis of the mean wall thickness and the vessel wall areas both demonstrated a significant correlation between MR imaging and histopathology. Due to motion artifacts affecting the thoracic aorta, previous authors have only focused on identification of atherosclerotic plaques in the abdominal aorta of New Zealand white rabbits (Skinner et al. 1995; Manninen et al. 1998). One of the difficulties for in vivo MR imaging is related to motion artifacts. Despite the cardiac and respiratory motion, we found that the thoracic aorta, which is adherent to the paraspinal structures, was relatively spared from these artifacts. Mean wall thickness and vessel wall areas showed a significant correlation between MR imaging and histopathology for the thoracic and supra renal aortic sections, a region of the aorta susceptible to respiratory artifacts from the diaphragm.

In this study we observed a small, consistent over-estimation of plaque components and vessel wall parameters by MR imaging as compared with histopathology. This involves both partial volume effects of MR imaging (as discussed above) plus the fact that histopathological specimen preparation leads to dessication and thus shrinkage. However, the correlation between the parameters was significant and consistent with previous studies (Skinner et al. 1995; McConnell et al. 1999).

Of interest is the fact that our study was conducted with a conventional coil and on a whole-body 1.5 Tesla clinical scanner. This indicates that our methods could be applied to the study of human atherosclerosis, and even coronary arteries, given the comparable size of the rabbit abdominal aorta. However, cardiac and respiratory motion, as well as spatial resolution, remain significant limitations for human coronary imaging. The use of 2-D imaging techniques, such as that used in this study, limits the "through-plane" or "z-axis" resolution. Thus, despite high "in-plane" resolution, the potential for "volume averaging" exists, leading to potential

errors in measurements. By assuring perpendicularity to the aorta of the MR image, and limiting the slice thickness, this can be attenuated. However, future efforts to improve resolution in all three axes using overlapping 2-D MR slices or especially using a 3-D imaging sequence warrant further study. Furthermore, the increased body mass of humans limits the signal-to-noise ratio for coronary artery MR imaging. In the future, the measurements of the different components of the plaque could provide a new prognostic tool useful in the management of atherosclerosis. This method may permit selection of the most appropriate treatment on the basis of the qualitative and quantitative characteristics of atherosclerotic lesions.

In conclusion, our data indicate that in vivo MR imaging has the potential to quantify noninvasively lipidic and fibrotic areas in atherosclerotic plaques using current clinical MR techniques. This method provides the basis for the continued development and investigation of the use of MR imaging to noninvasively assess changes in the composition of atherosclerotic lesions.

Chapter 7

SERIAL NONINVASIVE MAGNETIC RESONANCE IMAGING DOCUMENTS PROGRESSION AND REGRESSION OF INDIVIDUAL PLAQUES

TABLE OF CONTENTS

7. 1. INTRODUCTION

Atherosclerotic diseases remain the leading causes of morbidity and mortality in Western society (Theroux et al. 1998). The pathogenesis of the acute coronary syndromes is commonly atherosclerotic plaque disruption and subsequent thrombosis (Falk et al. 1995; Theroux et al. 1998). Atherosclerotic plaque composition, rather than the degree of arterial stenosis, appears to be a critical determinant of both risk of rupture and subsequent thrombogenicity (Fernandez-Ortiz et al. 1994; Toschi et al. 1997). In particular a large lipid core and a thin fibrous cap render a lesion susceptible or vulnerable to disruption and thrombosis (Falk et al. 1995; Davies 1996; Lee et al. 1997). Therapeutic interventions such as lipid lowering with statins have been shown to reduce cardiovascular mortality by 30-35% (Gould et al. 1998). Modification or stabilisation of the vulnerable plaques in the coronary arteries, by strengthening the fibrous cap and decreasing the lipid core, has been proposed as the mechanism responsible for the observed beneficial clinical effect of these lipid lowering therapies (Fuster et al. 1995; Archbold et al. 1998; Libby et al. 1998).

An imaging modality able to quantify atherosclerotic plaque composition could potentially allow not only the identification of these vulnerable atherosclerotic lesions, but also monitor effects of therapeutic interventions for stabilisation on the plaque composition (Fuster et al. 1999).

Magnetic resonance (MR) imaging is able to quantify and characterise noninvasively lesions in humans and animal models of atherosclerosis (Skinner et al. 1995; Toussaint et al. 1996; Fayad et al. 1998; Yuan et al. 1998; McConnell et al. 1999; Shinnar et al. 1999; Worthley et al. 2000). MR has been used to observe the difference in atherosclerotic plaque size between groups of animals under different

conditions (McConnell et al. 1999). However, the ability of MR to monitor serially changes in size and composition of a given atherosclerotic plaque over time has not been reported. This advance could allow the serial monitoring a given plaque over time, thus permitting studies of therapies for atherosclerotic plaque stabilisation.

We report the ability of serial noninvasive MR imaging to monitor changes in lipidic and fibrotic components of the same atherosclerotic plaques as well as plaque size and in a rabbit model, under conditions of dietary cholesterol lowering.

7. 2. METHODS

7. 2. 1. Animal Model of Experimental Atherosclerosis

Complex atherosclerotic aortic lesions were induced in New Zealand white rabbits (3.0 to 3.5 kg, n=15) by a combination of atherogenic diet (0.2% cholesterol) and sequential balloon denudation, one week and thirteen weeks after initiation of the atherogenic diet. Aortic denudation of the aorta from the aortic arch to the iliac bifurcation was performed by four withdrawals, with moderate resistance, of a 4Fr Fogarty embolectomy catheter introduced through the iliac artery. All procedures were performed under general anaesthesia by intramuscular injection of ketamine (Fort Dodge Animal Health, Fort Dodge, IA) (20mg/kg) and xylazine (Bayer Corporation, Shawnee Mission, KA) (10mg/kg) and were approved by the Mount Sinai School of Medicine animal management program, under accreditation from the American Association for the Accreditation of Laboratory Animal Care (AALAC).

7. 2. 2. Atherosclerosis Progression and Regression

A sub-group of animals (n=5) were sacrificed after atherosclerosis induction for validation of MR imaging with histopathology at this time-point. After 36 weeks of the atherogenic diet (atherosclerosis induction), the remaining animals were randomised to either continue the atherogenic diet (atherosclerosis progression, n=5) or resume normal chow (atherosclerosis regression, n=5) for a further 24 weeks. Thereafter, these animals were also sacrificed for comparison between the MR images and histopathology.

7. 2. 3. MR Imaging

MR imaging was performed at three time-points; baseline (prior to commencing the atherogenic diet), atherosclerosis induction and atherosclerosis progression or regression. Thus each animal acted as its own control, allowing serial imaging of individual atherosclerotic plaques. The animals were fully anaesthetised with ketamine and xylazine as described above and placed supine in a 1.5 Tesla MRI system (Signa, General Electric), using a conventional phased-array volume coil. Fast gradient-echo coronal images were used to localise the abdominal aorta. Sequential axial images (3-mm thickness) of the abdominal aorta from the renal arteries to the iliac bifurcation were obtained using a fast spin-echo sequence with an in plane resolution of 350 x 350 μm (PDW :TR/TE: 2300/17 msec; T2W: TR/TE:2300/60 msec, field of view (FOV)=9 x 9 cm, matrix 256 x 256, echo train length=8, signal averages=4). Inferior and superior radio frequency saturation pulses were used to null signal from flowing blood in the inferior vena cava and aorta. Fat suppression was used to null the signal from the peri-adventitial fat, in order to minimise chemical shift artifacts.

7. 2. 4. Histopathology

Rabbits were euthanased within 24 hours of MR imaging by intravenous injection of "Sleepaway" 5 mL IV (Fort Dodge Animal Health, Fort Dodge, IA) after receiving heparin (100 U/kg) to prevent post-mortem blood clotting. The aortas were immediately flushed with 250ml of physiological buffer (0.1mol/L PBS, pH 7.4) followed by perfusion fixation with 250ml cold (4^0C) 4% paraformaldehyde in 0.1% PBS at 100mmHg. After perfusion fixation, all specimens were immersed in fresh fixative and stored at 4^0C. Serial sections of the aorta were cut at intervals matching

corresponding MR images. Co-registration was carefully performed utilising the position of the renal arteries and iliac bifurcation. Aortic specimens were embedded in paraffin and sections 5-micron thick were cut and stained with combined Masson's trichrome elastin stain. A subset of abdominal aortic specimens was kept at -80^{0}C for specific lipid staining with Oil Red O.

7. 2. 5. Image and Data Analysis

Histopathological sections were digitised to a Macintosh computer from a Sony 3CCD video camera attached to a Zeiss Axioskop light microscope. The MR images were transferred to the same Macintosh computer and matched with the corresponding histopathological sections (atherosclerosis induction - n=50, atherosclerosis progression/regression – n=70). Cross-sectional areas of the lumen and outer boundary of each aortic section were determined for both MR images and histopathology by manual tracing with Image-Pro Plus (Media Cybernetics). From these measurements, mean wall thickness (MWT - a computer generated value), vessel wall area (VWA) and lumen area were calculated. Areas containing lipidic and fibrotic material were also measured, using T2W images as previously described. In brief, lipidic regions are low signal and fibrotic regions are high signal, thus potentially allowing differentiation. The ability of MR imaging to quantify these regions with computer assisted morphometry was reported in the previous chapter.

The study design allowed for the serial comparison between MR images from the same animals at the same aortic site (as confirmed by distance from the renal arteries and the iliac bifurcation) over the three time-points. Thus serial data about changes in the size and composition of the vessel wall with MR imaging could be analyzed. Histopathological measurements of mean wall thickness and vessel wall area were

analyzed with sections stained by combined Masson elastin stain (CME); lipidic and fibrotic areas were analyzed with Oil Red O staining. Two independent investigators blinded to the results of others performed the analyses.

7. 2. 6. Statistical Analysis

The correlations between measurements of mean wall thickness (MWT), vessel wall area (VWA), lipidic and fibrotic area by MR and histopathology were analyzed by simple linear regression with 95% confidence intervals (Statview, SAS Institute Inc). Comparisons of MR images of the same aortic sections from the same animals between different time points were made using paired students t-tests. All values are expressed as mean ± SEM. A p value < 0.05 was used to indicate statistical significance.

7. 3. RESULTS

7. 3. 1. Serum Lipid Profiles

The serum total cholesterol increased to 774±169 mg/dL after 9 months of the atherogenic diet. In the rabbits then randomised to dietary regression, the serum total cholesterol returned to the normal range, decreasing to 28±6 mg/dL, whereas in the dietary progression group the serum total cholesterol remained significantly elevated 936±340 mg/dL.

7. 3. 2. Serial MR Imaging of Vessel Wall Parameters

There was a significant ($p<0.0001$) increase in the atherosclerotic burden after the 9 month induction period. The vessel wall area (VWA) and mean wall thickness (MWT) increased from 4.62±0.09 mm^2 to 7.59±0.26 mm^2 and 0.38±0.01 mm to 0.65±0.02 mm respectively, as determined by serial MR imaging.

Comparison of vessel wall parameters determined by serial MR imaging in animals that were returned to normal chow diet after atherosclerosis induction (i.e. atherosclerosis regression group) confirms that there is a significant ($p<0.0001$) reduction in atherosclerotic burden in this group. Serial MR imaging at the three time points in these animals confirms the progression and regression of atherosclerosis in the same animals (Baseline: VWA 4.81±0.12 mm^2, MWT 0.38±0.01 mm; Atherosclerosis Induction: VWA 7.71±0.37 mm^2, MWT 0.62±0.03; Atherosclerosis Regression: VWA 6.21±0.24, MWT 0.52±0.02 mm - figure 7. 1).

Similarly in animals randomised to continued atherosclerosis progression with the continuation of the atherogenic diet, there was a further significant increase ($p<0.0001$) in atherosclerotic burden as determined by measurements of vessel wall parameters (Baseline: VWA 4.35±0.13 mm^2, MWT 0.38±0.01 mm; Atherosclerosis Induction: VWA 7.41±0.35 mm^2, MWT 0.70±0.02; Atherosclerosis Progression: VWA 9.75±0.40, MWT 0.96±0.03 mm - figure 7. 1).

Figure 7. 1

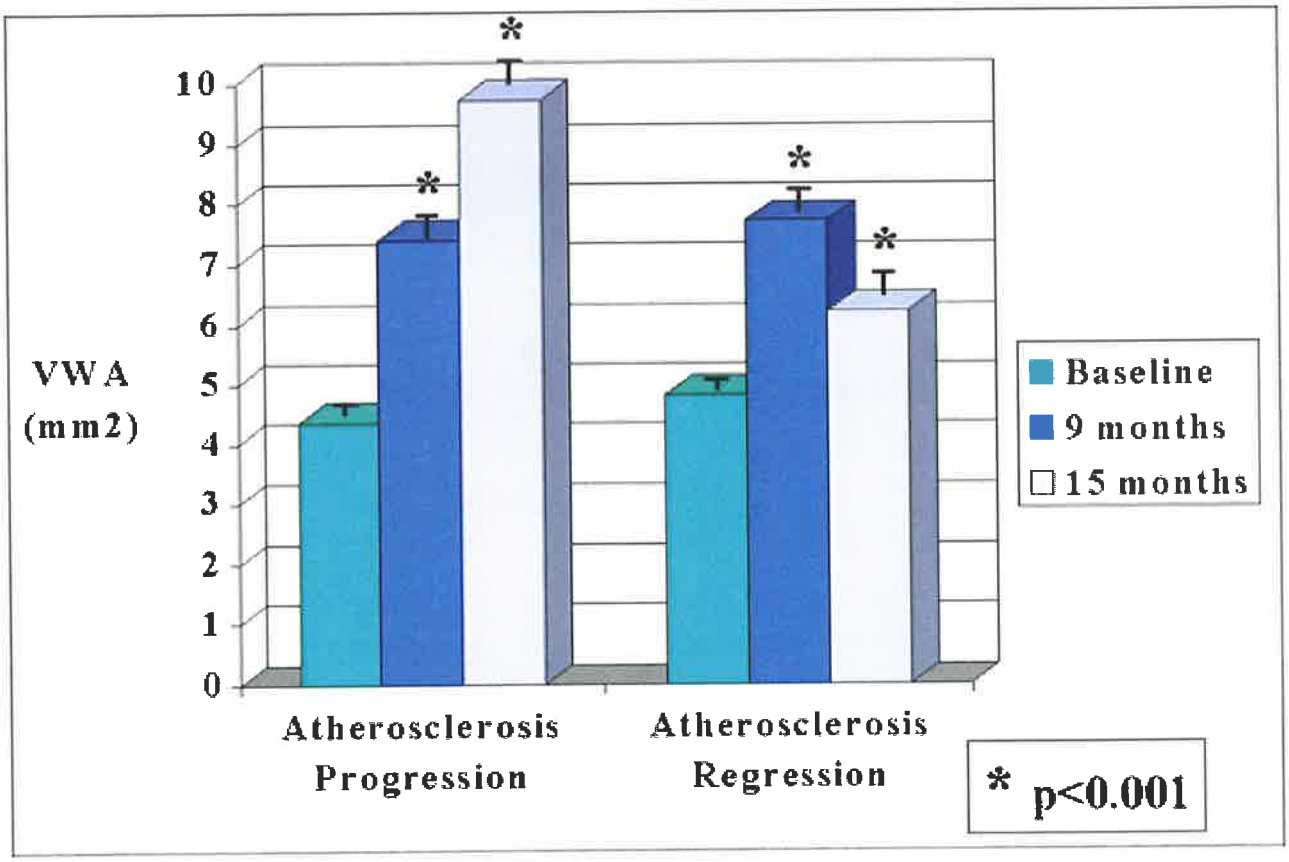

Graphic presentation allowing appreciation of the changes in the vessel wall area, as assessed by serial MR imaging in the Atherosclerotic Progression and Regression groups.

7. 3. 3. Serial MR Imaging of Fibrotic and Lipidic Plaque Components

Magnetic resonance imaging of animals after atherosclerosis induction, confirmed the presence of significant aortic atherosclerosis with both fibrotic (5.38±0.34 mm^2) and lipidic (0.93±0.19 mm^2) components identifiable. Serial imaging after atherosclerosis progression or regression thus allowed the study of plaque component changes over time.

There was no significant change in the fibrotic component of the atherosclerotic lesions (5.28±0.49 mm^2 to 5.58±0.30 mm^2), although there was a trend to an increase. However, there was a significant ($p=0.0007$) decrease in the lipidic component of these lesions (1.05±0.28 mm^2 to 0.13±0.16 mm^2) (figures 7. 2 and 7. 3).

Figure 7. 2

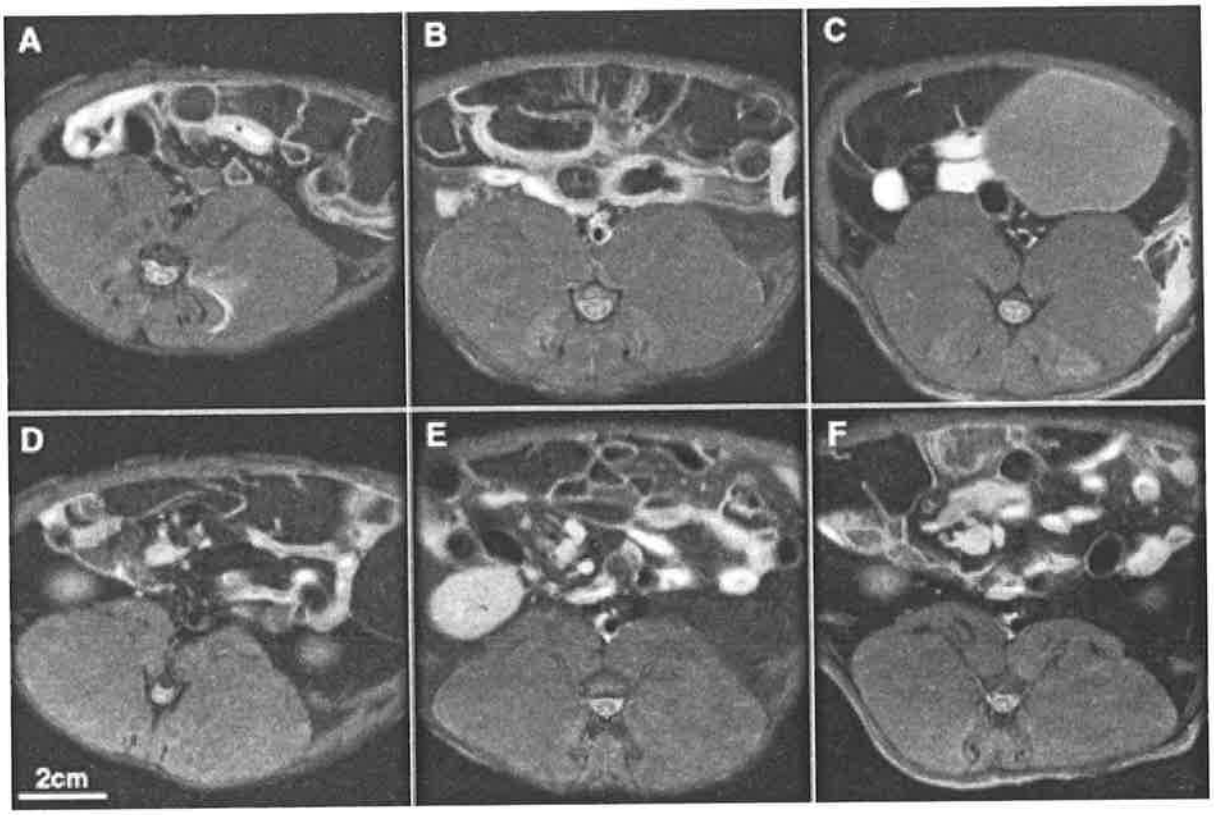

ATHEROSCLEROTIC REGRESSION

Sequential axial MR images of the abdominal aorta taken at the level of the first spinal artery (A, B and C) and the left renal artery (D, E and F) at baseline (A and D), 9 months (B and E) and 15 months (C and F).

Figure 7. 3

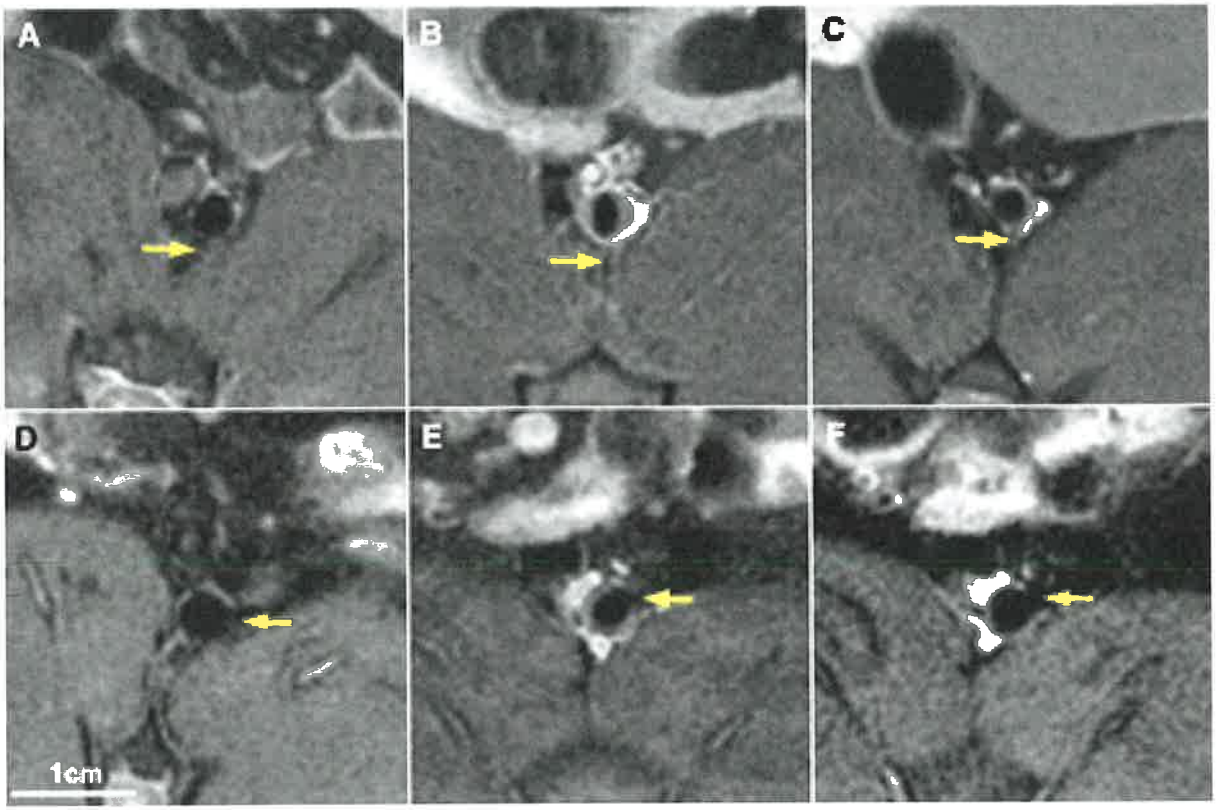

ATHEROSCLEROTIC REGRESSION

Magnification of the same MR images from figure 7. 2, depicting the sequential changes in the aortic wall over time at the level of the first spinal artery (A, B and C) and the left renal artery (D, E and F) as identified by the respective yellow arrows. At baseline (A and D) one can appreciate the very thin normal aortic wall. After 9 months of atherogenic diet (B and E) there has been a significant thickening of the aortic wall due to atherosclerosis. However after recommencing a normal diet, at 15 months (C and F) the atherosclerotic aortic wall has regressed towards the normal thin wall.

In those animals continued on the atherogenic diet (atherosclerosis progression), there was a small but significant (p=0.038) decrease in the fibrotic component of the lesions (5.53±0.42 mm^2 to 4.15±0.64 mm^2). Furthermore, there was a significant increase (p=0.002) in the lipidic component (0.76±0.23 mm^2 to 1.92±0.32 mm^2) (figures 7. 4 and 7. 5).

Figure 7. 4

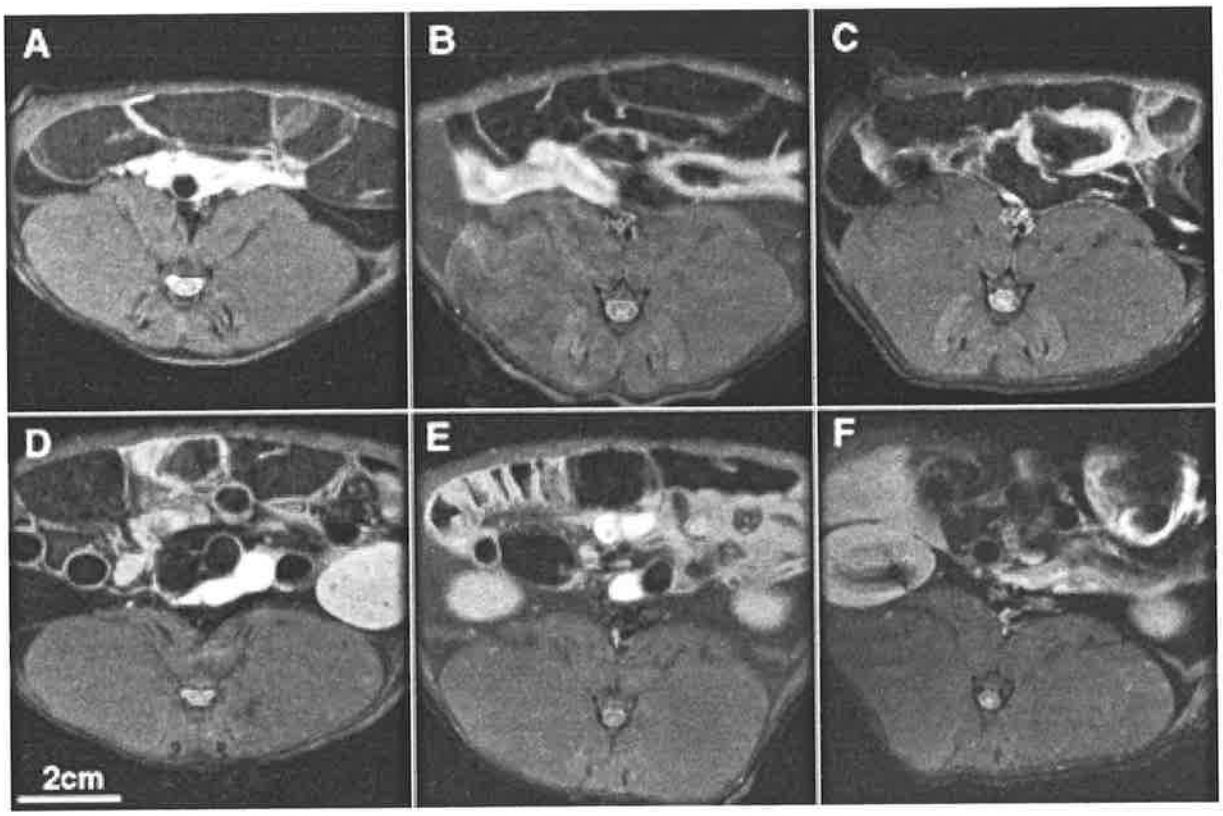

ATHEROSCLEROTIC PROGRESSION

Sequential axial MR images of the abdominal aorta taken at the level of the first spinal artery (A, B and C) and the left renal artery (D, E and F) at baseline (A and D), 9 months (B and E) and 15 months (C and F).

Figure 7. 5

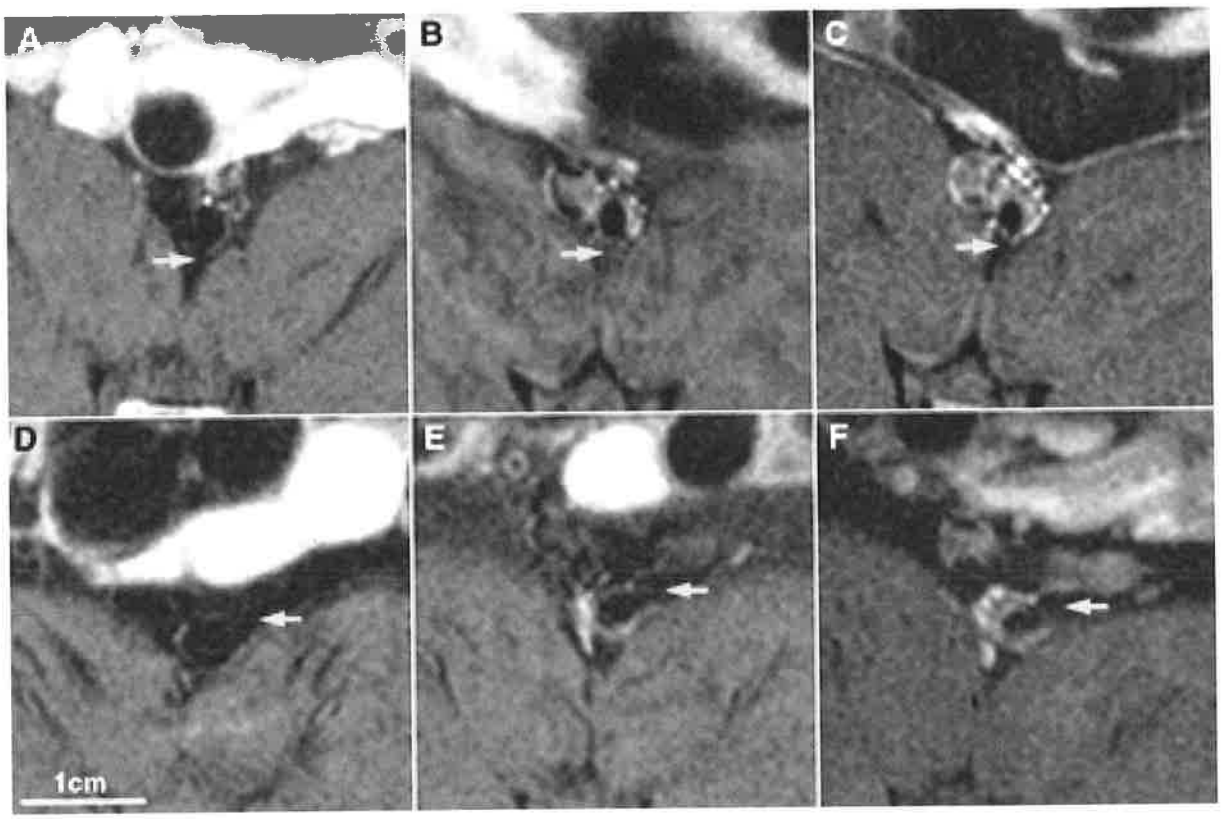

ATHEROSCLEROTIC PROGRESSION

Magnification of the same MR images from figure 7. 4, depicting the sequential changes in the aortic wall over time at the level of the first spinal artery (A, B and C) and the left renal artery (D, E and F) as identified by the respective yellow arrows. At baseline (A and D) one can appreciate the very thin normal aortic wall. After 9 months of atherogenic diet (B and E) there has been a significant thickening of the aortic wall due to atherosclerosis. In comparison to the regression of the atherosclerotic process appreciated in figure 7. 3, at 15 months (C and F) the atherosclerotic aortic wall has progressed with an even greater atherosclerotic burden, and one can readily appreciate the higher signal (white) fibrous cap from the lower signal (dark) lipid core.

7. 3. 4. Correlation Between MR Imaging and Histopathology

There was a good agreement between MR imaging and histopathology for the measurement of both vessel wall area ($r=0.81$, $p<0.0001$) and mean wall thickness ($r=0.86$, $p<0.0001$) as assessed by simple linear regression analysis.

Furthermore, a significant agreement between MR and histopathological measurements of lipidic and fibrotic areas existed (figure 4), confirming previous studies.

7. 4. DISCUSSION

Serial MR imaging not only documents atherosclerotic plaque composition and burden in this model, but allows the monitoring of changes over time and with different conditions of atherosclerotic lesions in the same animal. Although we used dietary modification as the means of observing atherosclerotic progression or regression, the potential exists for monitoring changes in atherosclerotic size and composition with a variety of therapies.

Magnetic resonance imaging has been used to document atherosclerotic composition ex vivo and in vivo in both animal models and humans (Skinner et al. 1995; Toussaint et al. 1996; Fayad et al. 1998; Yuan et al. 1998; McConnell et al. 1999; Shinnar et al. 1999; Worthley et al. 2000). The use of T2W imaging has emerged for the discrimination of fibrous and lipidic components of atherosclerotic lesions (Toussaint et al. 1995; Toussaint et al. 1996; McConnell et al. 1999; Worthley et al. 2000), although additional imaging sequences are required to assist with the differentiation of all the components of complex atherosclerotic lesions (Shinnar et al. 1999; Worthley et al. 2000). The experimental model used contains fibrotic and lipidic components only, and thus we are unable to comment on the ability of this MR imaging protocol to document serially changes in other atherosclerotic components. However, experimental and pathological data confirms the critical role the fibrotic and lipidic components play in atherosclerotic plaque vulnerability and thrombogenicity (Davies 1996; Lee et al. 1997; Fuster et al. 1999).

A recent study has shown the potential of MR imaging to document the different atherosclerotic burden in different rabbits subject to different dietary regimens (McConnell et al. 1999). However, serial data in the same animals at different time

points was not obtained. Thus, the ability to serially image with MR the same atherosclerotic lesions in the same animals over time could not be studied. Furthermore, the ability to document changes in the composition of aortic wall was unable to be studied as only one animal has evidence of fibrotic and lipidic components with MR imaging. Our study confirms and extends these findings, showing that not only is it possible to show changes in atherosclerotic burden in the same animals, but that changes in lesion composition can also be observed.

The significant changes in lipidic and fibrotic components over time in the different groups as documented by MR imaging do not necessarily apply to therapeutic modifications undertaken in patients. However, our results highlight the potential of MR imaging to provide serial data about atherosclerotic lesions in patients at different time points and in response to therapeutic interventions. Future studies with serial MR imaging of human atherosclerosis are warranted to clarify its potential role in the future.

The mechanisms by which these changes in the aortic wall have occurred are not elucidated in this study. However, as mentioned in the Chapter 1, the significant decrease in serum cholesterol associated with the return to a normal diet in the regression group, leads to an improvement in endothelial function, reverse cholesterol transport and decreased cellular and humoral mediators of inflammation, among other factors.

Magnetic resonance imaging is able to document changes in atherosclerotic plaque size and composition in response to dietary modification in this experimental model of atherosclerosis. The potential exists for serial studies of human atheroma with MR in response to therapies such as lipid lowering.

Chapter 8

SERIAL IN VIVO MAGNETIC RESONANCE IMAGING DOCUMENTS ARTERIAL REMODELLING IN EXPERIMENTAL ATHEROSCLEROSIS

TABLE OF CONTENTS

8. 1. INTRODUCTION

Atherosclerotic plaques may develop and even progress without compromising the arterial lumen in the early phases due to outward growth of the vessel wall; a concept known as "positive" or "outward" arterial remodelling (Glagov et al. 1987). Remodelling of the arterial wall is an important mechanism in determining luminal narrowing of native atherosclerotic lesions (Glagov et al. 1987; Shiran et al. 1999; Taylor et al. 1999; Weissman et al. 1999) and restenosis after percutaneous coronary interventions (Post et al. 1997; Dangas et al. 1999; Meine et al. 1999). However because of the difficulty in longitudinally studying atherosclerotic lesions over time, little is known about the mechanisms involved in the remodelling process (Taylor et al. 1999). Moreover, recent data has suggested that arterial remodelling may be "negative" or "inward" even in the early stages of plaque development (Taylor et al. 1999). To date, apart from post-mortem studies, intravascular ultrasound has been used to provide information on the remodelling phenomenon (Lim et al. 1997; Post et al. 1997; Dangas et al. 1999; Meine et al. 1999; Shiran et al. 1999; Weissman et al. 1999). However, this is an invasive imaging methodology that limits its usefulness for serial analysis of atherosclerotic lesions. Thus an imaging technique that could noninvasively and serially monitor the vessel wall could greatly assist our understanding of this process.

Magnetic resonance (MR) is a noninvasive imaging modality that has been used to document atherosclerotic burden in both humans and animal models of atherosclerosis (Skinner et al. 1995; Manninen et al. 1998; Yuan et al. 1998; McConnell et al. 1999; Worthley et al. 2000). It has been validated in a rabbit model of abdominal aortic atherosclerosis with cholesterol feeding and balloon injury

(Skinner et al. 1995; Manninen et al. 1998; McConnell et al. 1999), and permits serial imaging of the same atherosclerotic lesions.

The WHHL rabbit has an intrinsic deficiency in LDL receptors, thus more closely approximating humans with atherosclerosis than the cholesterol fed rabbit models (Watanabe 1980).

In this study, we have investigated arterial remodelling with serial MR imaging in WHHL rabbits that have undergone balloon injury to the abdominal aorta, in order to accelerate and localise the atherosclerosis.

8. 2. METHODS

8. 2. 1. Animal Model

WHHL rabbits (n=11, age=3months, weight=3.0 kg) underwent aortic denudation of the aorta from the renal arteries to the iliac bifurcation, one week after arrival to the institution as previously described (Skinner et al. 1995; McConnell et al. 1999). Full lipid profiles were analyzed from serum specimens obtained at the time of the MR imaging studies. The Mount Sinai School of Medicine animal management program approved all experiments.

8. 2. 2. MR Imaging

All rabbits had serial MR imaging performed on 2 occasions; immediately prior to aortic balloon denudation and 6 months later using a 1.5 Tesla MRI system (Signa GEMS) and a conventional phased-array volume coil. The MR imaging protocol used was based on previously validated work (Skinner et al. 1995; McConnell et al. 1999). Sequential axial images (3-mm thickness) of the aorta from the arch to the iliac bifurcation were obtained using a fast spin-echo sequence with an in plane resolution of 350 x 350μ (PDW :TR/TE: 2300/17msec; T2w: TR/TE:2300/60msec, field of view (FOV)=9x9cm, matrix 256x256, echo train length=8, signal averages=4). Fat suppression and flow saturation pulses were used as previously described (Skinner et al. 1995; McConnell et al. 1999).

8. 2. 3. MR Imaging Analysis

The MR images were transferred to a Macintosh computer for further analysis. The MR images from the same animals at the two time points were matched using distance from the renal arteries and the iliac bifurcation for registration. Thus, each segment of the abdominal aorta could be compared at baseline and 6 months with MR imaging, allowing true serial data to be obtained. The MR images from the validation subgroup were matched with corresponding histopathological sections for the aortic specimens as described above. Cross-sectional areas of the lumen and outer boundary of each aortic section were determined using manual tracing with Image Pro-Plus (Media Cybernetics) by an observer blinded to the identity of the rabbits. From these measurements lumen area, outer vessel area and vessel wall area (outer vessel area minus lumen area) were calculated. The outer wall was defined as the vessel wall-epicardial fat interface.

8. 2. 4. Histopathology

Euthanasia was performed within 24 hours of MR imaging of the rabbits (n=4) by intravenous injection of "Sleepaway" 5mL IV (Fort Dodge Animal Health, Fort Dodge, IA) after receiving heparin (100U/kg) to prevent post-mortem blood clotting. The aortas were excised and perfusion fixed as described (Skinner et al. 1995; McConnell et al. 1999). Serial sections of the aorta were cut at 3mm intervals matching corresponding MR images. The aortic specimens were embedded in paraffin and sections 5-micron thick were cut and stained with combined Masson's trichrome elastin stain.

8. 2. 5. Histopathology Analysis

The histopathological sections were digitised to the same computer and the same parameters analyzed with the method as described above for MR image analysis. The outer wall of the vessel was defined as the dense adventitial-epicardial fat interface on histopathology.

8. 2. 6. Statistical analysis

Paired student's t-tests were used to compare the MR image derived parameters from the same sites in the abdominal aorta at the two time points. Comparisons between MR and histopathology assessment of vessel parameters in the validation sub-group were performed using simple linear regression analysis. All probabilities are two-sided with statistical significance taken as $p<0.05$. All values are expressed as mean±SEM.

8. 3. RESULTS

8. 3. 1. Serum Lipid Profiles

The mean baseline serum cholesterol (age 3 months) was 990±91mg/dL. Six months later (age 9 months) it was 449±57mg/dL. This age related drop in serum cholesterol is a well described characteristic of WHHL rabbits (Watanabe 1980).

8. 3. 2. Validation Subgroup Data

In order to confirm the ability of MR imaging to assess changes in the arterial wall parameters, the correlation between the techniques was performed. There was a significant ($p<0.0001$) correlation between MR imaging and histopathological analysis for assessment of lumen area ($r=0.80$), outer vessel area ($r=0.84$) and vessel wall area ($r=0.83$), consistent with prior studies (figure 8. 1) (Manninen et al. 1998; McConnell et al. 1999).

8. 3. 3. Serial MR Imaging Data

To monitor changes in the lumen and outer vessel wall areas over time (indicating degree of stenosis and arterial remodelling respectively), we compared matched MR images of the abdominal aorta in the same rabbits at the two time points (figure 8. 2). At baseline, the mean areas for the pre-determined parameters were lumen area=4.36±0.16mm^2, outer vessel area=7.96±0.19mm^2, and vessel wall area=3.61±0.07mm^2. Six months after the balloon injury, the same parameters were lumen area=4.89±0.12mm^2, outer vessel area=10.46±0.19mm^2, and vessel wall area=5.57±0.09mm^2. Over this 6 month period there was a significant ($p<0.0001$)

increase in the vessel wall area, a surrogate of atherosclerotic thickening. Rather than a concomitant decrease in the lumen area there was a small, but significant ($p=0.006$), increase in the lumen area. An outward or positive remodelling accounted for this increase in atherosclerotic plaque burden, as evidenced by the significant ($p<0.0001$) increase in the outer vessel area.

Figure 8. 1

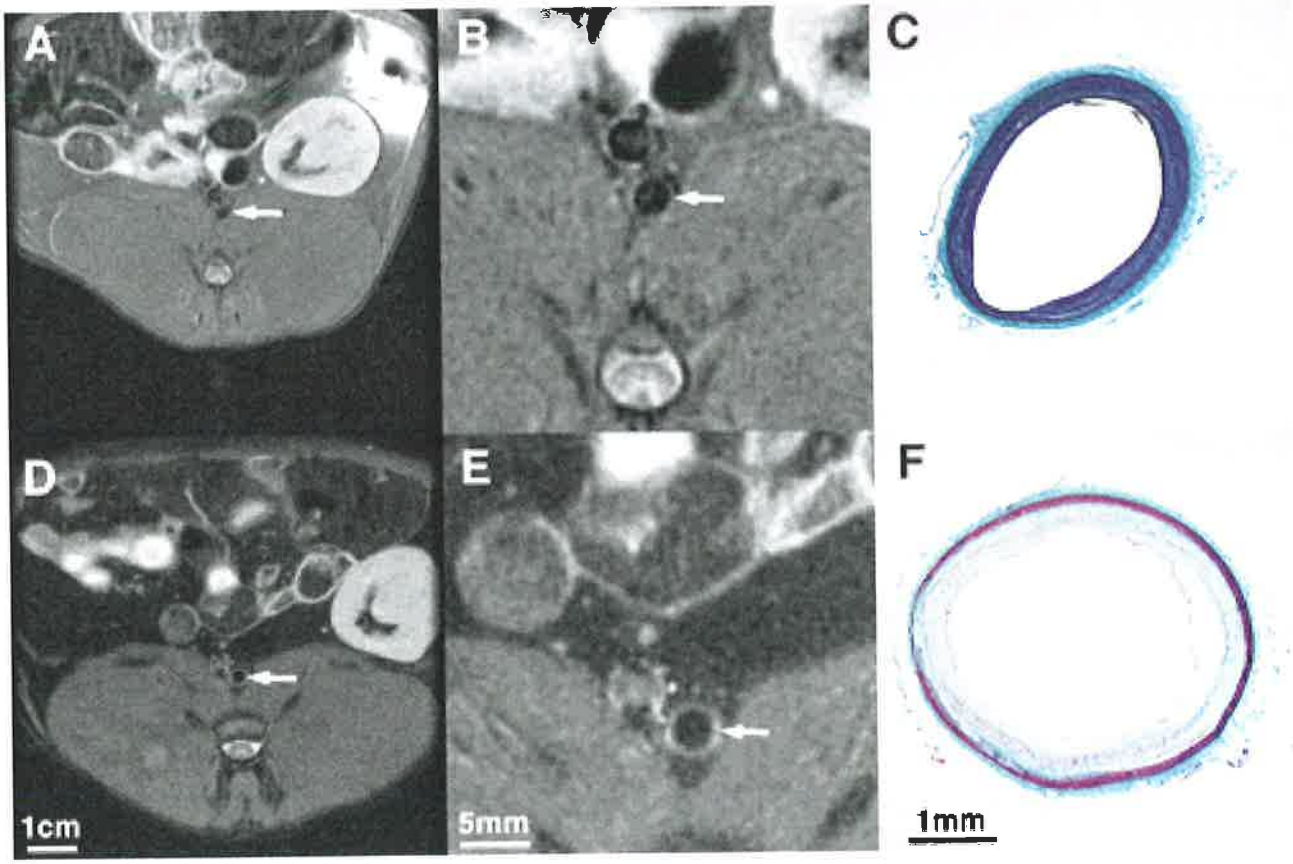

MR images and corresponding histopathology of the atherosclerotic aortas at baseline (i.e. 3 months of age) (A, B, C) and 6 months after balloon injury (i.e. 9 months of age) (D, E, F). The aortic images, although from different animals sacrificed as part of the validation sub-group, were selected at approximately the same level in the abdomen for comparability, as evidenced by the same appearance of the left kidney (right of image) both at baseline (A) and 6 months after balloon injury (D). Magnified MR images of the aortas in A and D show clearly the very thin aortic wall at baseline (B, arrow) and the more thickened wall 6 months later (E, arrow). Furthermore, it can be appreciated that there has been no luminal loss and that the increase in vessel wall area has been outward. Corresponding histopathology sections from A, B and D, E (C and F respectively) confirm the findings in the MR images. It can be appreciated that there is a greater atherosclerotic burden 6 months after the balloon injury, however the lumen is preserved. (Scale bars in D, E and F also refer to A, B and C respectively).

Figure 8. 2

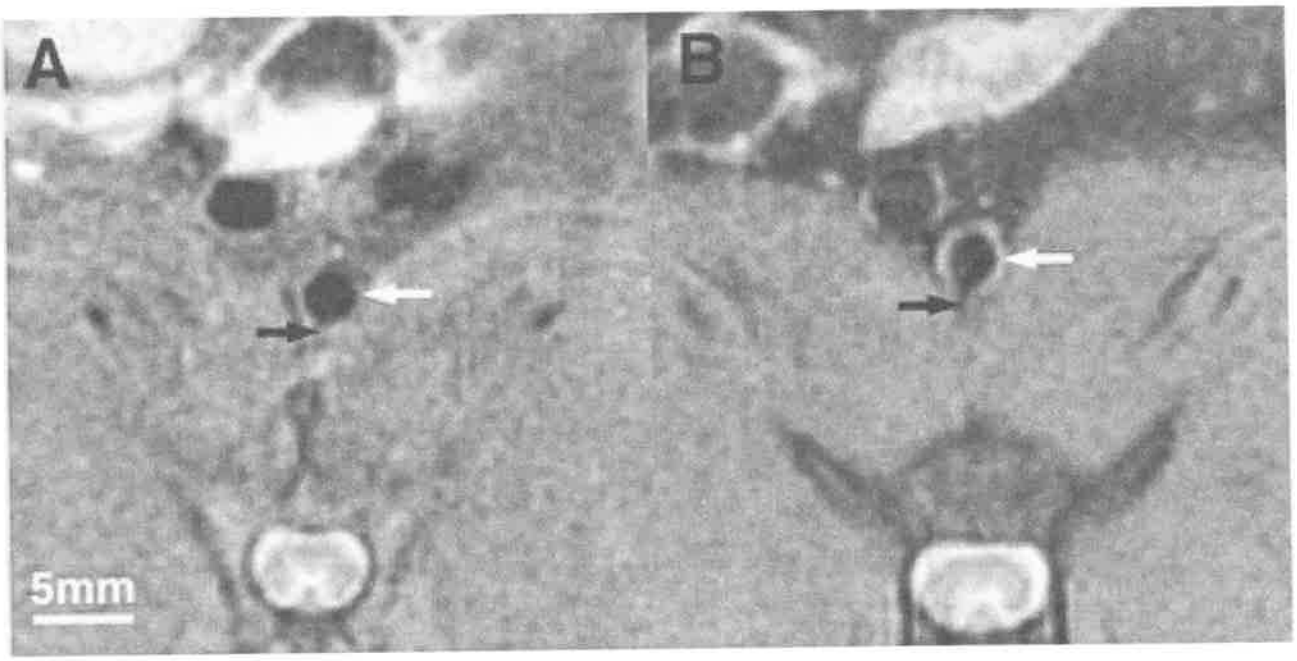

Serial MR images taken at baseline (A) and 6 months after balloon injury (B). Co-registration is confirmed by the presence of the spinal artery (black arrows) and the small bright signal from perivascular lymphatics just superior to the aorta. The aortic wall is clearly thicker at 6 months after balloon injury (white arrows), although the aortic lumen is relatively preserved.

8. 4. DISCUSSION

Atherosclerosis has classically been assessed by the degree of luminal narrowing. However, it is now known that significant atherosclerosis can exist without any compromise to the lumen (Glagov et al. 1987). This concept is clearly demonstrated in this model of aortic atherosclerosis in WHHL rabbits. Noninvasive serial MR imaging accurately documents the increase in atherosclerotic burden despite no decrease in or even an increase in the arterial lumen, as indicated by the increase in vessel wall area over the 6 month period (positive arterial remodelling). Angiographic analysis would have indicated not only no increase in but a decrease in atherosclerotic burden over time, as noted by the small but significant increase in lumen area over the 6 month period. On the other hand, MR imaging allows the serial and noninvasive assessment of vessel wall parameters in this model, and thus the potential for providing insights into mechanisms and the natural history of arterial remodelling.

Arterial remodelling has been described for over 10 years (Glagov et al. 1987). However, the mechanisms involved remain uncertain because of the difficulty in obtaining longitudinal studies over the lengthy time interval during which remodelling likely occurs, and because of limited data from relevant animal models (Taylor et al. 1999). Although we are not able to draw conclusions about the early remodelling process in humans or even other animal models from our findings, the feasibility of using MR imaging to document arterial remodelling in vivo permits future studies at multiple time points. Indeed it is clear that early arterial remodelling is not always positive (Taylor et al. 1999). This further reinforces the need for an imaging modality that can serially and noninvasively provide information about the arterial remodelling process in humans. Intravascular ultrasound has been the only

imaging technique used to study the effects of remodelling and atherosclerosis (Lim et al. 1997; Post et al. 1997; Dangas et al. 1999; Meine et al. 1999; Shiran et al. 1999; Weissman et al. 1999). However, it is an intrinsically invasive modality, thus limiting its usefulness for longitudinal studies.

Magnetic resonance imaging has been shown to accurately quantify the vessel wall area in the abdominal aortic of rabbits fed cholesterol (Skinner et al. 1995; Manninen et al. 1998; McConnell et al. 1999). Furthermore, in rabbit models of atherosclerosis, both intravascular ultrasound and surface MR imaging accurately estimate vessel wall area and thus atherosclerotic burden when compared to histology (Manninen et al. 1998). The ability of MR to provide serial and noninvasive information about the arterial wall in this model provides us with a useful imaging tool to assist the investigation of arterial remodelling in future studies, both in primary atherosclerosis and restenosis after percutaneous intervention.

Chapter 9

DISCUSSION AND SUMMARY

The primary aims of this thesis were specifically directed at validating a new noninvasive imaging modality, magnetic resonance imaging, for the purpose of providing information about the severity and composition of atherosclerotic lesions. This involved the use of a number of animal models and confirmation of the ability of this technique to serially image and characterise atherosclerotic lesions at different times and under different conditions.

As extensively reviewed in the introduction of this thesis, there is a need for an imaging modality (or modalities) that will provide information about the composition as well as the severity of atherosclerotic lesions, given the critical role that plaque composition plays in the acute thrombotic complications of atherosclerotic diseases. The aims of the thesis were to investigate the ability of high resolution MR imaging to both characterise and quantify atherosclerotic lesions in both porcine and rabbit models, and explore whether MR could be used to monitor serially changes in arterial wall parameters.

In Chapter 3, we confirmed the ability of MR imaging, in an ex vivo setting to be able to identify all of the components of complex atherosclerotic lesions in an experimental model. This first step, provided the basis for the possibility that if the techniques used in that Chapter could be translated to the in vivo setting, then the potential for characterising atheroma in humans could be eventually possible.

The work in Chapter 4 provided the first step towards translation of MR imaging techniques to in vivo coronary lesions, thus confirming the ability of the motion suppression techniques employed. The comparability of the in vivo and ex vivo MR images from the same sites in the coronary arteries provided compelling evidence that the imaging technique was robust for this purpose.

Chapter 5 confirmed and extended the work in Chapter 4 by providing definitive confirmation that MR imaging was accurate in its representation of the atherosclerotic lesion, by providing comparative histopathological sections of the regions imaged. Using the porcine model, where the coronary anatomy is comparable to the human, the feasibility of now translating these techniques to patients with coronary artery disease is proven.

Chapters 3 to 5 of the thesis were designed to permit a stepwise progression from feasibility of the technique for plaque characterisation to validity of the technique for this purpose in a live animal model of coronary disease that is comparable to humans. This now sets the stage for future work in human coronary atherosclerotic imaging, and opens a new realm of possibilities in the diagnosis and management of coronary artery disease. We have now shown the potential for normal and atherosclerotic human coronary wall imaging with high resolution black-blood methods. This may allow the identification of atherosclerotic disease before it is symptomatic. More importantly, perhaps, is the potential for risk stratification of patients with non-critical coronary disease who are not candidates for surgical or percutaneous coronary interventions, but by the composition of their coronary artery atherosclerotic disease, may be at high risk for a future acute coronary event. Further studies are necessary to assess lesions in asymptomatic patients and to monitor their outcomes.

Chapter 6 utilised MR imaging techniques in a cholesterol fed rabbit model of atherosclerosis to define both the composition of the lesion, as well as the extent of atherosclerotic burden. These findings have important implications for future studies.

The ability to noninvasively document the composition of atherosclerotic lesions in an experimental model allows us conceptually to monitor and document changes in lesion composition in response to various therapeutic interventions. For example, despite the pleiotropic postulates about the mechanisms involved for the risk reduction in mortality and recurrent coronary events in patients with coronary artery disease treated with lipid lowering therapy, in particular statins, the effect that these therapies have on the composition of atherosclerotic plaques is not definite. Despite pathological data suggesting a reduction in lipid and increase in fibrotic components of atherosclerotic lesions in response to dietary modification in animal models, the serial evaluation of the same lesions over time in response to a therapy will provide us with important data relevant to the concept of atherosclerotic plaque stabilisation.

Having discussed the theoretic ability of noninvasive MRI to serially image atherosclerosis, it remained to be shown that serial imaging at different time-points of the same atherosclerotic lesions could be performed. This crucial concept is central in the defining of compositional changes in atherosclerotic lesions. Having confirmed the ability of MRI to document the lipidic and fibrotic components of abdominal aortic atherosclerosis in the cholesterol fed rabbit model described in the previous chapter, the next step to serially image these lesions under circumstances of atherosclerotic progression and regression. In Chapter 7 we serially image the same atherosclerotic lesions in this model and define compositional changes as detected by MRI and later confirmed by histopathology. This is crucial in confirming the ability of MRI to identify the same atherosclerotic lesions in the same individuals at different time-points and to document compositional changes in these lesions.

Chapter 8 validates the ability of serial noninvasive MR imaging to document changes in aortic wall parameters, and thus monitor the arterial remodelling process,

in the Watanabe Heritable Hyperlipidaemic (WHHL) rabbit. We now know that significant atherosclerosis can exist without any compromise to the lumen. Furthermore, positive arterial remodelling appears to be associated with vulnerable atherosclerosis, thus enhancing the significance of its detection. This concept of arterial remodelling has been described for over 10 years. However, the mechanisms involved remain uncertain because of the difficulty in obtaining longitudinal studies over the lengthy time interval during which remodelling likely occurs, and because of limited data from relevant animal models. The feasibility of using MR imaging to document arterial remodelling in vivo permits future studies at multiple time points. Indeed it is clear that early arterial remodelling is not always positive. This further reinforces the need for an imaging modality that can serially and noninvasively provide information about the arterial remodelling process in humans. Intravascular ultrasound has been the only imaging technique used to study the effects of remodelling and atherosclerosis. However, it is an intrinsically invasive modality, thus limiting its usefulness for longitudinal studies. The ability of MR to provide serial and noninvasive information about the arterial wall in this model provides us with a useful imaging tool to assist the investigation of arterial remodelling in future studies, both in primary atherosclerosis and restenosis after percutaneous intervention.

Atherosclerotic imaging with MR has the potential to enhance our understanding of the pathobiology of this disease process and assist our understanding of the effect of therapies on atherosclerotic lesions. However, before this technology can become part of routine clinical practice, some issues will need to be addressed. This includes the cost and accessibility of the technology. Clearly, image quality (both in terms of temporal and spatial resolution) is just reaching the level required for routine clinical use of human atherosclerosis imaging. Further advances in MR imaging techniques such as imaging software, radiofrequency coil design and image sequence development will lead to improvements in image quality in the future, and allow us to move closer to this conceptual advance.

REFERENCES

Australian Institute of Health and Welfare (AIHW) 1999. Heart, stroke and vascular diseases, Australian facts. AIHW Cat. No. CVD 7. Canberra: AIHW and the Heart Foundation of Australia (Cardiovascular Disease Series No. 10).

Achenbach, S., Moshage, W., Ropers, D., et al. Value of electron-beam computed tomography for the noninvasive detection of high-grade coronary-artery stenoses and occlusions. N Engl J Med. 1998;339:1964-71.

Adam, E., Melnick, J. L., Probtsfield, J. L., et al. High levels of cytomegalovirus antibody in patients requiring vascular surgery for atherosclerosis. Lancet. 1987;2:291-3.

Aikawa, M., Rabkin, E., Okada, Y., et al. Lipid lowering by diet reduces matrix metalloproteinase activity and increases collagen content of rabbit atheroma: a potential mechanism of lesion stabilization. Circulation. 1998;97:2433-44.

Alderman, E. L., Corley, S. D., Fisher, L. D., et al. Five-year angiographic follow-up of factors associated with progression of coronary artery disease in the Coronary Artery Surgery Study (CASS). CASS Participating Investigators and Staff. J Am Coll Cardiol. 1993;22:1141-54.

Allen, S., Khan, S., Tam, S., et al. Expression of adhesion molecules by lp(a): a potential novel mechanism for its atherogenicity. FASEB J. 1998;12:1765-76.

Altbach, M. I., Mattingly, M. A., Brown, M. F., et al. Magnetic resonance imaging of lipid deposits in human atheroma via a stimulated-echo diffusion-weighted technique. Magn Reson Med. 1991;20:319-26.

Ambrose, J. A., Tannenbaum, M. A., Alexopoulos, D., et al. Angiographic progression of coronary artery disease and the development of myocardial infarction. J Am Coll Cardiol. 1988;12:56-62.

Amento, E. P., Ehsani, N., Palmer, H., et al. Cytokines and growth factors positively and negatively regulate interstitial collagen gene expression in human vascular smooth muscle cells. Arterioscler Thromb. 1991;11:1223-30.

Anderson, J. L., Muhlestein, J. B., Carlquist, J., et al. Randomized secondary prevention trial of azithromycin in patients with coronary artery disease and serological evidence for Chlamydia pneumoniae infection: The Azithromycin in Coronary Artery Disease: Elimination of Myocardial Infection with Chlamydia (ACADEMIC) study. Circulation. 1999;99:1540-7.

Ando, J., Tsuboi, H., Korenaga, R., et al. Shear stress inhibits adhesion of cultured mouse endothelial cells to lymphocytes by downregulating VCAM-1 expression. Am J Physiol. 1994;267:C679-87.

Ando, J., Tsuboi, H., Korenaga, R., et al. Down-regulation of vascular adhesion molecule-1 by fluid shear stress in cultured mouse endothelial cells. Ann N Y Acad Sci. 1995;748:148-56; discussion 156-7.

Annex, B. H., Denning, S. M., Channon, K. M., et al. Differential expression of tissue factor protein in directional atherectomy specimens from patients with stable and unstable coronary syndromes. Circulation. 1995;91:619-22.

Arad, Y., Spadaro, L. A., Goodman, K., et al. Predictive value of electron beam computed tomography of the coronary arteries. 19-month follow-up of 1173 asymptomatic subjects. Circulation. 1996;93:1951-3.

Archbold, R. A. and Timmis, A. D. Cholesterol lowering and coronary artery disease: mechanisms of risk reduction. Heart. 1998;80:543-7.

Arnold, J. A., Modaresi, K. B., Thomas, N., et al. Carotid plaque characterization by duplex scanning: observer error may undermine current clinical trials. Stroke. 1999;30:61-5.

Aronson, D., Rayfield, E. J. and Chesebro, J. H. Mechanisms determining course and outcome of diabetic patients who have had acute myocardial infarction. Ann Intern Med. 1997;126:296-306.

Aurigemma, G. P., Reichek, N., Axel, L., et al. Noninvasive determination of coronary artery bypass graft patency by cine magnetic resonance imaging. Circulation. 1989;80:1595-602.

Axel, L. and Dougherty, L. Heart wall motion: improved method of spatial modulation of magnetization for MR imaging. Radiology. 1989;172:349-50.

Axel, L. and Dougherty, L. MR imaging of motion with spatial modulation of magnetization. Radiology. 1989;171:841-5.

Babaev, V. R., Bobryshev, Y. V., Stenina, O. V., et al. Heterogeneity of smooth muscle cells in atheromatous plaque of human aorta. Am J Pathol. 1990;136:1031-42.

Badimon, J. J., Badimon, L., Turitto, V. T., et al. Platelet deposition at high shear rates is enhanced by high plasma cholesterol levels. In vivo study in the rabbit model. Arterioscler Thromb. 1991;11:395-402.

Badimon, J. J., Ortiz, A. F., Meyer, B., et al. Different response to balloon angioplasty of carotid and coronary arteries: effects on acute platelet deposition and intimal thickening. Atherosclerosis. 1998;140:307-14.

Baer, F. M., Voth, E., Theissen, P., et al. Gradient-echo magnetic resonance imaging during incremental dobutamine infusion for the localization of coronary artery stenoses. Eur Heart J. 1994;15:218-25.

Barter, P. J. and Rye, K. A. High density lipoproteins and coronary heart disease. Atherosclerosis. 1996;121:1-12.

Beanlands, R. Positron emission tomography in cardiovascular disease. Can J Cardiol. 1996;12:875-83.

Beyar, R., Weiss, J. L., Shapiro, E. P., et al. Small apex-to-base heterogeneity in radius-to-thickness ratio by three- dimensional magnetic resonance imaging. Am J Physiol. 1993;264:H133-40.

Bland, J. M. and Altman, D. G. Statistical methods for assessing agreement between two methods of clinical measurement. Lancet. 1986;1:307-10.

Blann, A. D., Kirkpatrick, U., Devine, C., et al. The influence of acute smoking on leucocytes, platelets and the endothelium. Atherosclerosis. 1998;141:133-9.

Boers, G. H. Hyperhomocysteinemia as a risk factor for arterial and venous disease. A review of evidence and relevance. Thromb Haemost. 1997;78:520-2.

Boers, G. H., Smals, A. G., Trijbels, F. J., et al. Heterozygosity for homocystinuria in premature peripheral and cerebral occlusive arterial disease. N Engl J Med. 1985;313:709-15.

Bolster, B. D., Jr., McVeigh, E. R. and Zerhouni, E. A. Myocardial tagging in polar coordinates with use of striped tags. Radiology. 1990;177:769-72.

Bombeli, T., Schwartz, B. R. and Harlan, J. M. Adhesion of activated platelets to endothelial cells: evidence for a GPIIbIIIa-dependent bridging mechanism and novel roles for endothelial intercellular adhesion molecule 1 (ICAM-1), alphavbeta3 integrin, and GPIbalpha. J Exp Med. 1998;187:329-39.

Booth, R. F., Honey, A. C., Martin, J. F., et al. Lipid characterization in an animal model of atherosclerosis using NMR spectroscopy and imaging. NMR Biomed. 1990;3:95-100.

Botnar, R. M., Stuber, M., Danias, P. G., et al. Improved coronary artery definition with T2-weighted, free-breathing, three-dimensional coronary MRA. Circulation. 1999;99:3139-48.

Bottomley, P. A. MR spectroscopy of the human heart: the status and the challenges. Radiology. 1994;191:593-612.

Braunwald, E., Jones, R. H., Mark, D. B., et al. Diagnosing and managing unstable angina. Agency for Health Care Policy and Research. Circulation. 1994;90:613-22.

Brezinski, M. E., Tearney, G. J., Weissman, N. J., et al. Assessing atherosclerotic plaque morphology: comparison of optical coherence tomography and high frequency intravascular ultrasound. Heart. 1997;77:397-403.

Brown, D. L., Hibbs, M. S., Kearney, M., et al. Identification of 92-kD gelatinase in human coronary atherosclerotic lesions. Association of active enzyme synthesis with unstable angina. Circulation. 1995;91:2125-31.

Brown, M. S. and Goldstein, J. L. Lipoprotein metabolism in the macrophage: implications for cholesterol deposition in atherosclerosis. Annu Rev Biochem. 1983;52:223-61.

Buchalter, M. B., Weiss, J. L., Rogers, W. J., et al. Noninvasive quantification of left ventricular rotational deformation in normal humans using magnetic resonance imaging myocardial tagging. Circulation. 1990;81:1236-44.

Buga, G. M., Gold, M. E., Fukuto, J. M., et al. Shear stress-induced release of nitric oxide from endothelial cells grown on beads. Hypertension. 1991;17:187-93.

Buhler, F. R., Vesanen, K., Watters, J. T., et al. Impact of smoking on heart attacks, strokes, blood pressure control, drug dose, and quality of life aspects in the International Prospective Primary Prevention Study in Hypertension. Am Heart J. 1988;115:282-8.

Burke, A. P., Farb, A., Malcom, G. T., et al. Coronary risk factors and plaque morphology in men with coronary disease who died suddenly. N Engl J Med. 1997;336:1276-82.

Busse, R., Pohl, U. and Luckhoff, A. Mechanisms controlling the production of endothelial autacoids. Z Kardiol. 1989;78:64-9.

Caiati, C., Montaldo, C., Zedda, N., et al. New noninvasive method for coronary flow reserve assessment: contrast- enhanced transthoracic second harmonic echo Doppler. Circulation. 1999;99:771-8.

Caiati, C., Zedda, N., Montaldo, C., et al. Contrast-enhanced transthoracic second harmonic echo Doppler with adenosine: a noninvasive, rapid and effective method for coronary flow reserve assessment. J Am Coll Cardiol. 1999;34:122-30.

Callister, T. Q., Raggi, P., Cooil, B., et al. Effect of HMG-CoA reductase inhibitors on coronary artery disease as assessed by electron-beam computed tomography. N Engl J Med. 1998;339:1972-8.

Campos, S., Martinez Sanjuan, V., Garcia Nieto, J. J., et al. New black blood pulse sequence for studies of the heart. Int J Card Imaging. 1999;15:175-83.

Carew, T. E., Schwenke, D. C. and Steinberg, D. Antiatherogenic effect of probucol unrelated to its hypocholesterolemic effect: evidence that antioxidants in vivo can selectively inhibit low density lipoprotein degradation in macrophage-rich fatty streaks and slow the progression of atherosclerosis in the Watanabe heritable hyperlipidemic rabbit. Proc Natl Acad Sci U S A. 1987;84:7725-9.

Carpenter, T. A., Hodgson, R. J., Herrod, N. J., et al. Magnetic resonance imaging in a model of atherosclerosis: use of a collar around the rabbit carotid artery. Magn Reson Imaging. 1991;9:365-71.

Carvalho, A. C., Colman, R. W. and Lees, R. S. Platelet function in hyperlipoproteinemia. N Engl J Med. 1974;290:434-8.

Casscells, W., Hathorn, B., David, M., et al. Thermal detection of cellular infiltrates in living atherosclerotic plaques: possible implications for plaque rupture and thrombosis. Lancet. 1996;347:1447-51.

Cathcart, M. K., McNally, A. K. and Chisolm, G. M. Lipoxygenase-mediated transformation of human low density lipoprotein to an oxidized and cytotoxic complex. J Lipid Res. 1991;32:63-70.

Celentano, D. C. and Frishman, W. H. Matrix metalloproteinases and coronary artery disease: a novel therapeutic target. J Clin Pharmacol. 1997;37:991-1000.

Celermajer, D. S. Noninvasive detection of atherosclerosis. N Engl J Med. 1998;339:2014-5.

Chamley-Campbell, J. H., Campbell, G. R. and Ross, R. Phenotype-dependent response of cultured aortic smooth muscle to serum mitogens. J Cell Biol. 1981;89:379-83.

Chandra, S., Clark, L. V., Coatney, R. W., et al. Application of serial in vivo magnetic resonance imaging to evaluate the efficacy of endothelin receptor antagonist SB 217242 in the rat carotid artery model of neointima formation. Circulation. 1998;97:2252-8.

Chang, M. Y., Sasahara, M., Chait, A., et al. Inhibition of hypercholesterolemia-induced atherosclerosis in the nonhuman primate by probucol. II. Cellular composition and proliferation. Arterioscler Thromb Vasc Biol. 1995;15:1631-40.

Chappey, O., Dosquet, C., Wautier, M. P., et al. Advanced glycation end products, oxidant stress and vascular lesions. Eur J Clin Invest. 1997;27:97-108.

Clark, N. R., Reichek, N., Bergey, P., et al. Circumferential myocardial shortening in the normal human left ventricle. Assessment by magnetic resonance imaging using spatial modulation of magnetization. Circulation. 1991;84:67-74.

Constantinides, P. Plaque fissures in human coronary thrombosis. J Atheroscler Res. 1966;6:1-17.

Correia, L. C., Atalar, E., Kelemen, M. D., et al. Intravascular magnetic resonance imaging of aortic atherosclerotic plaque composition. Arterioscler Thromb Vasc Biol. 1997;17:3626-32.

Corson, M. A., James, N. L., Latta, S. E., et al. Phosphorylation of endothelial nitric oxide synthase in response to fluid shear stress. Circ Res. 1996;79:984-91.

Dahlen, G. H., Guyton, J. R., Attar, M., et al. Association of levels of lipoprotein Lp(a), plasma lipids, and other lipoproteins with coronary artery disease documented by angiography. Circulation. 1986;74:758-65.

Danchin, N. Is myocardial revascularisation for tight coronary stenoses always necessary? Lancet. 1993;342:224-5.

Danesh, J., Collins, R. and Peto, R. Chronic infections and coronary heart disease: is there a link?. Lancet. 1997;350:430-6.

Dangas, G., Mintz, G. S., Mehran, R., et al. Preintervention arterial remodeling as an independent predictor of target-lesion revascularization after nonstent coronary intervention: an analysis of 777 lesions with intravascular ultrasound imaging. Circulation. 1999;99:3149-54.

Davi, G., Catalano, I., Averna, M., et al. Thromboxane biosynthesis and platelet function in type II diabetes mellitus. N Engl J Med. 1990;322:1769-74.

Davies, M. J. Stability and instability: two faces of coronary atherosclerosis. The Paul Dudley White Lecture 1995. Circulation. 1996;94:2013-20.

Davies, M. J. Coronary artery remodelling and the assessment of stenosis by pathologists. Histopathology. 1998;33:497-500.

Davies, M. J., Richardson, P. D., Woolf, N., et al. Risk of thrombosis in human atherosclerotic plaques: role of extracellular lipid, macrophage, and smooth muscle cell content. Br Heart J. 1993;69:377-81.

Davies, M. J. and Thomas, A. C. Plaque fissuring--the cause of acute myocardial infarction, sudden ischaemic death, and crescendo angina. Br Heart J. 1985;53:363-73.

Davies, P. F. Flow-mediated endothelial mechanotransduction. Physiol Rev. 1995;75:519-60.

de Feyter, P. J., Ozaki, Y., Baptista, J., et al. Ischemia-related lesion characteristics in patients with stable or unstable angina. A study with intracoronary angioscopy and ultrasound. Circulation. 1995;92:1408-13.

de Graaf, J., Hak-Lemmers, H. L., Hectors, M. P., et al. Enhanced susceptibility to in vitro oxidation of the dense low density lipoprotein subfraction in healthy subjects. Arterioscler Thromb. 1991;11:298-306.

de Jong, S. C., van den Berg, M., Rauwerda, J. A., et al. Hyperhomocysteinemia and atherothrombotic disease. Semin Thromb Hemost. 1998;24:381-5.

de Villiers, W. J., Smith, J. D., Miyata, M., et al. Macrophage phenotype in mice deficient in both macrophage-colony- stimulating factor (op) and apolipoprotein E. Arterioscler Thromb Vasc Biol. 1998;18:631-40.

Decossin, C., Tailleux, A., Fruchart, J. C., et al. Prevention of in vitro low-density lipoprotein oxidation by an albumin- containing Lp A-I subfraction. Biochim Biophys Acta. 1995;1255:31-8.

Dedichen, J. Thrombosing arteriosclerosis. Result of long-term anticogulant therapy. Br Med J. 1956;Nov. 3:1038-9.

den Heijer, P., Foley, D. P., Hillege, H. L., et al. The 'Ermenonville' classification of observations at coronary angioscopy--evaluation of intra- and inter-observer agreement. European Working Group on Coronary Angioscopy. Eur Heart J. 1994;15:815-22.

Deng, X., Marois, Y., How, T., et al. Luminal surface concentration of lipoprotein (LDL) and its effect on the wall uptake of cholesterol by canine carotid arteries. J Vasc Surg. 1995;21:135-45.

Detrano, R., Hsiai, T., Wang, S., et al. Prognostic value of coronary calcification and angiographic stenoses in patients undergoing coronary angiography. J Am Coll Cardiol. 1996;27:285-90.

Detrano, R., Kang, X., Mahaisavariya, P., et al. Accuracy of quantifying coronary hydroxyapatite with electron beam tomography. Invest Radiol. 1994;29:733-8.

Detrano, R. C., Wong, N. D., Doherty, T. M., et al. Coronary calcium does not accurately predict near-term future coronary events in high-risk adults. Circulation. 1999;99:2633-8.

Deutsch, H. J., Sechtem, U., Meyer, H., et al. Chronic aortic dissection: comparison of MR Imaging and transesophageal echocardiography. Radiology. 1994;192:645-50.

Diaz, M. N., Frei, B., Vita, J. A., et al. Antioxidants and atherosclerotic heart disease. N Engl J Med. 1997;337:408-16.

Dinkelborg, L. M., Duda, S. H., Hanke, H., et al. Molecular imaging of atherosclerosis using a technetium-99m-labeled endothelin derivative. J Nucl Med. 1998;39:1819-22.

Dinsmore, R. E., Liberthson, R. R., Wismer, G. L., et al. Magnetic resonance imaging of thoracic aortic aneurysms: comparison with other imaging methods. AJR Am J Roentgenol. 1986;146:309-14.

Djurovic, S. and Berg, K. Epidemiology of Lp(a) lipoprotein: its role in atherosclerotic/thrombotic disease. Clin Genet. 1997;52:281-92.

Doherty, T. M., Detrano, R. C., Mautner, S. L., et al. Coronary calcium: the good, the bad, and the uncertain. Am Heart J. 1999;137:806-14.

Doherty, T. M., Tang, W., Dascalos, S., et al. Ethnic origin and serum levels of 1alpha,25-dihydroxyvitamin D3 are independent predictors of coronary calcium mass measured by electron- beam computed tomography. Circulation. 1997;96:1477-81.

Edelman, R. R., Chien, D. and Kim, D. Fast selective black blood MR imaging. Radiology. 1991;181:655-60.

Edelman, R. R., Manning, W. J., Burstein, D., et al. Coronary arteries: breath-hold MR angiography. Radiology. 1991;181:641-3.

Eichenberger, A. C., Jenni, R. and von Schulthess, G. K. Aortic valve pressure gradients in patients with aortic valve stenosis: quantification with velocity-encoded cine MR imaging. AJR Am J Roentgenol. 1993;160:971-7.

Eichenberger, A. C., Schuiki, E., Kochli, V. D., et al. Ischemic heart disease: assessment with gadolinium-enhanced ultrafast MR imaging and dipyridamole stress. J Magn Reson Imaging. 1994;4:425-31.

Falcone, D. J., McCaffrey, T. A. and Vergilio, J. A. Stimulation of macrophage urokinase expression by polyanions is protein kinase C-dependent and requires protein and RNA synthesis. J Biol Chem. 1991;266:22726-32.

Falk, E. Plaque rupture with severe pre-existing stenosis precipitating coronary thrombosis. Characteristics of coronary atherosclerotic plaques underlying fatal occlusive thrombi. Br Heart J. 1983;50:127-34.

Falk, E. Morphologic features of unstable atherothrombotic plaques underlying acute coronary syndromes. Am J Cardiol. 1989;63:114E-120E.

Falk, E. Why do plaques rupture? Circulation. 1992;86:III30-42.

Falk, E., Shah, P. K. and Fuster, V. Coronary plaque disruption. Circulation. 1995;92:657-71.

Fallavollita, J. A., Brody, A. S., Bunnell, I. L., et al. Fast computed tomography detection of coronary calcification in the diagnosis of coronary artery disease. Circulation. 1994;89:285-90.

Fayad, Z. A., Fallon, J. T., Shinnar, M., et al. Noninvasive In vivo high-resolution magnetic resonance imaging of atherosclerotic lesions in genetically engineered mice. Circulation. 1998;98:1541-7.

Feld, S., Ganim, M., Carell, E. S., et al. Comparison of angioscopy, intravascular ultrasound imaging and quantitative coronary angiography in predicting clinical outcome after coronary intervention in high risk patients. J Am Coll Cardiol. 1996;28:97-105.

Felton, C. V., Crook, D., Davies, M. J., et al. Relation of plaque lipid composition and morphology to the stability of human aortic plaques. Arterioscler Thromb Vasc Biol. 1997;17:1337-45.

Fernandez-Ortiz, A., Badimon, J. J., Falk, E., et al. Characterization of the relative thrombogenicity of atherosclerotic plaque components: implications for consequences of plaque rupture. J Am Coll Cardiol. 1994;23:1562-9.

Fiorino, A. S. Electron-beam computed tomography, coronary artery calcium, and evaluation of patients with coronary artery disease. Ann Intern Med. 1998;128:839-47.

Fitzgerald, J. D. By what means might beta blockers prolong life after acute myocardial infarction? Eur Heart J. 1987;8:945-51.

Fleming, I., Bauersachs, J. and Busse, R. Calcium-dependent and calcium-independent activation of the endothelial NO synthase. J Vasc Res. 1997;34:165-74.

Frid, M. G., Aldashev, A. A., Dempsey, E. C., et al. Smooth muscle cells isolated from discrete compartments of the mature vascular media exhibit unique phenotypes and distinct growth capabilities. Circ Res. 1997;81:940-52.

Friedman, M. The coronary thrombus: its origin and fate. Hum Pathol. 1971;2:81-128.

Friedrich, G. J., Moes, N. Y., Muhlberger, V. A., et al. Detection of intralesional calcium by intracoronary ultrasound depends on the histologic pattern. Am Heart J. 1994;128:435-41.

Frink, R. J. Chronic ulcerated plaques: new insights into the pathogenesis of acute coronary disease. J Invasive Cardiol. 1994;6:173-85.

Fruebis, J., Gonzalez, V., Silvestre, M., et al. Effect of probucol treatment on gene expression of VCAM-1, MCP-1, and M- CSF in the aortic wall of LDL receptor-deficient rabbits during early atherogenesis. Arterioscler Thromb Vasc Biol. 1997;17:1289-302.

Fujimoto, J. G., Boppart, S. A., Tearney, G. J., et al. High resolution in vivo intra-arterial imaging with optical coherence tomography. Heart. 1999;82:128-133.

Fuster, V. Mechanisms of arterial thrombosis: foundation for therapy. Am Heart J. 1998;135:S361-6.

Fuster, V. and Badimon, J. J. Regression or stabilization of atherosclerosis means regression or stabilization of what we don't see in the arteriogram. Eur Heart J. 1995;16 Suppl E:6-12.

Fuster, V., Badimon, L., Badimon, J. J., et al. The pathogenesis of coronary artery disease and the acute coronary syndromes (1). N Engl J Med. 1992;326:242-50.

Fuster, V., Badimon, L., Badimon, J. J., et al. The pathogenesis of coronary artery disease and the acute coronary syndromes (2). N Engl J Med. 1992;326:310-8.

Fuster, V., Badimon, L., Badimon, J. J., et al. The porcine model for the understanding of thrombogenesis and atherogenesis. Mayo Clinic Proceedings. 1991;66:818-31.

Fuster, V., Badimon, L., Badimon, J. J., et al. The porcine model for the understanding of thrombogenesis and atherogenesis. Mayo Clin Proc. 1991;66:818-31.

Fuster, V., Chesebro, J. H., Frye, R. L., et al. Platelet survival and the development of coronary artery disease in the young adult: effects of cigarette smoking, strong family history and medical therapy. Circulation. 1981;63:546-51.

Fuster, V., Fallon, J. T., Badimon, J. J., et al. The unstable atherosclerotic plaque: clinical significance and therapeutic intervention. Thromb Haemost. 1997;78:247-55.

Fuster, V., Fayad, Z. A. and Badimon, J. J. Acute coronary syndromes: biology. Lancet. 1999;353 Suppl 2:SII5-9.

Fuster, V., Ip, J. H., Badimon, L., et al. Importance of experimental models for the development of clinical trials on thromboatherosclerosis. Circulation. 1991;83:IV15-25.

Galis, Z. S., Muszynski, M., Sukhova, G. K., et al. Cytokine-stimulated human vascular smooth muscle cells synthesize a complement of enzymes required for extracellular matrix digestion. Circ Res. 1994;75:181-9.

Gallo, R., Padurean, A., Toschi, V., et al. Prolonged thrombin inhibition reduces restenosis after balloon angioplasty in porcine coronary arteries. Circulation. 1998;97:581-8.

Gasser, R. N., Dienstl, F., Puschendorf, B., et al. New perspectives on the function of coronary artery spasm in acute myocardial infarction: the thromboischemic reentry mechanism. A review of 10 years research on the pathophysiology of AMI. Angiology. 1986;37:880-7.

Geppert, A., Graf, S., Beckmann, R., et al. Concentration of endogenous tPA antigen in coronary artery disease: relation to thrombotic events, aspirin treatment, hyperlipidemia, and multivessel disease. Arterioscler Thromb Vasc Biol. 1998;18:1634-42.

Giachelli, C. M., Liaw, L., Murry, C. E., et al. Osteopontin expression in cardiovascular diseases. Ann N Y Acad Sci. 1995;760:109-26.

Gibbons, G. H., Pratt, R. E. and Dzau, V. J. Vascular smooth muscle cell hypertrophy vs. hyperplasia. Autocrine transforming growth factor-beta 1 expression determines growth response to angiotensin II. J Clin Invest. 1992;90:456-61.

Ginsberg, H. N., Goldsmith, S. J. and Vallabhajosula, S. Noninvasive imaging of 99mtechnetium-labeled low density lipoprotein uptake by tendon xanthomas in hypercholesterolemic patients. Arteriosclerosis. 1990;10:256-62.

Giroud, D., Li, J. M., Urban, P., et al. Relation of the site of acute myocardial infarction to the most severe coronary arterial stenosis at prior angiography. Am J Cardiol. 1992;69:729-32.

Glagov, S., Weisenberg, E., Zarins, C. K., et al. Compensatory enlargement of human atherosclerotic coronary arteries. N Engl J Med. 1987;316:1371-5.

Go, R. T., Marwick, T. H., MacIntyre, W. J., et al. A prospective comparison of rubidium-82 PET and thallium-201 SPECT myocardial perfusion imaging utilizing a single dipyridamole stress in the diagnosis of coronary artery disease. J Nucl Med. 1990;31:1899-905.

Goldstein, J. L., Ho, Y. K., Basu, S. K., et al. Binding site on macrophages that mediates uptake and degradation of acetylated low density lipoprotein, producing massive cholesterol deposition. Proc Natl Acad Sci U S A. 1979;76:333-7.

Goto, S., Handa, S., Takahashi, E., et al. Synergistic effect of epinephrine and shearing on platelet activation. Thromb Res. 1996;84:351-9.

Gould, A. L., Rossouw, J. E., Santanello, N. C., et al. Cholesterol reduction yields clinical benefit: impact of statin trials. Circulation. 1998;97:946-52.

Grabowski, E. F., Jaffe, E. A. and Weksler, B. B. Prostacyclin production by cultured endothelial cell monolayers exposed to step increases in shear stress. J Lab Clin Med. 1985;105:36-43.

Grattan, M. T., Moreno-Cabral, C. E., Starnes, V. A., et al. Cytomegalovirus infection is associated with cardiac allograft rejection and atherosclerosis. JAMA. 1989;261:3561-6.

Griendling, K. K. and Alexander, R. W. Oxidative stress and cardiovascular disease. Circulation. 1997;96:3264-5.

Gronholdt, M. L., Dalager-Pedersen, S. and Falk, E. Coronary atherosclerosis: determinants of plaque rupture. Eur Heart J. 1998;19 Suppl C:C24-9.

Gurfinkel, E., Bozovich, G., Beck, E., et al. Treatment with the antibiotic roxithromycin in patients with acute non- Q-wave coronary syndromes. The final report of the ROXIS Study. Eur Heart J. 1999;20:121-7.

Gurfinkel, E., Bozovich, G., Daroca, A., et al. Randomised trial of roxithromycin in non-Q-wave coronary syndromes: ROXIS Pilot Study. ROXIS Study Group. Lancet. 1997;350:404-7.

Gussenhoven, W. J., Essed, C. E., Frietman, P., et al. Intravascular echographic assessment of vessel wall characteristics: a correlation with histology. Int J Card Imaging. 1989;4:105-16.

Haft, J. I., Haik, B. J., Goldstein, J. E., et al. Development of significant coronary artery lesions in areas of minimal disease. A common mechanism for coronary disease progression. Chest. 1988;94:731-6.

Hamsten, A., Wiman, B., de Faire, U., et al. Increased plasma levels of a rapid inhibitor of tissue plasminogen activator in young survivors of myocardial infarction. N Engl J Med. 1985;313:1557-63.

Han, J., Hajjar, D. P., Febbraio, M., et al. Native and modified low density lipoproteins increase the functional expression of the macrophage class B scavenger receptor, CD36. J Biol Chem. 1997;272:21654-9.

Hennekens, C. H., Buring, J. E., Manson, J. E., et al. Lack of effect of long-term supplementation with beta carotene on the incidence of malignant neoplasms and cardiovascular disease. N Engl J Med. 1996;334:1145-9.

Henry, P. D., Cabello, O. A. and Chen, C. H. Hypercholesterolemia and endothelial dysfunction. Curr Opin Lipidol. 1995;6:190-5.

Hermiller, J. B., Tenaglia, A. N., Kisslo, K. B., et al. In vivo validation of compensatory enlargement of atherosclerotic coronary arteries. Am J Cardiol. 1993;71:665-8.

Higgins, C. B., Herfkens, R., Lipton, M. J., et al. Nuclear magnetic resonance imaging of acute myocardial infarction in dogs: alterations in magnetic relaxation times. Am J Cardiol. 1983;52:184-8.

Hirsch, R., Kilner, P. J., Connelly, M. S., et al. Diagnosis in adolescents and adults with congenital heart disease. Prospective assessment of individual and combined roles of magnetic resonance imaging and transesophageal echocardiography. Circulation. 1994;90:2937-51.

Hodgson, J. M., Reddy, K. G., Suneja, R., et al. Intracoronary ultrasound imaging: correlation of plaque morphology with angiography, clinical syndrome and procedural results in patients undergoing coronary angioplasty. J Am Coll Cardiol. 1993;21:35-44.

Hopkins, P. N., Hunt, S. C., Schreiner, P. J., et al. Lipoprotein(a) interactions with lipid and non-lipid risk factors in patients with early onset coronary artery disease: results from the NHLBI Family Heart Study. Atherosclerosis. 1998;141:333-45.

Hoppe, U. C., Dederichs, B., Deutsch, H. J., et al. Congenital heart disease in adults and adolescents: comparative value of transthoracic and transesophageal echocardiography and MR imaging. Radiology. 1996;199:669-77.

Hsich, E., Johnson, T. M., Zhou, Y. F., et al. Cytomegalovirus infection increases development of atherosclerosis in apo-E knockout mice. FASEB J. 1999;13:A692. Abstract.

Hundley, W. G., Hamilton, C. A., Clarke, G. D., et al. Visualization and functional assessment of proximal and middle left anterior descending coronary stenoses in humans with magnetic resonance imaging. Circulation. 1999;99:3248-54.

Hunt, B. J. The relation between abnormal hemostatic function and the progression of coronary disease. Curr Opin Cardiol. 1990;5:758-65.

Janssens, S. P., Shimouchi, A., Quertermous, T., et al. Cloning and expression of a cDNA encoding human endothelium-derived relaxing factor/nitric oxide synthase. J Biol Chem. 1992;267:14519-22.

Johnson, J. M., Kennelly, M. M., Decesare, D., et al. Natural history of asymptomatic carotid plaque. Arch Surg. 1985;120:1010-2.

Johnston, D. L., Liu, P., Lauffer, R. B., et al. Use of gadolinium-DTPA as a myocardial perfusion agent: potential applications and limitations for magnetic resonance imaging. J Nucl Med. 1987;28:871-7.

Johnstone, M. T., Mittleman, M., Tofler, G., et al. The pathophysiology of the onset of morning cardiovascular events. Am J Hypertens. 1996;9:22S-28S.

Jonasson, L., Holm, J., Skalli, O., et al. Regional accumulations of T cells, macrophages, and smooth muscle cells in the human atherosclerotic plaque. Arteriosclerosis. 1986;6:131-8.

Kaufman, L., Crooks, L., Sheldon, P., et al. The potential impact of nuclear magnetic resonance imaging on cardiovascular diagnosis. Circulation. 1983;67:251-7.

Kawai, Y., Matsumoto, Y., Ikeda, Y., et al. [Regulation of antithrombogenicity in endothelium by hemodynamic forces]. Rinsho Byori. 1997;45:315-20.

Kennedy, J., Shavelle, R., Wang, S., et al. Coronary calcium and standard risk factors in symptomatic patients referred for coronary angiography. Am Heart J. 1998;135:696-702.

Keren, G. and Leon, M. B. Characterization of atherosclerotic lesions by intravascular ultrasound: possible role in unstable coronary syndromes and in interventional therapeutic procedures. Am J Cardiol. 1991;68:85B-91B.

Khoo, J. C., Miller, E., McLoughlin, P., et al. Enhanced macrophage uptake of low density lipoprotein after self- aggregation. Arteriosclerosis. 1988;8:348-58.

Khoo, J. C., Miller, E., Pio, F., et al. Monoclonal antibodies against LDL further enhance macrophage uptake of LDL aggregates. Arterioscler Thromb. 1992;12:1258-66.

Kilner, P. J., Firmin, D. N., Rees, R. S., et al. Valve and great vessel stenosis: assessment with MR jet velocity mapping. Radiology. 1991;178:229-35.

Kilner, P. J., Manzara, C. C., Mohiaddin, R. H., et al. Magnetic resonance jet velocity mapping in mitral and aortic valve stenosis. Circulation. 1993;87:1239-48.

Kimura, B. J., Bhargava, V. and DeMaria, A. N. Value and limitations of intravascular ultrasound imaging in characterizing coronary atherosclerotic plaque. Am Heart J. 1995;130:386-96.

Kita, T., Nagano, Y., Yokode, M., et al. Probucol prevents the progression of atherosclerosis in Watanabe heritable hyperlipidemic rabbit, an animal model for familial hypercholesterolemia. Proc Natl Acad Sci U S A. 1987;84:5928-31.

Kleber, F. X., Dopfmer, S. and Thieme, T. Invasive strategies to discriminate stable and unstable coronary plaques. Eur Heart J. 1998;19 Suppl C:C44-9.

Knight, L. C. Scintigraphic methods for detecting vascular thrombus. J Nucl Med. 1993;34:554-61.

Koyama, H., Raines, E. W., Bornfeldt, K. E., et al. Fibrillar collagen inhibits arterial smooth muscle proliferation through regulation of Cdk2 inhibitors. Cell. 1996;87:1069-78.

Kragel, A. H., Reddy, S. G., Wittes, J. T., et al. Morphometric analysis of the composition of atherosclerotic plaques in the four major epicardial coronary arteries in acute myocardial infarction and in sudden coronary death. Circulation. 1989;80:1747-56.

Kraiss, L. W., Raines, E. W., Wilcox, J. N., et al. Regional expression of the platelet-derived growth factor and its receptors in a primate graft model of vessel wall assembly. J Clin Invest. 1993;92:338-48.

Krams, R., Wentzel, J. J., Oomen, J. A., et al. Evaluation of endothelial shear stress and 3D geometry as factors determining the development of atherosclerosis and remodeling in human coronary arteries in vivo. Combining 3D reconstruction from angiography and IVUS (ANGUS) with computational fluid dynamics. Arterioscler Thromb Vasc Biol. 1997;17:2061-5.

Krantz, D. S., Kop, W. J., Santiago, H. T., et al. Mental stress as a trigger of myocardial ischemia and infarction. Cardiol Clin. 1996;14:271-87.

Ku, D. N., Giddens, D. P., Zarins, C. K., et al. Pulsatile flow and atherosclerosis in the human carotid bifurcation. Positive correlation between plaque location and low oscillating shear stress. Arteriosclerosis. 1985;5:293-302.

Kubota, R., Kubota, K., Yamada, S., et al. Microautoradiographic study for the differentiation of intratumoral macrophages, granulation tissues and cancer cells by the dynamics of fluorine-18-fluorodeoxyglucose uptake. J Nucl Med. 1994;35:104-12.

Lacoste, L., Lam, J. Y., Hung, J., et al. Hyperlipidemia and coronary disease. Correction of the increased thrombogenic potential with cholesterol reduction. Circulation. 1995;92:3172-7.

Laissy, J. P., Blanc, F., Soyer, P., et al. Thoracic aortic dissection: diagnosis with transesophageal echocardiography versus MR imaging. Radiology. 1995;194:331-6.

Lee, R. T. and Kamm, R. D. Vascular mechanics for the cardiologist. J Am Coll Cardiol. 1994;23:1289-95.

Lee, R. T. and Libby, P. The unstable atheroma. Arterioscler Thromb Vasc Biol. 1997;17:1859-67.

Lee, W. M. and Lee, K. T. Advanced coronary atherosclerosis in swine produced by combination of balloon-catheter injury and cholesterol feeding. Exp Mol Pathol. 1975;23:491-9.

Lees, A. M., Lees, R. S., Schoen, F. J., et al. Imaging human atherosclerosis with 99mTc-labeled low density lipoproteins. Arteriosclerosis. 1988;8:461-70.

Lees, R. S., Lees, A. M. and Strauss, H. W. External imaging of human atherosclerosis. J Nucl Med. 1983;24:154-6.

Leonard, E. J. and Yoshimura, T. Human monocyte chemoattractant protein-1 (MCP-1). Immunol Today. 1990;11:97-101.

Libby, P. Molecular bases of the acute coronary syndromes. Circulation. 1995;91:2844-50.

Libby, P. and Aikawa, M. New insights into plaque stabilisation by lipid lowering. Drugs. 1998;56:9-13; discussion 33.

Libby, P., Geng, Y. J., Aikawa, M., et al. Macrophages and atherosclerotic plaque stability. Curr Opin Lipidol. 1996;7:330-5.

Libby, P. and Ross, R. Cytokines and growth regulatory molecules. Philadelpia: Lippincott-Raven; 1996.

Libby, P., Sukhova, G., Lee, R. T., et al. Molecular biology of atherosclerosis. Int J Cardiol. 1997;62 Suppl 2:S23-9.

Lichtlen, P. R., Nikutta, P., Jost, S., et al. Anatomical progression of coronary artery disease in humans as seen by prospective, repeated, quantitated coronary angiography. Relation to clinical events and risk factors. The INTACT Study Group. Circulation. 1992;86:828-38.

Lim, T. T., Liang, D. H., Botas, J., et al. Role of compensatory enlargement and shrinkage in transplant coronary artery disease. Serial intravascular ultrasound study. Circulation. 1997;95:855-9.

Lima, J. A., Jeremy, R., Guier, W., et al. Accurate systolic wall thickening by nuclear magnetic resonance imaging with tissue tagging: correlation with sonomicrometers in normal and ischemic myocardium. J Am Coll Cardiol. 1993;21:1741-51.

Lin, C. S., Penha, P. D., Zak, F. G., et al. Morphodynamic interpretation of acute coronary thrombosis, with special reference to volcano-like eruption of atheromatous plaque caused by coronary artery spasm. Angiology. 1988;39:535-47.

Lin, M. C., Almus-Jacobs, F., Chen, H. H., et al. Shear stress induction of the tissue factor gene. J Clin Invest. 1997;99:737-44.

Lin, W., Abendschein, D. R. and Haacke, E. M. Contrast-enhanced magnetic resonance angiography of carotid arterial wall in pigs. J Magn Reson Imaging. 1997;7:183-90.

Linker, D. T., Kleven, A., Gronningsaether, A., et al. Tissue characterization with intra-arterial ultrasound: special promise and problems. Int J Card Imaging. 1991;6:255-63.

Little, W. C., Constantinescu, M., Applegate, R. J., et al. Can coronary angiography predict the site of a subsequent myocardial infarction in patients with mild-to-moderate coronary artery disease? Circulation. 1988;78:1157-66.

Loree, H. M., Tobias, B. J., Gibson, L. J., et al. Mechanical properties of model atherosclerotic lesion lipid pools. Arterioscler Thromb. 1994;14:230-4.

MacIsaac, A. I., Thomas, J. D. and Topol, E. J. Toward the quiescent coronary plaque. J Am Coll Cardiol. 1993;22:1228-41.

Maddahi, J., Schelbert, H., Brunken, R., et al. Role of thallium-201 and PET imaging in evaluation of myocardial viability and management of patients with coronary artery disease and left ventricular dysfunction. J Nucl Med. 1994;35:707-15.

Mahaisavariya, P., Detrano, R., Kang, X., et al. Quantitation of in vitro coronary artery calcium using ultrafast computed tomography. Cathet Cardiovasc Diagn. 1994;32:387-93.

Majno, G. and Joris, I. Apoptosis, oncosis, and necrosis. An overview of cell death. Am J Pathol. 1995;146:3-15.

Malek, A. M., Jackman, R., Rosenberg, R. D., et al. Endothelial expression of thrombomodulin is reversibly regulated by fluid shear stress. Circ Res. 1994;74:852-60.

Malik, N., Greenfield, B. W., Wahl, A. F., et al. Activation of human monocytes through CD40 induces matrix metalloproteinases. J Immunol. 1996;156:3952-60.

Mann, J. M. and Davies, M. J. Vulnerable plaque. Relation of characteristics to degree of stenosis in human coronary arteries. Circulation. 1996;94:928-31.

Manninen, H. I., Vanninen, R. L., Laitinen, M., et al. Intravascular ultrasound and magnetic resonance imaging in the assessment of atherosclerotic lesions in rabbit aorta. Correlation to histopathologic findings. Invest Radiol. 1998;33:464-71.

Manning, W. J., Atkinson, D. J., Grossman, W., et al. First-pass nuclear magnetic resonance imaging studies using gadolinium- DTPA in patients with coronary artery disease. J Am Coll Cardiol. 1991;18:959-65.

Manning, W. J., Li, W. and Edelman, R. R. A preliminary report comparing magnetic resonance coronary angiography with conventional angiography. N Engl J Med. 1993;328:828-32.

Margolis, J. R., Chen, J. T., Kong, Y., et al. The diagnostic and prognostic significance of coronary artery calcification. A report of 800 cases. Radiology. 1980;137:609-16.

Maseri, A., L'Abbate, A., Baroldi, G., et al. Coronary vasospasm as a possible cause of myocardial infarction. A conclusion derived from the study of "preinfarction" angina. N Engl J Med. 1978;299:1271-7.

Matheijssen, N. A., de Roos, A., van der Wall, E. E., et al. Acute myocardial infarction: comparison of T2-weighted and T1-weighted gadolinium-DTPA enhanced MR imaging. Magn Reson Med. 1991;17:460-9.

Mautner, G. C., Mautner, S. L., Froehlich, J., et al. Coronary artery calcification: assessment with electron beam CT and histomorphometric correlation. Radiology. 1994;192:619-23.

Mautner, S. L., Mautner, G. C., Froehlich, J., et al. Coronary artery disease: prediction with in vitro electron beam CT. Radiology. 1994;192:625-30.

McConnell, M. V., Aikawa, M., Maier, S. E., et al. MRI of rabbit atherosclerosis in response to dietary cholesterol lowering. Arterioscler Thromb Vasc Biol. 1999;19:1956-9.

McConnell, M. V., Khasgiwala, V. C., Savord, B. J., et al. Prospective adaptive navigator correction for breath-hold MR coronary angiography. Magn Reson Med. 1997;37:148-52.

McGill, J. B., Schneider, D. J., Arfken, C. L., et al. Factors responsible for impaired fibrinolysis in obese subjects and NIDDM patients. Diabetes. 1994;43:104-9.

McLean, J. W., Tomlinson, J. E., Kuang, W. J., et al. cDNA sequence of human apolipoprotein(a) is homologous to plasminogen. Nature. 1987;330:132-7.

McNamara, M. T., Higgins, C. B., Ehman, R. L., et al. Acute myocardial ischemia: magnetic resonance contrast enhancement with gadolinium-DTPA. Radiology. 1984;153:157-63.

Meade, T. W. Fibrinogen and cardiovascular disease. J Clin Pathol. 1997;50:13-5.

Mehta, D., Curwin, J., Gomes, J. A., et al. Sudden death in coronary artery disease: acute ischemia versus myocardial substrate. Circulation. 1997;96:3215-23.

Meine, T. J., Bauman, R. P., Yock, P. G., et al. Coronary artery restenosis after atherectomy is primarily due to negative remodeling. Am J Cardiol. 1999;84:141-6.

Mendall, M. A., Goggin, P. M., Molineaux, N., et al. Relation of Helicobacter pylori infection and coronary heart disease. Br Heart J. 1994;71:437-9.

Minar, E., Ehringer, H., Dudczak, R., et al. Indium-111-labeled platelet scintigraphy in carotid atherosclerosis. Stroke. 1989;20:27-33.

Mitchell, L., Jenkins, J. P., Watson, Y., et al. Diagnosis and assessment of mitral and aortic valve disease by cine- flow magnetic resonance imaging. Magn Reson Med. 1989;12:181-97.

Mizuno, K., Satomura, K., Miyamoto, A., et al. Angioscopic evaluation of coronary-artery thrombi in acute coronary syndromes. N Engl J Med. 1992;326:287-91.

Moore, E. H., Webb, W. R., Verrier, E. D., et al. MRI of chronic posttraumatic false aneurysms of the thoracic aorta. AJR Am J Roentgenol. 1984;143:1195-6.

Morel, D. W., Hessler, J. R. and Chisolm, G. M. Low density lipoprotein cytotoxicity induced by free radical peroxidation of lipid. J Lipid Res. 1983;24:1070-6.

Moreno, P. R., Bernardi, V. H., Lopez-Cuellar, J., et al. Macrophages, smooth muscle cells, and tissue factor in unstable angina. Implications for cell-mediated thrombogenicity in acute coronary syndromes. Circulation. 1996;94:3090-7.

Moreno, P. R., Falk, E., Palacios, I. F., et al. Macrophage infiltration in acute coronary syndromes. Implications for plaque rupture. Circulation. 1994;90:775-8.

Moriwaki, H., Matsumoto, M., Handa, N., et al. Functional and anatomic evaluation of carotid atherothrombosis. A combined study of indium 111 platelet scintigraphy and B-mode ultrasonography. Arterioscler Thromb Vasc Biol. 1995;15:2234-40.

Muhlestein, J. B., Anderson, J. L., Hammond, E. H., et al. Infection with Chlamydia pneumoniae accelerates the development of atherosclerosis and treatment with azithromycin prevents it in a rabbit model. Circulation. 1998;97:633-6.

Muller, J. E., Stone, P. H., Turi, Z. G., et al. Circadian variation in the frequency of onset of acute myocardial infarction. N Engl J Med. 1985;313:1315-22.

Muller, W. A., Weigl, S. A., Deng, X., et al. PECAM-1 is required for transendothelial migration of leukocytes. J Exp Med. 1993;178:449-60.

Nagel, E., Lehmkuhl, H. B., Bocksch, W., et al. Noninvasive diagnosis of ischemia-induced wall motion abnormalities with the use of high-dose dobutamine stress MRI: comparison with dobutamine stress echocardiography. Circulation. 1999;99:763-70.

Napoli, C., D'Armiento, F. P., Mancini, F. P., et al. Fatty streak formation occurs in human fetal aortas and is greatly enhanced by maternal hypercholesterolemia. Intimal accumulation of low density lipoprotein and its oxidation precede monocyte recruitment into early atherosclerotic lesions. J Clin Invest. 1997;100:2680-90.

Navab, M., Berliner, J. A., Watson, A. D., et al. The Yin and Yang of oxidation in the development of the fatty streak. A review based on the 1994 George Lyman Duff Memorial Lecture. Arterioscler Thromb Vasc Biol. 1996;16:831-42.

Nesto, R. W., Waxman, S., Mittleman, M. A., et al. Angioscopy of culprit coronary lesions in unstable angina pectoris and correlation of clinical presentation with plaque morphology. Am J Cardiol. 1998;81:225-8.

Nienaber, C. A., von Kodolitsch, Y., Nicolas, V., et al. The diagnosis of thoracic aortic dissection by noninvasive imaging procedures. N Engl J Med. 1993;328:1-9.

Nishida, K., Harrison, D. G., Navas, J. P., et al. Molecular cloning and characterization of the constitutive bovine aortic endothelial cell nitric oxide synthase. J Clin Invest. 1992;90:2092-6.

Nishimura, R. A., Edwards, W. D., Warnes, C. A., et al. Intravascular ultrasound imaging: in vitro validation and pathologic correlation. J Am Coll Cardiol. 1990;16:145-54.

Nishimura, T., Yamada, Y., Kozuka, T., et al. Value and limitation of gadolinium-DTPA contrast enhancement in the early detection of acute canine myocardial infarction. Am J Physiol Imaging. 1987;2:181-5.

Nobuyoshi, M., Tanaka, M., Nosaka, H., et al. Progression of coronary atherosclerosis: is coronary spasm related to progression? J Am Coll Cardiol. 1991;18:904-10.

Ohno, M., Cooke, J. P., Dzau, V. J., et al. Fluid shear stress induces endothelial transforming growth factor beta- 1 transcription and production. Modulation by potassium channel blockade. J Clin Invest. 1995;95:1363-9.

Ohtsuka, A., Ando, J., Korenaga, R., et al. The effect of flow on the expression of vascular adhesion molecule-1 by cultured mouse endothelial cells. Biochem Biophys Res Commun. 1993;193:303-10.

Olofsson, B. O., Dahlen, G. and Nilsson, T. K. Evidence for increased levels of plasminogen activator inhibitor and tissue plasminogen activator in plasma of patients with angiographically verified coronary artery disease. Eur Heart J. 1989;10:77-82.

Omenn, G. S., Goodman, G. E., Thornquist, M. D., et al. Effects of a combination of beta carotene and vitamin A on lung cancer and cardiovascular disease. N Engl J Med. 1996;334:1150-5.

Ossei-Gerning, N., Moayyedi, P., Smith, S., et al. Helicobacter pylori infection is related to atheroma in patients undergoing coronary angiography. Cardiovasc Res. 1997;35:120-4.

Ossewaarde, J. M., Feskens, E. J., De Vries, A., et al. Chlamydia pneumoniae is a risk factor for coronary heart disease in symptom-free elderly men, but Helicobacter pylori and cytomegalovirus are not. Epidemiol Infect. 1998;120:93-9.

Pasceri, V., Cammarota, G., Patti, G., et al. Association of virulent Helicobacter pylori strains with ischemic heart disease. Circulation. 1998;97:1675-9.

Pattynama, P. M., Lamb, H. J., Van der Velde, E. A., et al. Reproducibility of MRI-derived measurements of right ventricular volumes and myocardial mass. Magn Reson Imaging. 1995;13:53-63.

Pattynama, P. M., Willems, L. N., Smit, A. H., et al. Early diagnosis of cor pulmonale with MR imaging of the right ventricle. Radiology. 1992;182:375-9.

Paul, O. Background of the prevention of cardiovascular disease. II. Arteriosclerosis, hypertension, and selected risk factors. Circulation. 1989;80:206-14.

Pauly, R. R., Passaniti, A., Bilato, C., et al. Migration of cultured vascular smooth muscle cells through a basement membrane barrier requires type IV collagenase activity and is inhibited by cellular differentiation. Circ Res. 1994;75:41-54.

Pennell, D. J., Underwood, S. R., Manzara, C. C., et al. Magnetic resonance imaging during dobutamine stress in coronary artery disease. Am J Cardiol. 1992;70:34-40.

Peshock, R. M., Malloy, C. R., Buja, L. M., et al. Magnetic resonance imaging of acute myocardial infarction: gadolinium diethylenetriamine pentaacetic acid as a marker of reperfusion. Circulation. 1986;74:1434-40.

Pirich, C. and Sinzinger, H. Evidence for lipid regression in humans in vivo performed by 123iodine- low-density lipoprotein scintiscanning. Ann N Y Acad Sci. 1995;748:613-21.

Post, M. J., Borst, C. and Kuntz, R. E. The relative importance of arterial remodeling compared with intimal hyperplasia in lumen renarrowing after balloon angioplasty. A study in the normal rabbit and the hypercholesterolemic Yucatan micropig. Circulation. 1994;89:2816-21.

Post, M. J., de Smet, B. J., van der Helm, Y., et al. Arterial remodeling after balloon angioplasty or stenting in an atherosclerotic experimental model. Circulation. 1997;96:996-1003.

Powell, J. T. Vascular damage from smoking: disease mechanisms at the arterial wall. Vasc Med. 1998;3:21-8.

Prasad, K. Homocysteine, a Risk Factor for Cardiovascular Disease. International Journal Of Angiology. 1999;8:76-86.

Qiao, J. H., Tripathi, J., Mishra, N. K., et al. Role of macrophage colony-stimulating factor in atherosclerosis: studies of osteopetrotic mice. Am J Pathol. 1997;150:1687-99.

Quinn, M. T., Parthasarathy, S., Fong, L. G., et al. Oxidatively modified low density lipoproteins: a potential role in recruitment and retention of monocyte/macrophages during atherogenesis. Proc Natl Acad Sci U S A. 1987;84:2995-8.

Rajavashisth, T. B., Andalibi, A., Territo, M. C., et al. Induction of endothelial cell expression of granulocyte and macrophage colony-stimulating factors by modified low-density lipoproteins. Nature. 1990;344:254-7.

Rathbone, B., Martin, D., Stephens, J., et al. Helicobacter pylori seropositivity in subjects with acute myocardial infarction. Heart. 1996;76:308-11.

Raynaud, J. S., Bridal, S. L., Toussaint, J. F., et al. Characterization of atherosclerotic plaque components by high resolution quantitative MR and US imaging. J Magn Reson Imaging. 1998;8:622-9.

Reaven, P. D., Khouw, A., Beltz, W. F., et al. Effect of dietary antioxidant combinations in humans. Protection of LDL by vitamin E but not by beta-carotene. Arterioscler Thromb. 1993;13:590-600.

Redberg, R. F., Sobol, Y., Chou, T. M., et al. Adenosine-induced coronary vasodilation during transesophageal Doppler echocardiography. Rapid and safe measurement of coronary flow reserve ratio can predict significant left anterior descending coronary stenosis. Circulation. 1995;92:190-6.

Rehr, R., Disciascio, G., Vetrovec, G., et al. Angiographic morphology of coronary artery stenoses in prolonged rest angina: evidence of intracoronary thrombosis. J Am Coll Cardiol. 1989;14:1429-37.

Richardson, P. D., Davies, M. J. and Born, G. V. Influence of plaque configuration and stress distribution on fissuring of coronary atherosclerotic plaques. Lancet. 1989;2:941-4.

Rieder, M. J., Carmona, R., Krieger, J. E., et al. Suppression of angiotensin-converting enzyme expression and activity by shear stress. Circ Res. 1997;80:312-9.

Rimm, E. B., Stampfer, M. J., Ascherio, A., et al. Vitamin E consumption and the risk of coronary heart disease in men. N Engl J Med. 1993;328:1450-6.

Rosen, J. M., Butler, S. P., Meinken, G. E., et al. Indium-111-labeled LDL: a potential agent for imaging atherosclerotic disease and lipoprotein biodistribution. J Nucl Med. 1990;31:343-50.

Rosenfeld, M. Z., Morzed, T. C., Ricks, J., et al. Chronic infection with *Chlamydia pneumonia* accelerates atherosclerosis in apolipoprotein E deficient mice. Circulation. 1998;98(suppl I):I-142. Abstract.

Ross, J. J., Jr., Mintz, G. S. and Chandrasekaran, K. Transthoracic two-dimensional high frequency (7.5 MHz) ultrasonic visualization of the distal left anterior descending coronary artery. J Am Coll Cardiol. 1990;15:373-7.

Ross, R. The pathogenesis of atherosclerosis--an update. N Engl J Med. 1986;314:488-500.

Ross, R. The pathogenesis of atherosclerosis: a perspective for the 1990s. Nature. 1993;362:801-9.

Ross, R. The pathogenesis of atherosclerosis: a perspective for the 1990s. Nature. 1993;362:801-9.

Ross, R. Atherosclerosis--an inflammatory disease. N Engl J Med. 1999;340:115-26.

Ross, R., Bowen-Pope, D. F. and Raines, E. W. Platelet-derived growth factor and its role in health and disease. Philos Trans R Soc Lond B Biol Sci. 1990;327:155-69.

Ross, R. and Glomset, J. A. Atherosclerosis and the arterial smooth muscle cell: Proliferation of smooth muscle is a key event in the genesis of the lesions of atherosclerosis. Science. 1973;180:1332-9.

Rowsell, H. C., Hegardt, B., Downie, H. G., et al. Adrenaline and experimental thrombosis. Br J Haematol. 1966;12:66-73.

Rubanyi, G. M., Romero, J. C. and Vanhoutte, P. M. Flow-induced release of endothelium-derived relaxing factor. Am J Physiol. 1986;250:H1145-9.

Rumberger, J. A., Schwartz, R. S., Simons, D. B., et al. Relation of coronary calcium determined by electron beam computed tomography and lumen narrowing determined by autopsy. Am J Cardiol. 1994;73:1169-73.

Runge, V. M., Clanton, J. A., Wehr, C. J., et al. Gated magnetic resonance imaging of acute myocardial ischemia in dogs: application of multiecho techniques and contrast enhancement with GD DTPA. Magn Reson Imaging. 1985;3:255-66.

Saikku, P., Leinonen, M., Mattila, K., et al. Serological evidence of an association of a novel Chlamydia, TWAR, with chronic coronary heart disease and acute myocardial infarction. Lancet. 1988;2:983-6.

Salomaa, V., Stinson, V., Kark, J. D., et al. Association of fibrinolytic parameters with early atherosclerosis. The ARIC Study. Atherosclerosis Risk in Communities Study. Circulation. 1995;91:284-90.

Sampath, R., Kukielka, G. L., Smith, C. W., et al. Shear stress-mediated changes in the expression of leukocyte adhesion receptors on human umbilical vein endothelial cells in vitro. Ann Biomed Eng. 1995;23:247-56.

Sasahara, M., Raines, E. W., Chait, A., et al. Inhibition of hypercholesterolemia-induced atherosclerosis in the nonhuman primate by probucol. I. Is the extent of atherosclerosis related to resistance of LDL to oxidation? J Clin Invest. 1994;94:155-64.

Scanu, A. M. Atherothrombogenicity of lipoprotein(a): the debate. Am J Cardiol. 1998;82:26Q-33Q.

Scholz, T. D., Martins, J. B. and Skorton, D. J. NMR relaxation times in acute myocardial infarction: relative influence of changes in tissue water and fat content. Magn Reson Med. 1992;23:89-95.

Schwartz, R. S. Neointima and arterial injury: dogs, rats, pigs, and more. Lab Invest. 1994;71:789-91.

Secci, A., Wong, N., Tang, W., et al. Electron beam computed tomographic coronary calcium as a predictor of coronary events: comparison of two protocols. Circulation. 1997;96:1122-9.

Sechtem, U., Pflugfelder, P. W., White, R. D., et al. Cine MR imaging: potential for the evaluation of cardiovascular function. AJR Am J Roentgenol. 1987;148:239-46.

Seed, M., Hoppichler, F., Reaveley, D., et al. Relation of serum lipoprotein(a) concentration and apolipoprotein(a) phenotype to coronary heart disease in patients with familial hypercholesterolemia. N Engl J Med. 1990;322:1494-9.

Sessa, W. C., Harrison, J. K., Barber, C. M., et al. Molecular cloning and expression of a cDNA encoding endothelial cell nitric oxide synthase. J Biol Chem. 1992;267:15274-6.

Shah, P. K., Falk, E., Badimon, J. J., et al. Human monocyte-derived macrophages induce collagen breakdown in fibrous caps of atherosclerotic plaques. Potential role of matrix-degrading metalloproteinases and implications for plaque rupture. Circulation. 1995;92:1565-9.

Sharefkin, J. B., Diamond, S. L., Eskin, S. G., et al. Fluid flow decreases preproendothelin mRNA levels and suppresses endothelin-1 peptide release in cultured human endothelial cells. J Vasc Surg. 1991;14:1-9.

Sherman, C. T., Litvack, F., Grundfest, W., et al. Coronary angioscopy in patients with unstable angina pectoris. N Engl J Med. 1986;315:913-9.

Shinnar, M., Fallon, J. T., Wehrli, S., et al. The Diagnostic Accuracy of Ex Vivo MRI for Human Atherosclerotic Plaque Characterization. Arterioscler Thromb Vasc Biol. 1999;19:2756-2761.

Shiomi, M., Ito, T., Tsukada, T., et al. Reduction of serum cholesterol levels alters lesional composition of atherosclerotic plaques. Effect of pravastatin sodium on

atherosclerosis in mature WHHL rabbits. Arterioscler Thromb Vasc Biol. 1995;15:1938-44.

Shiran, A., Mintz, G. S., Leiboff, B., et al. Serial volumetric intravascular ultrasound assessment of arterial remodeling in left main coronary artery disease. Am J Cardiol. 1999;83:1427-32.

Shyy, J. Y., Lin, M. C., Han, J., et al. The cis-acting phorbol ester "12-O-tetradecanoylphorbol 13-acetate"- responsive element is involved in shear stress-induced monocyte chemotactic protein 1 gene expression. Proc Natl Acad Sci U S A. 1995;92:8069-73.

Silva, J. A., Escobar, A., Collins, T. J., et al. Unstable angina. A comparison of angioscopic findings between diabetic and nondiabetic patients. Circulation. 1995;92:1731-6.

Simionescu, N., Vasile, E., Lupu, F., et al. Prelesional events in atherogenesis. Accumulation of extracellular cholesterol-rich liposomes in the arterial intima and cardiac valves of the hyperlipidemic rabbit. Am J Pathol. 1986;123:109-25.

Simons, D. B., Schwartz, R. S., Edwards, W. D., et al. Noninvasive definition of anatomic coronary artery disease by ultrafast computed tomographic scanning: a quantitative pathologic comparison study. J Am Coll Cardiol. 1992;20:1118-26.

Sinzinger, H., Rodrigues, M. and Kritz, H. (1996). Radioisotope imaging of atheroma. Syndromes of atherosclerosis: correlations of clinical imaging and pathology. V. Fuster. Armonk, NY, Futura Publishing Company, Inc: 369-83.

Sinzinger, H. and Virgolini, I. Nuclear medicine and atherosclerosis. Eur J Nucl Med. 1990;17:160-78.

Skinner, M. P., Yuan, C., Mitsumori, L., et al. Serial magnetic resonance imaging of experimental atherosclerosis detects lesion fine structure, progression and complications in vivo. Nat Med. 1995;1:69-73.

Slyper, A. H. Low-density lipoprotein density and atherosclerosis. Unraveling the connection. JAMA. 1994;272:305-8.

Small, D. M. George Lyman Duff memorial lecture. Progression and regression of atherosclerotic lesions. Insights from lipid physical biochemistry. Arteriosclerosis. 1988;8:103-29.

Sorlie, P. D., Adam, E., Melnick, S. L., et al. Cytomegalovirus/herpesvirus and carotid atherosclerosis: the ARIC Study. J Med Virol. 1994;42:33-7.

Spalding, A., Vaitkevicius, H., Dill, S., et al. Mechanism of epinephrine-induced platelet aggregation. Hypertension. 1998;31:603-7.

Springer, T. A. and Cybulsky, M. I. (1996). Traffic signals on endothelium for leukocytes in health, inflammation, and atherosclerosis. Atherosclerosis and coronary artery disease. F. V, R. R and T. EJ. Philadelphia, Lippincott-Raven. **1:** 595-606.

St Clair, R. W. Atherosclerosis regression in animal models: current concepts of cellular and biochemical mechanisms. Prog Cardiovasc Dis. 1983;26:109-32.

Stamper, J. J. and Pohost, G. M. Assessing myocardial ischemic insult using nuclear magnetic resonance spectroscopy. Am J Card Imaging. 1992;6:244-58.

Stampfer, M. J., Hennekens, C. H., Manson, J. E., et al. Vitamin E consumption and the risk of coronary disease in women. N Engl J Med. 1993;328:1444-9.

Stary, H. C., Chandler, A. B., Glagov, S., et al. A definition of initial, fatty streak, and intermediate lesions of atherosclerosis. A report from the Committee on Vascular Lesions of the Council on Arteriosclerosis, American Heart Association. Circulation. 1994;89:2462-78.

Steele, P. M., Chesebro, J. H., Stanson, A. W., et al. Balloon angioplasty. Natural history of the pathophysiological response to injury in a pig model. Circ Res. 1985;57:105-12.

Steffans, J. C., Sakuma, H., Bourne, M. W., et al. Magnetic resonance imaging in ischemic heart disease. Am Heart J. 1996;132:156-73.

Steinberg, D. Low density lipoprotein oxidation and its pathobiological significance. J Biol Chem. 1997;272:20963-6.

Stemme, S., Faber, B., Holm, J., et al. T lymphocytes from human atherosclerotic plaques recognize oxidized low density lipoprotein. Proc Natl Acad Sci U S A. 1995;92:3893-7.

Stephens, N. G., Parsons, A., Schofield, P. M., et al. Randomised controlled trial of vitamin E in patients with coronary disease: Cambridge Heart Antioxidant Study (CHAOS). Lancet. 1996;347:781-6.

Stewart, R. E., Schwaiger, M., Molina, E., et al. Comparison of rubidium-82 positron emission tomography and thallium-201 SPECT imaging for detection of coronary artery disease. Am J Cardiol. 1991;67:1303-10.

Strauss, L. G. and Conti, P. S. The applications of PET in clinical oncology. J Nucl Med. 1991;32:623-48; discussion 649-50.

Strong, J. P., Bhattacharyya, A. K., Eggen, D. A., et al. Long-term induction and regression of diet-induced atherosclerotic lesions in rhesus monkeys. I. Morphological and chemical evidence for regression of lesions in the aorta and carotid and peripheral arteries. Arterioscler Thromb. 1994;14:958-65.

Taams, M. A., Gussenhoven, E. J., Cornel, J. H., et al. Detection of left coronary artery stenosis by transoesophageal echocardiography. Eur Heart J. 1988;9:1162-6.

Takada, Y., Shinkai, F., Kondo, S., et al. Fluid shear stress increases the expression of thrombomodulin by cultured human endothelial cells. Biochem Biophys Res Commun. 1994;205:1345-52.

Tang, W., Detrano, R. C., Brezden, O. S., et al. Racial differences in coronary calcium prevalence among high-risk adults. Am J Cardiol. 1995;75:1088-91.

Taylor, A. J., Burke, A. P., Farb, A., et al. Arterial remodeling in the left coronary system: the role of high- density lipoprotein. J Am Coll Cardiol. 1999;34:760-7.

Theroux, P. and Fuster, V. Acute coronary syndromes: unstable angina and non-Q-wave myocardial infarction. Circulation. 1998;97:1195-206.

Thieme, T., Wernecke, K. D., Meyer, R., et al. Angioscopic evaluation of atherosclerotic plaques: validation by histomorphologic analysis and association with stable and unstable coronary syndromes. J Am Coll Cardiol. 1996;28:1-6.

Thiruvikraman, S. V., Guha, A., Roboz, J., et al. In situ localization of tissue factor in human atherosclerotic plaques by binding of digoxigenin-labeled factors VIIa and X. Lab Invest. 1996;75:451-61.

Thom, D. H., Grayston, J. T., Siscovick, D. S., et al. Association of prior infection with Chlamydia pneumoniae and angiographically demonstrated coronary artery disease. JAMA. 1992;268:68-72.

Thompson, S. G., Kienast, J., Pyke, S. D., et al. Hemostatic factors and the risk of myocardial infarction or sudden death in patients with angina pectoris. European Concerted Action on Thrombosis and Disabilities Angina Pectoris Study Group. N Engl J Med. 1995;332:635-41.

Tillisch, J., Brunken, R., Marshall, R., et al. Reversibility of cardiac wall-motion abnormalities predicted by positron tomography. N Engl J Med. 1986;314:884-8.

Tobis, J. M., Mallery, J., Mahon, D., et al. Intravascular ultrasound imaging of human coronary arteries in vivo. Analysis of tissue characterizations with comparison to in vitro histological specimens. Circulation. 1991;83:913-26.

Topol, E. J. and Nissen, S. E. Our preoccupation with coronary luminology. The dissociation between clinical and angiographic findings in ischemic heart disease. Circulation. 1995;92:2333-42.

Toschi, V., Gallo, R., Lettino, M., et al. Tissue factor modulates the thrombogenicity of human atherosclerotic plaques. Circulation. 1997;95:594-9.

Toussaint, J. F., LaMuraglia, G. M., Southern, J. F., et al. Magnetic resonance images lipid, fibrous, calcified, hemorrhagic, and thrombotic components of human atherosclerosis in vivo. Circulation. 1996;94:932-8.

Toussaint, J. F., Southern, J. F., Fuster, V., et al. T2-weighted contrast for NMR characterization of human atherosclerosis. Arterioscler Thromb Vasc Biol. 1995;15:1533-42.

Toussaint, J. F., Southern, J. F., Fuster, V., et al. Water diffusion properties of human atherosclerosis and thrombosis measured by pulse field gradient nuclear magnetic resonance. Arterioscler Thromb Vasc Biol. 1997;17:542-6.

Toussaint, J. F., Southern, J. F., Kantor, H. L., et al. Behavior of atherosclerotic plaque components after in vitro angioplasty and atherectomy studied by high field MR imaging. Magn Reson Imaging. 1998;16:175-83.

Traub, O. and Berk, B. C. Laminar shear stress: mechanisms by which endothelial cells transduce an atheroprotective force. Arterioscler Thromb Vasc Biol. 1998;18:677-85.

Tribble, D. L., Holl, L. G., Wood, P. D., et al. Variations in oxidative susceptibility among six low density lipoprotein subfractions of differing density and particle size. Atherosclerosis. 1992;93:189-99.

Tsao, P. S., Lewis, N. P., Alpert, S., et al. Exposure to shear stress alters endothelial adhesiveness. Role of nitric oxide. Circulation. 1995;92:3513-9.

Tscholakoff, D., Higgins, C. B., Sechtem, U., et al. Occlusive and reperfused myocardial infarcts: effect of Gd-DTPA on ECG- gated MR imaging. Radiology. 1986;160:515-9.

Uchida, Y., Nakamura, F., Tomaru, T., et al. Prediction of acute coronary syndromes by percutaneous coronary angioscopy in patients with stable angina. Am Heart J. 1995;130:195-203.

Uchida, Y., Tomaru, T., Nakamura, F., et al. Percutaneous coronary angioscopy in patients with ischemic heart disease. Am Heart J. 1987;114:1216-22.

Ulevitch, R. J., Johnston, A. R. and Weinstein, D. B. New function for high density lipoproteins. Isolation and characterization of a bacterial lipopolysaccharide-high density lipoprotein complex formed in rabbit plasma. J Clin Invest. 1981;67:827-37.

Vallabhajosula, S. and Fuster, V. Atherosclerosis: imaging techniques and the evolving role of nuclear medicine. J Nucl Med. 1997;38:1788-96.

Vallabhajosula, S. and Goldsmith, S. J. 99mTc-low density lipoprotein: intracellularly trapped radiotracer for noninvasive imaging of low density lipoprotein metabolism in vivo. Semin Nucl Med. 1990;20:68-79.

Vallabhajosula, S., Paidi, M., Badimon, J. J., et al. Radiotracers for low density lipoprotein biodistribution studies in vivo: technetium-99m low density lipoprotein versus radioiodinated low density lipoprotein preparations. J Nucl Med. 1988;29:1237-45.

Van Belle, E., Lablanche, J. M., Bauters, C., et al. Coronary angioscopic findings in the infarct-related vessel within 1 month of acute myocardial infarction: natural history and the effect of thrombolysis. Circulation. 1998;97:26-33.

van der Wal, A. C., Becker, A. E., van der Loos, C. M., et al. Site of intimal rupture or erosion of thrombosed coronary atherosclerotic plaques is characterized by an inflammatory process irrespective of the dominant plaque morphology. Circulation. 1994;89:36-44.

van der Wal, A. C., Das, P. K., Bentz van de Berg, D., et al. Atherosclerotic lesions in humans. In situ immunophenotypic analysis suggesting an immune mediated response. Lab Invest. 1989;61:166-70.

van der Wall, E. E., Vliegen, H. W., de Roos, A., et al. Magnetic resonance imaging in coronary artery disease. Circulation. 1995;92:2723-39.

van Rugge, F. P., van der Wall, E. E., de Roos, A., et al. Dobutamine stress magnetic resonance imaging for detection of coronary artery disease. J Am Coll Cardiol. 1993;22:431-9.

Vanhoutte, P. M. Endothelium and control of vascular function. State of the Art lecture. Hypertension. 1989;13:658-67.

Vaughan, C. J., Murphy, M. B. and Buckley, B. M. Statins do more than just lower cholesterol. Lancet. 1996;348:1079-82.

Vaughan, D. E. Plasminogen activator inhibitor-1: a common denominator in cardiovascular disease. J Investig Med. 1998;46:370-6.

Virgolini, I., Rauscha, F., Lupattelli, G., et al. Autologous low-density lipoprotein labelling allows characterization of human atherosclerotic lesions in vivo as to presence of foam cells and endothelial coverage. Eur J Nucl Med. 1991;18:948-51.

von Rokitansky, C. (1852). . A Manual of Pathological Anatomy. Berlin, Sydenham Society. **4:** 261.

Wagner, W. D., St. Clair, R. W., Clarkson, T. B., et al. A study of atherosclerosis regression in Macaca mulatta: III. Chemical changes in arteries from animals with atherosclerosis induced for 19 months and regressed for 48 months at plasma cholesterol concentrations of 300 or 200 mg/dl. Am J Pathol. 1980;100:633-50.

Walpola, P. L., Gotlieb, A. I., Cybulsky, M. I., et al. Expression of ICAM-1 and VCAM-1 and monocyte adherence in arteries exposed to altered shear stress. Arterioscler Thromb Vasc Biol. 1995;15:2-10.

Watanabe, Y. Serial inbreeding of rabbits with hereditary hyperlipidemia (WHHL-rabbit). Atherosclerosis. 1980;36:261-8.

Weissman, N. J., Sheris, S. J., Chari, R., et al. Intravascular ultrasonic analysis of plaque characteristics associated with coronary artery remodeling. Am J Cardiol. 1999;84:37-40.

Wesbey, G. E., Higgins, C. B., McNamara, M. T., et al. Effect of gadolinium-DTPA on the magnetic relaxation times of normal and infarcted myocardium. Radiology. 1984;153:165-9.

Wexler, L., Brundage, B., Crouse, J., et al. Coronary artery calcification: pathophysiology, epidemiology, imaging methods, and clinical implications. A statement for health professionals from the American Heart Association. Writing Group. Circulation. 1996;94:1175-92.

White, R. D., Caputo, G. R., Mark, A. S., et al. Coronary artery bypass graft patency: noninvasive evaluation with MR imaging. Radiology. 1987;164:681-6.

White, R. D., Pflugfelder, P. W., Lipton, M. J., et al. Coronary artery bypass grafts: evaluation of patency with cine MR imaging. AJR Am J Roentgenol. 1988;150:1271-4.

Wight, T. N. Cell biology of arterial proteoglycans. Arteriosclerosis. 1989;9:1-20.

Wilcox, J. N., Smith, K. M., Schwartz, S. M., et al. Localization of tissue factor in the normal vessel wall and in the atherosclerotic plaque. Proc Natl Acad Sci U S A. 1989;86:2839-43.

Willerson, J. T., Golino, P., Eidt, J., et al. Specific platelet mediators and unstable coronary artery lesions. Experimental evidence and potential clinical implications. Circulation. 1989;80:198-205.

Williams, E. S., Kaplan, J. I., Thatcher, F., et al. Prolongation of proton spin lattice relaxation times in regionally ischemic tissue from dog hearts. J Nucl Med. 1980;21:449-53.

Willich, S. N., Linderer, T., Wegscheider, K., et al. Increased morning incidence of myocardial infarction in the ISAM Study: absence with prior beta-adrenergic blockade. ISAM Study Group. Circulation. 1989;80:853-8.

Winniford, M. D., Wheelan, K. R., Kremers, M. S., et al. Smoking-induced coronary vasoconstriction in patients with atherosclerotic coronary artery disease: evidence for adrenergically mediated alterations in coronary artery tone. Circulation. 1986;73:662-7.

Winocour, P. D. Platelet abnormalities in diabetes mellitus. Diabetes. 1992;41 Suppl 2:26-31.

Worthley, S. G., Helft, G., Fuster, V., et al. High resolution ex vivo magnetic resonance imaging of in situ coronary and aortic atherosclerotic plaque in a porcine model. Atherosclerosis. 2000;150:321-9.

Worthley, S. G., Helft, G., Fuster, V., et al. Serial in vivo MRI documents arterial remodeling in experimental atherosclerosis. Circulation. 2000;101:586-9.

Yoshida, K., Yoshikawa, J., Hozumi, T., et al. Detection of left main coronary artery stenosis by transesophageal color Doppler and two-dimensional echocardiography. Circulation. 1990;81:1271-6.

Yuan, C., Beach, K. W., Smith, L. H., Jr., et al. Measurement of atherosclerotic carotid plaque size in vivo using high resolution magnetic resonance imaging. Circulation. 1998;98:2666-71.

Yuan, C., Petty, C., O'Brien, K. D., et al. In vitro and in situ magnetic resonance imaging signal features of atherosclerotic plaque-associated lipids. Arterioscler Thromb Vasc Biol. 1997;17:1496-503.

Yuan, C., Skinner, M. P., Kaneko, E., et al. Magnetic resonance imaging to study lesions of atherosclerosis in the hyperlipidemic rabbit aorta. Magn Reson Imaging. 1996;14:93-102.

Zerhouni, E. A., Parish, D. M., Rogers, W. J., et al. Human heart: tagging with MR imaging--a method for noninvasive assessment of myocardial motion. Radiology. 1988;169:59-63.

Zhu, J., Quyyumi, A., Norman, J. E., et al. Potential role of hepatitis A virus in coronary artery disease. J Am Coll Cardiol. 1999;33(suppl):Abstract.

Zimmermann-Paul, G. G., Quick, H. H., Vogt, P., et al. High-resolution intravascular magnetic resonance imaging: monitoring of plaque formation in heritable hyperlipidemic rabbits. Circulation. 1999;99:1054-61.